1991

A pairwise interaction theory for determining the linear acoustic properties of dilute bubbly liquids

Ashok S. Sangani, *Syracuse University*

J. Fluid Mech. (1991), *vol.* 232, *pp.* 221–284
Printed in Great Britain

A pairwise interaction theory for determining the linear acoustic properties of dilute bubbly liquids

By A. S. SANGANI
Department of Chemical Engineering, Syracuse University, Syracuse, NY 13244, USA

(Received 23 May 1990 and in revised form 27 March 1991)

The problem of determining the acoustic properties of dilute bubbly liquids is examined using the method of ensemble-averaged equations and pairwise interactions. The phase speed and attenuation of sound waves in the small-amplitude regime are determined as a function of frequency of sound waves including the effects of finite surface tension, small viscosity of the liquid, and non-adiabatic thermal changes, and compared with the experimental data available in the literature. An excellent agreement is found for frequencies smaller than about 1.3 times the natural frequency of the bubbles, but the discrepancy is substantial at larger frequencies.

1. Introduction

The presence of gas bubbles dispersed in a liquid affects rather profoundly the acoustic behaviour of the liquid. For example, while the speed of sound in pure water at ordinary temperatures and pressures is approximately 1500 m s^{-1}, its speed, under similar conditions of temperatures and pressures and at relatively low frequencies, in water containing 5% by volume of air bubbles is only about 60 m s^{-1}, which is even lower than the speed of sound in pure air (330 m s^{-1}). The reason for such a drastic effect is now well understood. The speed of sound in the medium depends roughly on the product of the compressibility and the density of the medium. Since the former is primarily determined by the amount of gas bubbles and the latter by the amount of liquid, the resulting speed of sound in the mixture is quite different from that of the pure liquid or the pure gas.

A number of investigators have studied theoretically the problem of acoustic wave propagation in bubbly liquids, both in the linear small-amplitude regime and the weakly nonlinear regime, when the volume fraction β of the gas bubbles is small compared to unity (Foldy 1945; Carstensen & Foldy 1947; Twerski 1962; Batchelor 1969; van Wijngaarden 1972; Caflisch *et al.* 1985*a*, *b*; Prosperetti & Kim 1989). Foldy (1945) treated the bubbles as point scatterers and gave the following expression for C_{ef}, the speed of sound in the mixture:

$$\frac{1}{C_{ef}^2} = \frac{1}{C_L^2} + \beta \frac{\rho_L}{\gamma P_e} \frac{1}{1-\omega_r^2} + o(\beta), \tag{1.1}$$

where C_L is the speed in pure liquid, ρ_L is the density of the liquid, γ is the ratio of the constant pressure and constant volume specific heats of the gas, P_e is the equilibrium pressure in the gas bubbles, and ω_r is the ratio of the frequency ω of the sound wave and the adiabatic natural frequency ω_c of the gas bubbles given by

$$\omega_c^2 = 3\gamma P_e/\rho_L R^2, \tag{1.2}$$

R being the radius of the bubbles. For most gas–liquid mixtures, the coefficient of β in (1.1) is much greater than the $O(1)$ term. For example, for an air–water mixture at atmospheric pressures, the ratio $\rho_L C_L^2/\gamma P_e$ is $O(10^4)$ and, therefore, unless β is smaller than 10^{-4}, the speed of sound in the mixture deviates significantly from that of the pure liquid.

In deriving (1.1), surface tension and viscosity effects were neglected and the gas bubbles were assumed to undergo adiabatic volume changes. The effects of these variables have also been studied by several investigators and the reader is referred to the review articles by van Wijngaarden (1972) and Prosperetti (1984) for details. We also note that there is actually a correction of $O(\beta)$ multiplying $1/C_L^2$ in (1.1) but, in view of the fact that $1/C_L^2 \ll \rho_L/\gamma P_e$, this correction is of no practical significance.

The earlier theoretical results were obtained based on somewhat heuristic grounds and it was not clear under what quantitative conditions these results were correct. Recently, Caflisch *et al.* (1985*a*, *b*) have presented a method of two-scale homogenization to derive rigorously the equations that describe the acoustic behaviour of bubbly liquids on a macroscale, i.e. on a lengthscale large compared to the radius of the bubbles, by starting from the equations of motion satisfied by the individual phases on the microscale. Using this method, these investigators have determined exact conditions under which various expressions apply. In particular, they have examined carefully the limits $\omega_r \to 0$ and $\beta \to 0$.

As a result of the pressure variations in the acoustic wave, and owing to the unequal densities of the gas and liquid, the bubbles undergo both radial and displacement oscillations. When β is very small but ω_r is $O(1)$, Caflisch *et al.* (1985*a*) found that the $O(\beta)$ term given by the Foldy approximation (1.1) is correct and that the primary mode of the bubble oscillations is radial. In this limit the pressure around each bubble is approximately uniform and the disturbance in the velocity potential or the pressure around each bubble may be approximated by a monopole situated at the centre of the bubble. These investigators, however, did not specify the order of magnitude of the error in (1.1). On the other hand, when β is $O(1)$ and $\omega_r \to 0$, Caflisch *et al.* (1985*b*) found the primary mode of the bubble oscillations to be the volume-preserving displacement oscillation. In other words, the disturbance velocity potential or the pressure around each bubble may be approximated, to the leading order, by a dipole situated at the centre of the bubble. This result can be explained physically as follows. When the frequency is small, the temporal variations in pressure occur slowly, and so the radial velocity at the surface of each bubble and the strength of the monopole are small in magnitude. However, since the bubbles have density different from that of the liquid, the ratio of their displacement acceleration to the mixture acceleration remains finite even as $\omega_r \to 0$. In this case the Foldy approximation given by (1.1) with $\omega_r = 0$ is still valid and the correction, which is $O(\beta^2)$, was explicitly determined by Caflisch *et al.* (1985*b*) (cf. (3.40)). The term $(\beta\rho_L)/(\gamma P_e(1-\omega_r^2))$ in the Foldy approximation is actually a sum of two terms: $(\beta\rho_L)/(\gamma P_e)$, which represents the compressibility of the medium, and $[(\beta\rho_L)/(\gamma P_e)]$ $[(\omega_r^2)/(1-\omega_r^2)]$, which is proportional to the strength of monopole. Since the compressibility of the gas bubbles plays a very significant role in determining the speed of sound, the first term in the Foldy approximation is always valid when β is small. It is only when one considers the corrections to it for higher β-values that the leading dipole-like behaviour of the bubbles become important in the case of $\omega_r \to 0$. Once again, although the correction to (1.1) is exactly specified in this case, Caflisch *et al.* (1985*b*) did not provide any quantitative criterion for how small ω_r must be in order that this approximation to (1.1) becomes valid.

The homogenization method has also been applied in recent years to the problem of determining the viscous and thermal attenuation of sound waves due to non-zero viscosity and non-adiabatic expansions and to examine the effect of finite surface tension resulting in deformation of the bubbles from the spherical shape (Miksis & Ting 1986, 1987*a*, *b*).

In all of the studies mentioned above, only the interaction of a single bubble with the medium was employed in determining the behaviour of dilute bubbly liquids, an exception being the work of Rubinstein (1985) who considered the special case of bubbles arranged in a periodic array and determined the first, $O(\beta^{\frac{1}{3}})$, correction to the Foldy's expression. When the spatial arrangement of bubbles is random and β larger it is necessary to examine the interaction of a pair of bubbles as has been done in the determination of the other macroscopic properties of suspensions, such as effective conductivity, sedimentation coefficient, and effective permeability (Jeffrey 1973; Batchelor 1974; Howells 1974). It is surprising, however, that in spite of well developed techniques for analysing such interactions, no attempts seem to have been made in the literature to analyse the acoustic behaviour of non-dilute bubbly liquids in a rigorous manner. In this paper we employ the method of ensemble averages developed by Hinch (1977) to provide a relatively simple and less formal alternative to the two-space homogenization method for deriving the macroscale behaviour of bubbly liquids. The method is particularly suitable for incorporating pairwise interactions among bubbles when the finite-wavelength effect is important or for incorporating the results of large-scale numerical multi-particle calculations which are now made possible because of the improved computational resources. The results of such numerical calculations will be presented in a future paper; here we use the method to determine the correction to (1.1) in terms of β for finite ω_{r}. Since the $O(\beta)$ correction in (1.1) is usually much larger than the $1/C_{\mathrm{L}}^2$ term for β-values that are not exceedingly small and for ω_{r} not much greater than unity, we may ignore the $O(1)$ term in (1.1) for the purpose of higher-order calculations. This amounts to treating the liquid as incompressible and the bubbles as the sole source of compressibility of the mixture. As a consequence, the subsequent corrections to (1.1) have a much different dependence on β than what would have been obtained had the bubbles been viewed as making only $O(\beta)$ changes in the effective properties of the mixture over those of the pure liquid.

1.1. *A summary of important results*

For the benefit of a reader who is not interested in the details of the mathematical analysis, and in view of the length of the article, we summarize here some of the important findings.

In §2, we present the governing equations for inviscid and adiabatic changes due to a pressure wave propagating through a mixture of liquid and gas bubbles. The ensemble-averaged equations of continuity and momentum conservation are derived and it is shown that the effective speed in the mixture can be evaluated in terms of four coefficients λ_p, λ_v, $\lambda_{\sigma c}$, and $\lambda_{\sigma m}$. Of these, the first two are the most important ones in determining the speed. The coefficient λ_p may be interpreted as the ratio of the amplitude of the pressure variation in the gas phase to that in the mixture, and the coefficient λ_v as the ratio of the amplitudes of the gas and mixture velocities.

In §3.1, we determine the above four coefficients to $O(1)$ by examining the interaction of a single bubble with the pressure wave and thereby recover Foldy's approximation (1.1) with a few minor modifications accounting for the finite surface tension and the finite compressibility of the liquid. Although these modifications *per*

se are not of great practical significance, the derivation has some methodological interest and the details of the calculations aid later calculations in incorporating the effects of finite wavelength. The finite compressibility of the liquid renders C_{ef} a complex quantity indicating an attenuation of sound waves even in the absence of viscous and non-adiabatic thermal effects due to what is known as the acoustic radiation damping: the energy of sound waves is stored in part as elastic energy in the liquid and then converted back into the kinetic energy resulting in a phase difference between the pressure fluctuations in the gas phase and the mixture. (This makes λ_p and, hence, C_{ef} a complex quantity.)

In §3.2, we determine the corrections to (1.1) that are of $O(\beta^2)$ or larger. The analysis is restricted to the values of β that are small compared to unity but large compared to $\gamma P_e/\rho_L C_L^2$. In this limit, the liquid may be regarded as incompressible and the estimates of λ_p correct to $O(\beta)$ and λ_v and $\lambda_{\sigma m}$ to $O(1)$ are needed. Thus, this section is concerned mainly with the determination of λ_p correct to $O(\beta)$ by accounting for the pairwise interactions among bubbles. A straightforward method of doing this by determining the change in the pressure amplitude inside a given bubble due to the presence of a second bubble at a distance S from it, multiplying this change by the probability of finding the second bubble at that distance, and integrating over the all possible S cannot be applied to determine this $O(\beta)$ correction as the second bubble modifies the pressure in the given bubble by an $O(R/S)$ amount when S is large, making the resulting integral diverge. The use of ensemble-averaged equations as suggested by Hinch (1977) avoids such convergence difficulties. Using this rigorous method, we show that the calculation of λ_p correct to $O(\beta)$ can be decomposed essentially into two parts. The first part consists of determining the pressure inside a single bubble placed in an effective medium whose compressibility is determined by the amount of bubbles in the mixture, and the second part consists of determining the effect of the presence of a second bubble. It is shown that the first part already accounts for the first two reflections, i.e. the terms of $O(R/S)$ and $O((R/S)^2)$ in the two-bubble interactions, and thereby the remainder is now integrable (see further discussion on this in the next paragraph). The leading correction to λ_p, which results from the first part, is shown to be $O(\beta^{\frac{1}{2}})$ and this contributes mostly to the acoustic radiation damping. The magnitude of this damping is shown to be proportional to $\omega R/C_{ef}$ compared with the magnitude $\omega R/C_L$ reported in earlier studies. Since C_{ef} can be an order of magnitude or more smaller than C_L, this finding is quite significant and, in fact, responsible for predicting the attenuation values for sound waves near the resonance frequency of bubbles that are in a very good agreement with the experimental data available in the literature.

As mentioned above, the second part of the calculation requires integrating the pairwise interaction effect with the first two reflections omitted. The effective wavelength in the mixture is large, of $O(R\beta^{-\frac{1}{2}})$. If we take this wavelength to be infinite, then the pressure felt by the two bubbles is exactly the same and consequently the third reflection in the two bubbles interacting in an incompressible liquid behaves as $(R/S)^3$ for large S, making the resulting integral diverge logarithmically. The fact that the wavelength is finite, however, makes the pressures in the two bubbles slightly different from each other and accounting for this fact results in an $O(\beta \ln \beta)$ correction to λ_p.

To evaluate the $O(\beta)$ correction to λ_p, we need to integrate the two-bubble interaction effect with the first three reflections omitted. This effect decays as $(R/S)^4$ for large S and the effective wavelength may be taken to be infinite in evaluating it. The details of the two-bubble interactions are given in Appendix A. A pair of bubbles

resonates in two different modes. The first mode corresponds to the two bubbles resonating in phase with each other and the second corresponds to the two bubbles resonating 180° out of phase with each other. The frequencies at which they resonate depend on the separation distance between the bubbles. For example, when the non-dimensional surface tension $\sigma^* \equiv \sigma/(\rho_L R^3 \omega^2)$ is large, two widely separated bubbles resonate at the frequency ω_c corresponding to the resonance of isolated bubbles and two bubbles in close contact resonate at about $0.83\omega_c$ in the in-phase mode and at an infinite frequency in the out-of-phase mode. In other words, when the surface tension is large and when $0.828\omega_c \leqslant \omega < \infty$, there is always a pair of bubbles in the mixture that is resonating either in the in-phase mode or in the out-of-phase mode. This suggests that the resonance effects in pairs of bubbles may play a very significant role in the acoustic properties of bubbly liquids for a fairly wide range of frequencies. In Appendix A, we show that the magnitudes by which the in-phase and the out-of-phase modes are excited are proportional, respectively, to the mean and the difference of the pressures felt by the two bubbles. Now the latter, being inversely proportional to the effective wavelength of the mixture, is a small, $O(\beta^{\frac{1}{2}})$, quantity compared to the former and hence in determining the leading-order pairwise interaction effect, i.e. in calculating the $O(\beta)$ correction to λ_p, only the in-phase mode resonance is important. The out-of-phase mode is important in the next, $O(\beta^{\frac{3}{2}})$, correction to λ_p, but we have not pursued its evaluation in the present study. Likewise, the three-bubble interaction will exhibit even more complex resonance behaviour in the $O(\beta^2)$ and higher-order corrections to λ_p.

The constant 0.83 in the above discussion corresponds to the resonance frequency of two nearly touching bubbles undergoing in-phase radial mode resonance when the surface tension is large. Here, by radial we mean the volume oscillations that result from temporal variations in the pressure around the bubbles. This constant decreases as the surface tension is lowered and, in fact, becomes zero for $\sigma^* = \frac{1}{12}$. At this value of σ^*, the P_2 component of the shape of the second bubble is strongly affected and this, in turn, causes the radial oscillations of the first bubble to become very large even at zero frequency. Here, P_2 is the second Legendre polynomial. Similarly, the other components of the shape deformation also cause the radial resonances at zero frequency. It may be noted that these effects of finite surface tension and shape-dependent resonances occur in the $O(\beta)$ correction to λ_p and not in the $O(1)$ estimate that gives the Foldy's approximation (1.1). This is because the radial oscillations in a bubble are affected by the surface tension only when there is a second bubble in its vicinity which is undergoing large shape deformations.

Although these resonance effects of pairs of bubbles are interesting, our detailed calculations of the $O(\beta)$ coefficient of λ_p suggests a rather weak influence. This can be explained as follows. Let us consider the case of large surface tension and let ω be greater than $0.83\omega_c$. Then there exists a critical separation distance, say S_c, for pairs of bubbles to undergo a resonance at this frequency. The bubbles with a separation distance less than S_c are already past their resonance frequency and so the pressure in such bubbles is 180° out of phase with the mixture pressure. (Note that λ_p, which is a ratio of the pressure amplitude inside the gas phase to that in the mixture, to the leading order is given by $1/(1-\omega_r^2)$ and this implies that the pressure inside the bubbles is negative or out of phase with respect to the pressure in the mixture when the frequency is larger than the resonance frequency.) On the other hand, the bubbles with separation distance greater than S_c have resonance frequencies larger than ω and so the pressure inside them is positive or in phase with the pressure in the mixture. In determining the $O(\beta)$ correction to λ_p, we must integrate the pressure

inside the gas phase for all possible separation distances and our calculations then show that the effect of large positive pressures for S slightly greater than S_c is cancelled by the large negative pressures for S less than S_c, resulting in a finite contribution to λ_p for most frequencies. Only when ω equals $0.83\omega_c$, corresponding to pairs of bubbles in contact with each other resonating, is there a divergence in λ_p and this divergence is shown to be logarithmic only and thus weak. This calculation is carried out in the limit of vanishingly small damping due to viscous and thermal effects. It is shown that, while the real part of λ_p remains finite for $\omega > 0.83\omega_c$ due to the cancellation effects of resonances, the imaginary part becomes relatively large indicating a large attenuation due to the resonance of pairs of bubbles in the limit of vanishingly small viscous or thermal damping.

In §3.3, we examine the acoustic behaviour for frequencies small compared to ω_c. In this case the temporal variations in the pressure are occurring so slowly that the pressure inside the gas phase is essentially the same as the pressure in the mixture and λ_p is approximately unity for all values of β. The calculations of §3.2 for λ_p correct to $O(\beta)$ indicate that taking λ_p to unity is likely to result in an error in effective speed of less than a few percent whenever $\omega_r \equiv \omega/\omega_c$ is less than 0.3. In this case it turns out that C_{ef}^{-2} can be determined to $O(\beta^3)$ by determining λ_v correct only to $O(\beta)$. Thus, §3.3 is primarily concerned with the determination of λ_v correct to $O(\beta)$ in the limit of small ω_r. To the leading order, i.e. to $O(1)$, λ_v, which can be interpreted as the ratio of the velocity in the massless bubble to the mixture velocity, equals 3 and is independent of the surface tension. The $O(\beta)$ correction, which is to be evaluated from pairwise interactions, is, however, dependent on σ^*. The calculation of λ_v is closely related to that for determining the added mass coefficient for bubbles in an inviscid liquid. The $O(\beta)$ correction to the added mass coefficient for the case of $\sigma^* = \infty$ corresponding to spherical bubbles has been determined by van Wijngaarden (1972). We confirm his result and determine the $O(\beta)$ correction for the entire range of σ^*. In particular, we find once again resonance effects among pairs of bubbles for σ^* less than 0.11. These effects arise from the excitation of the shape deformation resonance of the second bubble due to the uneven pressure distribution created by the presence of the first bubble and which, in turn, giving rise to the resonance in the velocity or the displacement of the first bubble. It is shown that in the limit of $\sigma^* \to 0$, the $O(\beta)$ coefficient of λ_v goes through a countably infinite number of discontinuities. The divergence at each of these discontinuities is shown to be only logarithmic and thus rather weak.

A comparison between the predicted values of C_{ef} and the experimental data of Micaelli (1982) is made at the end of §3.3. This comparison is limited to small ω_r where the determination of λ_v is the most significant. An excellent agreement between the theory and experiments is found for β-values of about 0.2, up to which the experimental data are available. A comparison with the experimental data at large frequencies is made in §5 and this is discussed later.

Since the consideration of pairwise interactions under small-amplitude conditions resulted in the resonance behaviour for a fairly wide range of frequency and surface tension, it is important to assess how much these resonances will be damped by the viscous and non-adiabatic effects that are usually present. The damping due to these effects is also significant under most experimental conditions and thus they must be analysed before a comparison between the theory and experimental data on attenuation can be made. Thus §§4 and 5 are devoted to these effects and a comparison with the experimental data on attenuation by Silberman (1957) is made at the end of §5.

In §4, we examine in detail the effects of small viscosity on the coefficients λ_p and λ_v and on the ensemble-averaged momentum equation. The non-dimensional viscosity $\mu^* \equiv \mu/(\rho_L \omega R^2)$ is usually small in most practical applications and so the analysis is confined to this case. Thus the effect of viscosity is essentially confined to a thin Stokes layer near the surface of each bubble. A method is developed to account for this effect for pairwise bubble interactions. We have examined only the case of gas–liquid systems which are relatively free of the surface-active impurities. For such systems the appropriate boundary condition at the surface of the bubbles is a continuity of tangential stress. In a separate study, Sangani, Zhang & Prosperetti (1991) have examined the case of relatively small bubbles in the presence of surface-active impurities for which the appropriate boundary condition at the surface of the bubbles is the no-slip condition.

Section 5.1 deals with the study of non-adiabatic effects. As a result of pressure variations, there are temperature variations in the system and thus there is an exchange of energy between the gas and the liquid phase. The surface area of the bubbles is slightly greater when the bubbles expand and thus there is a greater exchange of energy when the bubbles expand than when they contract and consequently there is a net exchange of energy between the two phases during one cycle giving rise thereby to the attenuation of waves. The thermal diffusivity of the liquid is usually much larger than that of the gas and so the thermal effects are important only inside the bubble. Moreover, only the spherically symmetric part of the pressure and velocity inside the bubble is affected by the presence of the bubbles. This makes it relatively easy to include the thermal effects in the pairwise interactions calculations.

It may be noted that since the thermal effect is closely dependent on the volume oscillations, it becomes relatively less important at small frequencies. The acoustic radiation damping which is inversely proportional to the effective wavelength of the sound waves in the mixture is also small at small frequencies. Thus the viscous damping is the only effective mechanism at small frequencies and the resonance effects in λ_v for small frequencies described in §3.3 can only be damped by the viscous effects. The detailed calculations in §4 with some representative values of μ^*, however, suggest that the displacement resonances are only slightly damped by viscosity. Thus the presence of these resonances could give rise to a relatively large scatter in the measurement of the effective speed at small frequencies if σ^* is less than about 0.15.

Section 5.2 is concerned with the comparison between the theory and experimental data on the attenuation of sound waves for frequencies comparable with the resonance frequency of isolated bubbles. First, a summary of the various expressions derived in the present study including the viscous and thermal effects is given. The relative magnitudes of these effects for an air–water system with bubbles of diameter 5 mm are given. The $O(\beta \ln \beta)$ and $O(\beta)$ corrections to λ_p determined in the present study turned out to be of large magnitude for ω_r comparable to unity and so the expressions for C_{ef} are recast in a different form in order to yield finite estimates of C_{ef} and attenuation for the complete range of ω_r.

Most of our discussion so far applies to the case when ω_r is less than unity. As the Foldy's approximation (1.1) suggests, the effective speed is not a real quantity even in the absence of thermal, viscous, and acoustic radiation effects when $\omega_r > 1$. This is because the pressure variations in the bubbles become out-of-phase with the variations in the mixture at frequencies larger than the natural frequency of the bubbles. Thus, the bubbles behave as though they have a negative compressibility.

The compressibility of the liquid being negligible, this implies a negative compressibility of the medium and, consequently, the intensity of sound waves decays exponentially in the medium. Of course, at sufficiently large ω_r, given approximately by $\omega_r^2 \approx \beta\rho_L C_L^2/(\gamma P_e)$, the compressibility of the liquid becomes important and the attenuation of sound waves in the absence of other damping mechanisms then becomes vanishingly small and the speed of sound approaches that of pure liquid.

The expressions for the attenuation derived in the present study are compared with the data from Silberman as they are believed to be the most reliable in terms of the uniformity of the size of bubbles. There is an excellent agreement between the theory and experiments for frequencies close to and smaller than the resonance frequency of the bubbles. Under these experimental conditions, it turned out that the thermal damping was of sufficiently large magnitude to suppress the resonance effects of pairs of bubbles that are discussed in §3.2. The new magnitude of the acoustic radiation damping found in the present theory seems to be the most important factor in achieving the good agreement between the theory and an experimental value for ω_r of about 0.9.

The theory, however, does not seem to give good agreement with the experimental data at larger frequencies and the reason for this is not fully understood at present. A discrepancy by as much as a factor of 2 remains for larger frequencies. Whether this discrepancy is as a result of some attenuation mechanism that is overlooked, or because of large scatter in experiments that is possible at such large frequencies and because of the pair resonance effects, or simply the effect of multi-bubble interactions that is not accounted for adequately by the dilute theory examined here remains to be further investigated. As mentioned earlier, we expect the out-of-phase-mode resonance effects to become important whenever ω_r is greater than unity. These effects appear in the $O(\beta^{\frac{3}{2}})$ correction to λ_p which we have not evaluated, but it is quite plausible that these effects are important for $\beta = 0.01$. It is also possible that such resonance effects may produce a larger scatter in the experimental data making them unreliable. We are currently calculating the effective speed and attenuation by direct numerical simulation of the multi-bubble interaction effects without making any assumption about the smallness of β. The results of these calculations will provide the answers to some of these questions.

2. The governing equations and the ensemble averages

2.1. *The governing equations*

Let us consider sound waves propagating through a liquid in which bubbles of equal size are homogeneously dispersed. The viscosities of the liquid and gas are small and the intensity of sound waves is sufficiently small so that the nonlinear terms in the equations of motion can be linearized. The equations of mass and momentum conservation in both the liquid and gas phases then simplify to

$$\frac{1}{\rho}\frac{\partial \rho}{\partial t} + \nabla \cdot \boldsymbol{u} = 0, \tag{2.1}$$

$$\rho \frac{\partial \boldsymbol{u}}{\partial t} + \nabla p = 0, \tag{2.2}$$

where ρ is the density, t is the time, $\boldsymbol{u}$ is the velocity, and p is the pressure. The density derivative in (2.1) can be expressed in the usual manner in terms of the

pressure derivative by the introduction of a compressibility factor $\partial\rho/\partial p$ evaluated at a constant entropy s for reversible adiabatic changes, which we shall assume is the case. The effects of viscosity and non-adiabatic changes will be examined separately in §§4 and 5. Thus (2.1) can be expressed as

$$\frac{1}{\rho}\left(\frac{\partial\rho}{\partial p}\right)_s \frac{\partial p}{\partial t} + \nabla\cdot\boldsymbol{u} = 0. \tag{2.3}$$

The compressibility factors for the pure liquid and the gas, assumed to be ideal, are well known and can be expressed by means of a single expression

$$\frac{1}{\rho}\left(\frac{\partial\rho}{\partial p}\right)_s = \frac{1}{\rho_{\mathrm{L}} C_{\mathrm{L}}^2} + \left(\frac{1}{\gamma P_{\mathrm{e}}} - \frac{1}{\rho_{\mathrm{L}} C_{\mathrm{L}}^2}\right) g(\boldsymbol{x}, t), \tag{2.4}$$

where $g(\boldsymbol{x}, t)$ is a generalized function of the position coordinate and time whose value is unity for $\boldsymbol{x}$ inside the gas bubbles and zero for $\boldsymbol{x}$ in the liquid. Similarly the density in the momentum equation (2.2) can be expressed as

$$\rho = \rho_{\mathrm{L}} + (\rho_{\mathrm{G}} - \rho_{\mathrm{L}})\, g(\boldsymbol{x}, t), \tag{2.5}$$

where ρ_{G} is the density of the gas. For most gas–liquid systems, ρ_{G} is small and, therefore, we shall take it to be zero.

The boundary conditions are the usual kinematic and stress conditions at the surface of the bubbles. The normal component of the velocity is continuous across the interface and is related to the deformation of the bubbles by the kinematic condition

$$\frac{\partial\eta}{\partial t} = \boldsymbol{n}\cdot\boldsymbol{u}, \tag{2.6}$$

where $\boldsymbol{n}$ is the unit normal at the interface and η is the deformation of the bubble from its equilibrium size. In other words, the surface of a representative bubble, with its centre taken as the origin, is assumed to be given by $r = R + \eta$. The stress boundary condition is

$$p_{\mathrm{G}} - p_{\mathrm{L}} = \sigma\nabla\cdot\boldsymbol{n}, \tag{2.7}$$

where p_{G} and p_{L} are the pressures on the two sides of the gas–liquid interface and σ is the surface tension, which we shall assume to be uniform over the entire surface of the bubble. Since the intensity of the sound is small, we are interested in $|\eta| \ll R$, so that we may write

$$\nabla\cdot\boldsymbol{n} = \left[\frac{2}{R} - \frac{1}{R^2}(2\eta + \nabla_{\mathrm{s}}^2\eta)\right] + O(\eta^2), \tag{2.8}$$

where ∇_{s}^2 denotes the surface Laplacian operator. For the purpose of the calculations later we find it convenient to decompose η in the Legendre polynomials P_n^m as

$$\eta = \sum_{n=0}^{\infty} \sum_{m=-n}^{n} \eta_{nm} P_n^m(\cos\theta)\, \mathrm{e}^{\mathrm{i}m\phi}, \tag{2.9}$$

where θ and ϕ are the spherical polar angles measured with respect to the centre of the bubble. Since $\rho_{\mathrm{G}} = 0$, it can be seen from (2.2) that the pressure inside the gas bubbles is uniform. Therefore, using the adiabatic law, $pV^\gamma = \text{const.}$, we find that η_{00} is related to p_{G} by

$$p_{\mathrm{G}} - P_{\mathrm{e}} = -\frac{3\gamma\eta_{00}}{R} P_{\mathrm{e}}. \tag{2.10}$$

Using the well-known identity

$$\nabla_s^2[P_n^m(\cos\theta)\,e^{im\phi}] = -n(n+1)P_n^m(\cos\theta)\,e^{im\phi}, \tag{2.11}$$

we can express the dynamic condition as

$$p_{nm}(R) = \left[-3\gamma P_e R^{-1}\delta_{n0}\delta_{m0} + \frac{\sigma}{R^2}(2-n(n+1))\right]\eta_{nm}, \tag{2.12}$$

where $p_{nm}(r)$ are the coefficients of the Legendre polynomials in the expansion of $p_L - P$ around the centre of the bubble and P is the equilibrium pressure in the liquid given by $P = P_e - 2\sigma/R$.

Since the governing equations are linear, it is convenient to analyse the acoustic behaviour for various frequency components separately. Thus we may assume that the velocity, pressure, and deformation are all proportional to $e^{i\omega t}$. The dynamic and kinematic conditions at the undeformed surface of the bubbles may then be combined into a single equation for the Legendre components of the pressure on the liquid side of the interface by introducing a velocity potential φ, with $\boldsymbol{u} = \nabla\varphi$ and $p = -i\omega\rho_L\varphi$, and eliminating η_{nm} from (2.6)–(2.8) and (2.12):

$$p_{nm} = \sigma^*[2-n(n+1)]Rp'_{nm} \quad \text{for} \quad n>0 \quad \text{and} \quad \omega_r^2 p_{00} + Rp'_{00} = 0, \tag{2.13}$$

where $\sigma^* = \sigma/\rho_L R^3\omega^2$ is the non-dimensional surface tension, the prime indicates the radial derivative of pressure components evaluated at the undeformed bubble surface on the liquid side, and ω_r is the ratio of ω and the natural frequency ω_c of the bubbles defined by

$$\omega_c^2 = \frac{3\gamma^* P_e}{\rho_L R^2} \quad \text{with} \quad \gamma^* = \gamma - \frac{2\sigma}{3RP_e}. \tag{2.14}$$

Note that we have modified slightly the original definition of the natural frequency (cf. (1.2)) to account for the finite surface tension. The quantity $2\sigma/(RP_e) \equiv 2/We$, where We is the Weber number, is always less than 1 so that $\gamma > \gamma^* \geqslant \gamma - \frac{1}{3}$. If we take $\sigma = 70$ dynes/cm, a typical value for pure water, and assume P_e to equal the atmospheric pressure, then γ^* differs from γ by less than 5% whenever R is greater than 10^{-3} cm. It should also be noted that the non-dimensional surface tension σ^*, which is a function of frequency, may also be expressed in terms of the Weber number as $\sigma^* = 1/(3We\gamma^*\omega_r^2)$. Since We is large in many practical situations, we shall treat σ^* as an $O(1)$ quantity even when ω_r is small.

This completes the description of the governing equations.

2.2. *The ensemble-averaged equations*

We now proceed to derive the ensemble-averaged equations for the velocity and pressure fields. We shall denote the unconditionally averaged pressure and velocity fields by p_0 and $\boldsymbol{u}_0$, and conditionally averaged fields with the centre of a bubble fixed at $\boldsymbol{x}_1$ by p_1 and $\boldsymbol{u}_1$, etc. The ensemble average of a product of two quantities or more will be denoted by enclosing it in a curly bracket. We note that, with the introduction of the generalized function g, (2.1) and (2.2), together with (2.4) and (2.5), are valid at all points in the medium except at the interface, where we must supplement these equations with the kinematic and stress conditions before taking the ensemble averages. Alternatively, the ensemble-averaged equations for the mixture can also be obtained by first writing the ensemble-averaged equations for the individual phases and then combining them. The latter procedure is easy to implement and can also be employed in a relatively straightforward manner to derive the averaged equations

when the deformations are not small. Thus, for example, multiplying (2.3) with g, using (2.4) to evaluate the density derivative in the gas phase, and then taking the unconditional ensemble average yields

$$\frac{1}{\gamma P_e}\left\{g\frac{\partial p_G}{\partial t}\right\}_0 + \{g\nabla\cdot\boldsymbol{u}_G\}_0 = 0. \tag{2.15}$$

A similar equation can be obtained for the liquid phase by multiplying (2.3) with $1-g$, and adding the two equations then yields

$$\frac{1}{\rho_L C_L^2}\left\{(1-g)\frac{\partial p_L}{\partial t}\right\}_0 + \frac{1}{\gamma P_e}\left\{g\frac{\partial p_G}{\partial t}\right\}_0 + \{(1-g)\nabla\cdot\boldsymbol{u}_L\}_0 + \{g\nabla\cdot\boldsymbol{u}_G\}_0 = 0. \tag{2.16}$$

The ensemble-averaged pressure is given by

$$p_0 = \{gp_G + (1-g)p_L\}_0, \tag{2.17}$$

and a similar equation applies to $\boldsymbol{u}_0$. In terms of these two average quantities, (2.16) can be expressed as

$$\frac{1}{\rho_L C_L^2}\left[\frac{\partial p_0}{\partial t} + \left\{\frac{\partial g}{\partial t}(p_L - p_G)\right\}_0\right] + \left(\frac{1}{\gamma P_e} - \frac{1}{\rho_L C_L^2}\right)\left\{g\frac{\partial p_G}{\partial t}\right\}_0 + \nabla\cdot\boldsymbol{u}_0 + \{(\boldsymbol{u}_L - \boldsymbol{u}_G)\cdot\nabla g\}_0 = 0. \tag{2.18}$$

Similarly, the ensemble average of the momentum equation (2.2) with $\rho_G = 0$ yields

$$\rho_L\left[\frac{\partial \boldsymbol{u}_0}{\partial t} - \left\{g\frac{\partial \boldsymbol{u}_G}{\partial t}\right\}_0 + \left\{(\boldsymbol{u}_L - \boldsymbol{u}_G)\frac{\partial g}{\partial t}\right\}_0\right] + \nabla p_0 + \{(p_L - p_G)\nabla g\}_0 = 0. \tag{2.19}$$

Now ∇g may be evaluated from

$$\nabla g = -\boldsymbol{n}\delta(\boldsymbol{x} - \boldsymbol{x}_i(t)), \tag{2.20}$$

$\boldsymbol{x}_i(t)$ being points on the interface, and $\partial g/\partial t$ from

$$\frac{\partial g}{\partial t} = -\boldsymbol{u}\cdot\nabla g = \boldsymbol{n}\cdot\boldsymbol{u}\delta(\boldsymbol{x} - \boldsymbol{x}_i(t)), \tag{2.21}$$

which is valid in the absence of any mass transfer or phase change at the interface. Since $\boldsymbol{u}_G\cdot\boldsymbol{n} = \boldsymbol{u}_L\cdot\boldsymbol{n}$ at the interface, it can be easily shown, on using (2.20) and (2.21), that the terms involving $\boldsymbol{u}_L - \boldsymbol{u}_G$ in (2.18) and (2.19) vanish. The remaining terms depend on the details of the spatial configuration of the bubbles and we shall evaluate them for the case of small deformations and small volume fraction β of the gas bubbles. To evaluate these terms, we first solve for the conditionally averaged pressure and velocity fields with one bubble fixed for small β and then use relations such as

$$\left\{g\frac{\partial p_G}{\partial t}\right\}_0(\boldsymbol{x}) = \int_{\boldsymbol{x}\in V_1} P(\boldsymbol{x}_1)\frac{\partial p_1}{\partial t}(\boldsymbol{x}\,|\,\boldsymbol{x}_1)\,\mathrm{d}V_1, \tag{2.22}$$

where $P(\boldsymbol{x}_1)$ is the probability density for finding a bubble at $\boldsymbol{x}_1$ occupying the region V_1 such that $\boldsymbol{x}$ lies inside the bubble. Since $P(\boldsymbol{x}_1)$ is proportional to β, the unconditionally averaged momentum and continuity equations (2.18) and (2.19) can be evaluated to $O(\beta)$ by determining the conditionally averaged pressure and velocity correct only to $O(1)$.

If we assume that the bubbles' spatial distribution is isotropic on a macroscale, then the integral in (2.22), being scalar, can depend only on scalar quantities such as

p_0, $\nabla^2 p_0$, $\nabla^4 p_0$, $\nabla\cdot\boldsymbol{u}_0$, and $\nabla^2(\nabla\cdot\boldsymbol{u}_0)$. However, since we anticipate that p_0 will satisfy a wave equation for the case of small deformations, $\nabla^2 p_0$, etc. are linearly related to p_0, and since $\nabla\cdot\boldsymbol{u}_0$, etc. are also expected to be linearly related to p_0 (cf. (2.27), (2.28)), we can write quite generally that

$$\left\{g\frac{\partial p_{\mathrm{G}}}{\partial t}\right\}_0(\boldsymbol{x}) = \beta\lambda_p\frac{\partial p_0}{\partial t}(\boldsymbol{x}), \tag{2.23}$$

where λ_p is a function of β and ω. Using similar arguments we write

$$\left\{g\frac{\partial \boldsymbol{u}_{\mathrm{G}}}{\partial t}\right\}_0(\boldsymbol{x}) = \beta\lambda_v\frac{\partial \boldsymbol{u}_0}{\partial t}(\boldsymbol{x}), \tag{2.24}$$

$$\left\{(p_{\mathrm{L}}-p_{\mathrm{G}})\frac{\partial g}{\partial t}\right\}_0(\boldsymbol{x}) = \beta\lambda_{\sigma c}\frac{\partial p_0}{\partial t}(\boldsymbol{x}), \tag{2.25}$$

$$\{(p_{\mathrm{L}}-p_{\mathrm{G}})\nabla g\}_0(\boldsymbol{x}) = \beta\lambda_{\sigma m}\nabla p_0(\boldsymbol{x}), \tag{2.26}$$

where λ_v, $\lambda_{\sigma c}$, and $\lambda_{\sigma m}$ are other constants that also depend on β and ω.

Substitution of (2.23)–(2.26) into (2.18) and (2.19) then yields

$$\left[\frac{1}{\rho_{\mathrm{L}}C_{\mathrm{L}}^2}\{1+\beta(\lambda_{\sigma c}-\lambda_p)\}+\frac{\beta\lambda_p}{\gamma P_{\mathrm{e}}}\right]\frac{\partial p_0}{\partial t}+\nabla\cdot\boldsymbol{u}_0 = 0, \tag{2.27}$$

$$\rho_{\mathrm{L}}(1-\beta\lambda_v)\frac{\partial \boldsymbol{u}_0}{\partial t}+(1+\beta\lambda_{\sigma m})\nabla p_0 = 0, \tag{2.28}$$

from which it is easy to show that both p_0 and $\boldsymbol{u}_0$ satisfy the wave equation and that the speed of sound in the mixture is given by

$$\frac{1}{C_{\mathrm{ef}}^2} = \frac{1-\beta\lambda_v}{1+\beta\lambda_{\sigma m}}\left[\frac{1}{C_{\mathrm{L}}^2}\{1+\beta(\lambda_{\sigma c}-\lambda_p)\}+\frac{\beta\rho_{\mathrm{L}}\lambda_p}{\gamma P_{\mathrm{e}}}\right]. \tag{2.29}$$

Thus we see that to determine the speed of sound correct to $O(\beta)$, we must estimate the coefficients λ_p, λ_v, $\lambda_{\sigma c}$, and $\lambda_{\sigma m}$ correct to $O(1)$. It may be noted that since p_0, $\boldsymbol{u}_0$, and their derivatives are all linearly related to each other, there is a slight arbitrariness involved in defining these coefficients via (2.23)–(2.26). Since the resulting averaged continuity and momentum equations (2.27) and (2.28) are homogeneous, we can determine the average pressure and velocity only to within a multiplicative constant by solving these equations. The dispersion relation, i.e. the relation between C_{ef} and ω, on the other hand is unique and does not depend on what definitions we employ to evaluate various average quantities appearing in (2.23)–(2.26).

It may be noted that the spatial distribution of the bubbles in many practical situations such as the bubbles rising under the influence of buoyancy forces is likely to be anisotropic and for such cases the speed of sound will depend on the direction of its propagation. Relations such as (2.23)–(2.26) are not valid in such situations and perhaps it is most convenient to first evaluate quantities such as $\{g\,\partial p_{\mathrm{G}}/\partial t\}_0$ by taking $p_0(\boldsymbol{x}) = P+\hat{p}_{\mathrm{a}}\exp(\mathrm{i}\omega t-\mathrm{i}\boldsymbol{k}\cdot\boldsymbol{x})$ and $\boldsymbol{u}_0 = \hat{\boldsymbol{u}}_{\mathrm{a}}\exp(\mathrm{i}\omega t-\mathrm{i}\boldsymbol{k}\cdot\boldsymbol{x})$ and determining the effective wavenumber $\boldsymbol{k}$ and hence $C_{\mathrm{ef}}(\boldsymbol{k}/k)$ from the averaged continuity and momentum equations (2.18) and (2.19). This procedure is illustrated in Appendix B where we have briefly examined the effect of buoyancy. In the main text of the paper, however, we shall continue to use the coefficients λ_p, etc. as it is convenient to refer to various averaged quantities such as $\{g\,\partial p_{\mathrm{G}}/\partial t\}_0$ in terms of suitable coefficients.

3. Estimates of the coefficients appearing in (2.29)

3.1. *Calculations of* λ_p, λ_v, $\lambda_{\sigma c}$, *and* $\lambda_{\sigma m}$ *to* $O(1)$

In this section we shall obtain the $O(1)$ estimates of the coefficients appearing in (2.29) and thereby determine $C_{\rm ef}^{-2}$ correct to $O(\beta)$. The analysis will recover Foldy's approximation (1.1) with a few minor modifications accounting for the effect of finite surface tension and compressibility of the liquid. As mentioned in the Introduction, although these modifications by themselves are not of much practical significance, the methodology will have some interest and the calculations will be needed in the subsequent sections when we determine the higher-order corrections to $C_{\rm ef}^{-2}$.

The conditional ensemble averages of (2.1) and (2.2) with the centre of a bubble fixed at $\boldsymbol{x}_1$ and for x outside the bubble are given by

$$\frac{1}{\rho_{\rm L} C_{\rm L}^2}\frac{\partial p_1}{\partial t}+\boldsymbol{\nabla}\cdot\boldsymbol{u}_1=\left[\frac{1}{\rho_{\rm L} C_{\rm L}^2}-\frac{1}{\gamma P_{\rm e}}\right]\left\{g\frac{\partial p_{\rm G}}{\partial t}\right\}_1-\frac{1}{\rho_{\rm L} C_{\rm L}^2}\left\{(p_{\rm L}-p_{\rm G})\frac{\partial g}{\partial t}\right\}_1, \tag{3.1}$$

$$\rho_{\rm L}\frac{\partial \boldsymbol{u}_1}{\partial t}+\boldsymbol{\nabla}p_1=\rho_{\rm L}\left\{g\frac{\partial \boldsymbol{u}_{\rm G}}{\partial t}\right\}_1-\{(p_{\rm L}-p_{\rm G})\,\boldsymbol{\nabla}g\}_1. \tag{3.2}$$

Now since the terms on the right-hand sides of the above equations are proportional to β, we can determine $\boldsymbol{u}_1$ and p_1 to $O(1)$ by simply setting the right-hand sides of these equations to zero and requiring that $\boldsymbol{u}_1$ and p_1 approach the corresponding unconditional fields to $O(1)$ as $|\boldsymbol{x}-\boldsymbol{x}_1|\to\infty$.

Assuming that $p_1\to p_0=P+\hat{p}_{\rm a}\,{\rm e}^{{\rm i}\omega t-{\rm i}\boldsymbol{k}\cdot\boldsymbol{x}}$ far away from the bubble with $|\hat{p}_{\rm a}|\ll {\rm P}$ and $k=\omega/C_{\rm ef}$ ($C_{\rm ef}=C_{\rm L}$ at the present level of approximation in small β), we determine the pressure and the velocity fields around the bubble. The solution of (3.1) and (3.2), with their right-hand sides set equal to zero, can be expressed in terms of multipoles as

$$p_1=P+\hat{p}_{\rm a}\,{\rm e}^{{\rm i}\omega t-{\rm i}\boldsymbol{k}\cdot\boldsymbol{x}_1}\left[{\rm e}^{-{\rm i}\boldsymbol{k}\cdot\boldsymbol{s}}+\sum_{n=0}^{\infty}\sum_{m=-n}^{n}A_{nm}\,{\rm Y}_n^m\left(\frac{\partial}{\partial s_1},\frac{\partial}{\partial s_2},\frac{\partial}{\partial s_3}\right)G(ks)\right] \tag{3.3}$$

and

$$-{\rm i}\omega\rho_{\rm L}\boldsymbol{u}_1=\boldsymbol{\nabla}p_1, \tag{3.4}$$

where $\boldsymbol{s}=\boldsymbol{x}-\boldsymbol{x}_1$ and G is the fundamental solution of the wave equation, i.e.

$$G(ks)=\frac{{\rm e}^{-{\rm i}ks}}{s}=-{\rm i}kh_0(ks), \tag{3.5}$$

corresponding to an outgoing spherically symmetric scattered wave from the centre of the bubble. Here $h_n\equiv h_n^{(2)}=j_n-{\rm i}y_n$ is the spherical Bessel function of the third kind (Abramowitz & Stegun 1972), j_n and y_n are the spherical Bessel functions of the first and second kind, ${\rm Y}_n^m$ is an nth-order homogeneous differential operator defined by

$${\rm Y}_n^m(s_1,s_2,s_3)=s^n P_n^m(\cos\theta)\,{\rm e}^{{\rm i}m\phi}, \tag{3.6}$$

s, θ, and ϕ being the polar coordinates for the corresponding Cartesian coordinates s_1, s_2, s_3. In other words, the differential operator ${\rm Y}_n^m$ is obtained by first writing it as the nth degree homogeneous polynomial in s_1, s_2, and s_3 and then replacing these arguments by $\partial/\partial s_1$, $\partial/\partial s_2$, and $\partial/\partial s_3$, respectively. The constants A_{nm} are to be determined from the boundary conditions on the surface of the bubble. These constants will be referred to as the strengths of the multipoles, e.g. A_{00} as the strength of the monopole and A_{1m} as the components of the dipole strength. To determine them, we expand p_1 in Legendre polynomials as

$$p_1=P+\hat{p}_{\rm a}\,{\rm e}^{{\rm i}\omega t-{\rm i}\boldsymbol{k}\cdot\boldsymbol{x}_1}\sum_{n=0}^{\infty}\sum_{m=-n}^{n}[C_{nm}j_n(ks)+D_{nm}h_n(ks)]P_n^m\,{\rm e}^{{\rm i}m\phi}, \tag{3.7}$$

where the constants C_{nm} and D_{nm} are related to A_{nm}. Let us choose the s_1-axis to coincide with the direction of the wave vector $\boldsymbol{k}$ so that A_{nm}, C_{nm}, and D_{nm} are all non-zero only for $m = 0$, and, using the general theorems for the differentiation and the integration of the Legendre polynomials given by Hobson (1931), it can be shown that (see also Appendix A)

$$D_{n0} = \mathrm{i}(-k)^{n+1} A_{n0} \tag{3.8}$$

and

$$C_{n0} = (-\mathrm{i})^n (2n+1). \tag{3.9}$$

The boundary condition (2.13) now yields

$$\frac{A_{00}}{R} = -\frac{\mathrm{i}}{z}\frac{\omega_{\mathrm{r}}^2 j_0 + z j_0'}{\omega_{\mathrm{r}}^2 h_0 + z h_0'}, \quad z \equiv kR, \tag{3.10}$$

$$A_{n0} = \mathrm{i}^{n-1}(2n+1)\, k^{-n-1} \frac{j_n - \sigma^*[2-n(n+1)]\, z j_n'}{h_n - \sigma^*[2-n(n+1)]\, z h_n'}, \tag{3.11}$$

where j_n, h_n, and their derivatives are all evaluated at $z = kR$. Since kR is typically much smaller than unity, we need only the leading-order estimates of A_{n0}:

$$\frac{A_{00}}{R} = t_0 - \mathrm{i}z t_0^2 - \frac{z^2(1+2\omega_{\mathrm{r}}^6)}{3(1-\omega_{\mathrm{r}}^2)^3} + O(z^3), \quad t_0 \equiv \frac{\omega_{\mathrm{r}}^2}{1-\omega_{\mathrm{r}}^2}, \tag{3.12}$$

$$A_{10} = -\mathrm{i}kR^3 + O(k^2R^4), \tag{3.13}$$

$$A_{n0} = O(k^n R^{2n+1}), \quad n \geqslant 2. \tag{3.14}$$

It may be noted that the above estimates for the strengths of monopoles and dipoles for small kR can also be obtained in a simpler manner by using a perturbation method in which the wave equation for p_1 is approximated, to the leading order, by a Laplace equation. This approximation is, of course, not uniformly valid in space and for distances s comparable to k^{-1} the neglected term in the wave equation becomes important so that a singular perturbation technique is needed for developing consistent approximations (see Prosperetti & Lezzi 1986 for details of such calculations). However, the leading-order terms can be obtained simply by solving Laplace equation near the surface of the bubble and requiring that

$$p_1 \to P + \hat{p}_{\mathrm{a}}\, \mathrm{e}^{\mathrm{i}\omega t - \mathrm{i}\boldsymbol{k}\cdot\boldsymbol{x}_1}(1 - \mathrm{i}ks_1) \quad \text{as} \quad s \to \infty, \tag{3.15}$$

obtained by expanding the far-field behaviour of p_1 for small $\boldsymbol{k}\cdot\boldsymbol{s}$.

We now proceed to obtain the leading-order estimates of λ_p, λ_v, $\lambda_{\sigma c}$, and $\lambda_{\sigma m}$ as $\beta \to 0$. Since $\partial g/\partial t$ is $O(\hat{p}_{\mathrm{a}})$ (cf. (2.21), $\boldsymbol{u}$ being $O(\hat{p}_{\mathrm{a}})$), we can approximate $p_{\mathrm{L}} - p_{\mathrm{G}}$ in the linear theory by its equilibrium value $-2\sigma/R$ in calculating $\lambda_{\sigma c}$ from (2.25). Thus we obtain

$$\beta\lambda_{\sigma c}\frac{\partial p_0}{\partial t} = -\frac{2\sigma}{R}\frac{\partial g_0}{\partial t} = -\frac{2\sigma}{R}\int_{|\boldsymbol{x}-\boldsymbol{x}_1|=R} (\boldsymbol{n}\cdot\boldsymbol{u})(\boldsymbol{x}\,|\,\boldsymbol{x}_1)\, P(\boldsymbol{x}_1)\, \mathrm{d}S_1. \tag{3.16}$$

Note that to this leading-order approximation, the bubble surface may be taken to be the undeformed spherical surface and $P(\boldsymbol{x}_1)$ may be approximated by its equilibrium value. Assuming that the spatial distribution of the bubbles is homogeneous in the equilibrium state, $P(\boldsymbol{x}_1)$ equals β/V_{b}, $V_{\mathrm{b}} = 4\pi R^3/3$ being the volume of a bubble at equilibrium.

We shall encounter integrals similar to that in (3.16) in subsequent calculations and therefore it is useful to obtain a general formula for evaluating such integrals.

Integrands such as $(\boldsymbol{n}\cdot\boldsymbol{u})(\boldsymbol{x}\,|\,\boldsymbol{x}_1)$ can be generally expressed as $e^{i\omega t-i\boldsymbol{k}\cdot\boldsymbol{x}_1}$ times a function of $\boldsymbol{s}\equiv\boldsymbol{x}-\boldsymbol{x}_1$. Therefore, let us suppose that we wish to determine the surface integral of a function $f(\boldsymbol{x}\,|\,\boldsymbol{x}_1)$ given by

$$f(\boldsymbol{x}\,|\,\boldsymbol{x}_1)=e^{i\omega t-i\boldsymbol{k}\cdot\boldsymbol{x}_1}f^*(\boldsymbol{s})=e^{i\omega t-i\boldsymbol{k}\cdot\boldsymbol{x}_1}\sum_{n=0}^{\infty}\tilde{f}_n(s)\,P_n^0(\cos\theta), \tag{3.17}$$

where $\boldsymbol{k}$ is a vector with orientation along the s_1 axis. Then it can be easily shown that

$$\begin{aligned}\int_{s=R}f(\boldsymbol{x}\,|\,\boldsymbol{x}_1)\,dS_1&=e^{i\omega t-i\boldsymbol{k}\cdot\boldsymbol{x}}\,2\pi R^2\sum_{n=0}^{\infty}\tilde{f}_n\int_{-1}^{1}e^{ikRy}\,P_n^0(y)\,dy\\&=e^{i\omega t-i\boldsymbol{k}\cdot\boldsymbol{x}}\,4\pi R^2[\tilde{f}_0+\tfrac{1}{3}iz\tilde{f}_1+(iz)^2\,(\tfrac{1}{6}\tilde{f}_0+\tfrac{1}{15}\tilde{f}_2)+\ldots],\end{aligned} \tag{3.18}$$

where $\tilde{f}_n$ are evaluated at $s=R$. Similarly the volume integral can be evaluated from

$$\begin{aligned}\int_{s\leqslant R}f(\boldsymbol{x}\,|\,\boldsymbol{x}_1)\,dV_1=e^{i\omega t-i\boldsymbol{k}\cdot\boldsymbol{x}}\,4\pi\int_0^R s^2\,ds[\tilde{f}_0(s)\\+\tfrac{1}{3}iks\tilde{f}_1(s)+(iks)^2\,(\tfrac{1}{6}\tilde{f}_0(s)+\tfrac{1}{15}\tilde{f}_2(s))+\ldots].\end{aligned} \tag{3.19}$$

Now we evaluate the integral in (3.16) by making use of (3.18), (2.6), and (2.9) to obtain

$$\int_{|\boldsymbol{x}-\boldsymbol{x}_1|=R}(\boldsymbol{n}\cdot\boldsymbol{u})(\boldsymbol{x}\,|\,\boldsymbol{x}_1)\,P(\boldsymbol{x}_1)\,dS_1=i\omega\,e^{i\omega t-i\boldsymbol{k}\cdot\boldsymbol{x}}\frac{3\beta}{R}[\tilde{\eta}_{00}+O(z\tilde{\eta}_{10})]. \tag{3.20}$$

Noting now that $\partial p_0/\partial t=i\omega\hat{p}_a\,e^{i\omega t-i\boldsymbol{k}\cdot\boldsymbol{x}}$, and combining (3.16) and (3.20) we obtain

$$\hat{p}_a\frac{\partial g_0}{\partial t}=\beta\frac{\partial p_0}{\partial t}\frac{3}{R}[\tilde{\eta}_{00}+O(z\tilde{\eta}_{10})], \tag{3.21}$$

so that on substituting for $\tilde{\eta}_{00}$ from (2.12), (2.14), (3.7)–(3.12) and combining with (3.16) we obtain

$$\lambda_{\sigma c}=\frac{6\sigma^*\omega_r^2}{1-\omega_r^2(1-iz)}+O(z^2), \tag{3.22}$$

where we have made use of the fact that $\tilde{\eta}_{10}=O(z)$.

Similarly, to calculate $\lambda_{\sigma m}$ we write

$$\{(p_L-p_G)\nabla g\}_0=-\frac{2\sigma}{R}\nabla g_0-\int_{s=R}(\boldsymbol{n}(p_L-p_G)^a)\,(\boldsymbol{x}\,|\,\boldsymbol{x}_1)\,P(\boldsymbol{x}_1)\,dS_1, \tag{3.23}$$

where $(p_L-p_G)^a$ is the jump in the pressure at the surface of the bubble due to $O(\hat{p}_a)$ terms. Now the direct evaluation of the first term on the right-hand side of the above equation from the expression

$$\nabla g_0=\int_{x\in\partial V_1}(-\boldsymbol{n})\,(\boldsymbol{x}\,|\,\boldsymbol{x}_1)\,P(\boldsymbol{x}_1)\,dS_1, \tag{3.24}$$

∂V_1 being the (deformed) surface of the bubble at $\boldsymbol{x}_1$, is quite complicated since it requires evaluating both $P(\boldsymbol{x}_1)$ and the shape of the interface correct to $O(\hat{p}_a)$, the former being the most difficult to evaluate. Fortunately, we can make use of the fact that g_0 must satisfy the same wave equation as that satisfied by p_0 or $\boldsymbol{u}_0$. Thus we write

$$g_0=\beta[1+\hat{\beta}\,e^{i\omega t-i\boldsymbol{k}\cdot\boldsymbol{x}}], \tag{3.25}$$

where $\hat{\beta}$ is proportional to $\hat{p}_a$. Now determining $\hat{\beta}$ from the first equality in (3.16) and (3.22), we determine ∇g_0 without much additional effort to be given by

$$\frac{2\sigma}{R}\nabla g_0 = -\beta\lambda_{\sigma c}\nabla p_0 = -\nabla p_0(6\sigma^* t_0 + O(z)). \tag{3.26}$$

The second term on the right-hand side of (3.23) can be evaluated by noting that only the s_1 component is non-zero and $n_1 = \cos\theta = P_1^0(\cos\theta)$, so that on writing

$$(p_L - p_G)^a n_1 = \tfrac{1}{3}p_{10}P_0^0(\cos\theta) + (p_{00} - p_G^a + O(p_{20}))P_1^0(\cos\theta) + \ldots, \tag{3.27}$$

using $p_{10}(R) = 0$ (cf. (2.13)), relating $(p_{00} - p_G)^a(R)$ to η_{00}, and using (3.18) we obtain

$$\lambda_{\sigma m} = \frac{4\sigma^*\omega_r^2}{1 - \omega_r^2(1 - iz)} + O(z^2). \tag{3.28}$$

To calculate λ_p, we determine the time derivative of p_G from (2.10) as

$$\frac{\partial p_G}{\partial t} = -\frac{3\gamma P_e}{R}\frac{\partial \eta_{00}}{\partial t} \tag{3.29}$$

and then make use of the relation $p_{00} = -3\gamma^* P_e R^{-1}\eta_{00}$, obtained by combining (2.12) and (2.14), to yield

$$\frac{\partial p_G}{\partial t}(\boldsymbol{x}\,|\,\boldsymbol{x}_1) = \frac{\gamma}{\gamma^*}\frac{\partial p_{00}}{\partial t} = \frac{\gamma}{\gamma^*}\frac{\partial p_0}{\partial t}(\boldsymbol{x})\,e^{iks_1}\left(j_0(z) + \frac{e^{-iz}A_{00}}{R}\right). \tag{3.30}$$

The constant λ_p can be now readily evaluated to yield

$$\lambda_p = \frac{\gamma}{\gamma^*}\frac{1}{1 - \omega_r^2(1 - iz)} + O(z^2). \tag{3.31}$$

Finally, to calculate λ_v, we first determine the velocity field inside the bubble. Writing $\boldsymbol{u}_1 = \nabla\varphi_1$, and combining (2.1), (2.2), (2.6), and (2.10), we obtain

$$\varphi_1 = -p_1/(i\omega\rho_L) \quad \text{for} \quad s > R, \tag{3.32}$$

$$\nabla^2\varphi_1 = \frac{3}{R}\frac{\partial \eta_{00}}{\partial t} = \frac{3}{R}(\boldsymbol{u}_1\cdot\boldsymbol{n})_{00} \quad \text{for} \quad s \leqslant R, \tag{3.33}$$

where $(\boldsymbol{u}_1\cdot\boldsymbol{n})_{00}$ is the coefficient of P_0^0 in the expansion of the normal velocity at the surface of the bubble. The solution of (3.33) for $s \leqslant R$ can be expressed as

$$\varphi_1 = (\boldsymbol{u}_1\cdot\boldsymbol{n})_{00}\frac{s^2}{2R} + \sum_{n=1}^{n=\infty} E_{n0}\,s^n P_n^0(\cos\theta), \tag{3.34}$$

where the constants E_{n0} are to be determined from the requirement that $\boldsymbol{u}_1\cdot\boldsymbol{n}$ be continuous across $s = R$. For example,

$$E_{10} = (\boldsymbol{u}_1\cdot\boldsymbol{n})_{10} = -\frac{p'_{10}}{i\omega\rho_L} = \hat{p}_a\frac{3k}{\omega\rho_L}e^{i\omega t - i\boldsymbol{k}\cdot\boldsymbol{x}_1}. \tag{3.35}$$

The velocity inside the bubble can be calculated now by differentiating (3.34):

$$\boldsymbol{u}_1 = \frac{\boldsymbol{s}}{R}(\boldsymbol{u}_1\cdot\boldsymbol{n})_{00} + E_{10}\,\boldsymbol{e}_1 + O(k^2 s), \tag{3.36}$$

where $\boldsymbol{e}_1$ is a unit vector along the s_1-axis. Only the term containing E_{10} is important for determining the leading-order estimate of λ_v, and using (3.35), and noting that $\omega\rho_L\boldsymbol{u}_0 = \boldsymbol{k}\hat{p}_a e^{-i\omega t - i\boldsymbol{k}\cdot\boldsymbol{x}_1}$, we obtain

$$\lambda_v = 3 + O(z^2). \tag{3.37}$$

The above result, that the acceleration of an isolated bubble is three times the acceleration of the fluid, is, of course, the classical result for potential flow. We reproduced the essential steps in the derivation here only to aid us later when we calculate the $O(\beta)$ correction to λ_v.

With the above $O(1)$ estimates of $\lambda_{\sigma c}$, $\lambda_{\sigma m}$, λ_p, and λ_v, we now estimate the speed of sound to $O(\beta)$ from (2.29) to be given by

$$\frac{1}{C_{\rm ef}^2}=\frac{1}{C_{\rm L}^2}\left[1-\beta\left(3+\frac{1-2/(3We\gamma^*)}{1-\omega_{\rm r}^2(1-{\rm i}z)}\right)\right]+\frac{\beta\rho_{\rm L}}{\gamma^* P_{\rm e}}\frac{1}{1-\omega_{\rm r}^2(1-{\rm i}z)}, \tag{3.38}$$

which agrees with the Foldy approximation (1.1) with three minor modifications. First, γ is replaced by γ^* in the last term. Second, there is an extra $O(\beta)$ correction in the coefficient of $1/C_{\rm L}^2$, which, as mentioned in §1, is typically much smaller than the last term on the right-hand side of (3.38) and hence of no practical significance. And third, we see that the speed of sound is now a complex quantity so that there is an attenuation due to the term of $O(z)$. If we multiply the denominator of the second term on the right-hand side of (3.38) by $\omega_{\rm c}^2$ and write it as

$$\omega_{\rm c}^2-\omega^2+ib\omega^2, \tag{3.39}$$

then the damping parameter b equals z or $\omega R/C_{\rm L}$. This effect due to scattered waves from the surface of the bubbles is known as acoustic radiation damping.

From the above calculations we see that in the limit $\omega_{\rm r}\to 0$, the strength of the monopole A_{00} vanishes and $\lambda_p\to\gamma/\gamma^*$. This can also be seen from (2.13), where we obtain $p'_{00}=0$ on each bubble by substituting $\omega_{\rm r}=0$. Now since the potential flow approximation is valid near the surface of each bubble, p_{00} must be of the form $e^{i\omega t}(c_1+c_2/s)$ for each bubble with the constant c_2, being the strength of the monopole, equal to zero for $\omega_{\rm r}=0$. Moreover, the wavenumber k also becomes very small at small frequencies and so the $O(z)$ and higher-order terms that were not evaluated in determining various coefficients also remain negligibly small. This suggests that, in fact, $\lambda_p\to\gamma/\gamma^*$ for all values of β in the limit of $\omega_{\rm r}\to 0$. Thus from (2.29) we see that, with the $O(1)$ estimates of λ_v and $\lambda_{\sigma m}$ obtained here, it is in fact possible to calculate the effective speed to $O(\beta^2)$:

$$\frac{1}{C_{\rm ef}^2}=\frac{1}{C_{\rm L}^2}[1-4\beta+O(\beta^2)]+\frac{\beta\rho_{\rm L}}{\gamma^* P_{\rm e}}\left[1-3\beta\left(1+\frac{4}{9We\gamma^*}\right)\right],\quad \omega_{\rm r}\ll 1, \tag{3.40}$$

except for the unimportant $O(\beta^2)$ correction multiplying $C_{\rm L}^{-2}$. If we take $\gamma=\gamma^*$, the above expression agrees with that given by Caflisch *et al.* (1985*b*) who considered the case $We=\infty$.

When $\omega_{\rm r}$ is not small, we see from (2.29) that, if we ignore small corrections multiplying the $C_{\rm L}^{-2}$ term, then we need to determine only λ_p correct to $O(\beta)$ in order to determine $C_{\rm ef}^{-2}$ correct to $O(\beta^2)$. This we shall consider next.

3.2. *Determination of λ_p to $O(\beta)$*

Before we proceed to determine the higher-order corrections to λ_p, we make a simplification in the conditional-averaged equation (3.1). We recall that our interest is largely in determining the corrections to λ_p when $\omega_{\rm r}$ is $O(1)$. With the expression for $C_{\rm ef}^{-2}$ determined to $O(\beta)$ (cf. (3.38)), we can now express the effective wavenumber $k=\omega/C_{\rm ef}$ as

$$k^2R^2=k_{\rm L}^2R^2[1+O(\beta)]+\frac{3\beta\omega_{\rm r}^2}{1-\omega_{\rm r}^2+O(k_{\rm L}R)}, \tag{3.41}$$

where $k_L = \omega/C_L$ is the wavenumber for the pure liquid. We shall be interested in analysing situations for which ω_r is $O(1)$ and β is small, but $k_L^2 R^2 \ll \beta\omega_r^2/(1-\omega_r^2)$. We note that the ratio of the last two quantities is equivalent to $(C_L/C_{ef})^2$, which for β greater than 0.01 is 200 or larger for the air–water system. For β satisfying the above condition, the compressibility of the mixture may be considered to be solely due to the bubbles, and we may regard the liquid as incompressible. To put in another way, near each bubble the liquid may be considered essentially incompressible and the compressibility effects of the liquid are important only at distances of $O(k_L^{-1})$ from the bubble. If this distance is much larger than $O(R/\beta^{\frac{1}{2}})$, then the compressibility of the mixture due to non-zero volume fraction of the bubbles plays a much more significant role than the compressibility of the pure liquid. Thus setting $1/C_L$ and k_L to zero in (3.1) we obtain, for $|\boldsymbol{x}-\boldsymbol{x}_1| > R$:

$$\nabla\cdot\boldsymbol{u}_1 = -\frac{1}{\gamma P_e}\left\{g\frac{\partial p_G}{\partial t}\right\}_1. \tag{3.42}$$

Now to determine λ_p correct to $O(\beta)$, we must solve (3.2) and (3.42) subject to the condition that p_1 and $\boldsymbol{u}_1$ approach, respectively, p_0 and $\boldsymbol{u}_0$ correct to $O(\beta)$ as $|\boldsymbol{x}-\boldsymbol{x}_1|\to\infty$. From the $O(1)$ estimates of $\lambda_{\sigma m}$, λ_v and λ_p determined in the §3.1, we see that p_0 and $\boldsymbol{u}_0$ satisfy the following equations to $O(\beta)$:

$$\frac{\beta}{\gamma^* P_e}\frac{1}{1-\omega_r^2}\frac{\partial p_0}{\partial t} + \nabla\cdot\boldsymbol{u}_0 = 0, \tag{3.43}$$

$$\rho_L(1-3\beta)\frac{\partial \boldsymbol{u}_0}{\partial t} + (1+4\sigma^* t_0)\nabla p_0 = 0, \tag{3.44}$$

where $t_0 = \omega_r^2/(1-\omega_r^2)$. Eliminating the velocity field and denoting the amplitude of the fluctuations by a hat, e.g. $p_0 = P + \hat{p}_0 e^{i\omega t}$, we see that $\hat{p}_0$ satisfies the Helmholtz equation:

$$\nabla^2\hat{p}_0 + k^2\hat{p}_0 = 0, \tag{3.45}$$

where, to $O(\beta)$, k^2 is the same as that given by (3.41) with k_L set to zero, i.e.

$$k^2R^2 = 3\beta\frac{\omega_r^2}{1-\omega_r^2} = 3\beta t_0. \tag{3.46}$$

Thus the effective wavenumber is $O(R\beta^{\frac{1}{2}})$ when ω_r is $O(1)$. We shall require that $\hat{p}_1$ satisfies the same equation as $\hat{p}_0$ as $|\boldsymbol{x}-\boldsymbol{x}_1|\to\infty$. An equation for $\hat{p}_1$ correct to $O(\beta)$ can be obtained by eliminating $\boldsymbol{u}_1$ from (3.2) and (3.42) by first taking the divergence of (3.2) and subtracting $i\omega\rho_L$ times (3.42) from it. The divergence of the first term on the right-hand side of (3.2), with $\partial/\partial t$ replaced by $i\omega$, equals

$$i\omega\rho_L\left\{\int_{|\boldsymbol{x}-\boldsymbol{x}_2|=R}(-\boldsymbol{n}\cdot\hat{\boldsymbol{u}})_2(\boldsymbol{x})\,P_c\,dS_2 + \int_{|\boldsymbol{x}-\boldsymbol{x}_2|\leqslant R}\nabla\cdot\hat{\boldsymbol{u}}_2(\boldsymbol{x})\,P_c\,dV_2\right\}, \tag{3.47}$$

where $P_c \equiv P(\boldsymbol{x}_2\,|\,\boldsymbol{x}_1)$ is the conditional probability density for finding a bubble at $\boldsymbol{x}_2$ given that a bubble exists at $\boldsymbol{x}_1$. The subscript 2 in the above expression implies a conditional average with two bubbles fixed at $\boldsymbol{x}_1$ and $\boldsymbol{x}_2$. For brevity, we have suppressed the arguments of P_c. Now inside the bubble at $\boldsymbol{x}_2$, we have $\nabla\cdot\hat{\boldsymbol{u}}_2 = -i\omega\hat{p}_2/(\gamma P_e)$, so that the second term in (3.47) will cancel the right-hand side of (3.42), resulting in the following equation for $\hat{p}_1$ for $\boldsymbol{x}$ outside the bubble at $\boldsymbol{x}_1$:

$$\nabla^2\hat{p}_1 = -i\omega\rho_L\int_{|\boldsymbol{x}-\boldsymbol{x}_2|=R}(\boldsymbol{n}\cdot\hat{\boldsymbol{u}})_2(\boldsymbol{x})\,P_c\,dS_2 + \nabla\cdot\int_{\boldsymbol{x}\in\partial V_2}\{\boldsymbol{n}(\hat{p}_L-\hat{p}_G)\}_2(\boldsymbol{x})\,P_c\,dS_2. \tag{3.48}$$

Now instead of evaluating the right-hand side of the above equation as a function of $\boldsymbol{x}$ first and then solving for $\hat{p}_1$ subject to the boundary conditions, we follow the method of generalized functions presented by Hinch (1977) and relate the solution of the above problem directly to the solution of the two-bubble problem. Introducing generalized functions we write (3.48) for $\boldsymbol{x}$ outside the bubble at $\boldsymbol{x}_1$ as

$$\nabla^2\hat{p}_1 = -\int_{|\boldsymbol{x}_1-\boldsymbol{x}_2|\geqslant 2R} \mathrm{d}V_2 P_c \int_{\boldsymbol{x}'\in\partial V_2} \mathrm{d}S'[\mathrm{i}\omega\rho_L(\boldsymbol{n}'\cdot\hat{\boldsymbol{u}})_2(\boldsymbol{x}')\,\delta(\boldsymbol{x}-\boldsymbol{x}') + \{(\hat{p}_L-\hat{p}_G)(\boldsymbol{x}')\,\boldsymbol{n}'\cdot\nabla\delta(\boldsymbol{x}-\boldsymbol{x}')\}_2]. \quad (3.49)$$

Here, the second integration is carried out on the surface of a bubble placed at $\boldsymbol{x}_2$. The reason for doing this mathematical manipulation is to convert the integrals in (3.48), which are somewhat difficult to evaluate as they are carried out for all the different bubbles whose surfaces pass through the point $\boldsymbol{x}$, to the integrals on the surface of an individual bubble located at a fixed point $\boldsymbol{x}_2$. As we shall see later, the solution of (3.49) can be more easily related to the solution of the two-bubble problem, and therein lies the main advantage of the approach suggested by Hinch. According to the expression (3.49), the singularities in $\hat{p}_1$ outside the bubble at $\boldsymbol{x}_1$ are distributed on the surface of each second bubble where both $\hat{p}_1$ and the normal derivative $\boldsymbol{n}\cdot\nabla\hat{p}_1$ are discontinuous owing to the finite surface tension and the compressibility of the bubble.

Now since we require that $\hat{p}_1\to\hat{p}_0$ at infinity and since $\hat{p}_0$ satisfies the Helmholtz equation, it is useful to add the following identity to (3.49):

$$k^2\hat{p}_1(\boldsymbol{x}) = \frac{3\beta t_0}{4\pi R^2}\int_{|\boldsymbol{x}-\boldsymbol{x}_2|>R} 4\pi\delta(\boldsymbol{x}-\boldsymbol{x}_2)\,\hat{p}_1(\boldsymbol{x}_2)\,\mathrm{d}V_2, \quad (3.50)$$

which is valid for $\boldsymbol{x}$ outside V_1. Note that in this identity $\boldsymbol{x}_2$ is merely a dummy variable of integration and nothing is implied about the two-bubble problem. In fact the integration is carried out for $\hat{p}_1$ which is the conditionally averaged pressure with a single bubble fixed at $\boldsymbol{x}_1$. The advantage of adding this identity to (3.49) is that it converts the left-hand side of (3.49) into a Helmholtz operator, thereby making it easier to satisfy the boundary condition for $\hat{p}_1$ at infinity. Now let us decompose $\hat{p}_1$ into two parts: $\hat{p}_1 = \hat{p}_1^{\mathrm{e}}+\hat{p}_1^{\mathrm{p}}$. The effective-medium part satisfies

$$\nabla^2\hat{p}_1^{\mathrm{e}} + k^2\hat{p}_1^{\mathrm{e}} = 0 \quad (3.51)$$

together with the boundary conditions given by (2.13) at $|\boldsymbol{x}-\boldsymbol{x}_1| = R$ and $\hat{p}_1^{\mathrm{e}}\to\hat{p}_0$ $(=\hat{p}_a\,\mathrm{e}^{-\mathrm{i}k\cdot x})$ as $|\boldsymbol{x}-\boldsymbol{x}_1|\to\infty$. The solution for this part is straightforward and it is readily obtained from the solution presented in §3.1 with k now being given by (3.46). Since we now wish to calculate the terms to $O(\beta)$, we need to keep the $O(z^2)$ terms in (3.12) and (3.19). (Since the pressure inside the gas bubble is uniform, in evaluating the volume integral of $\partial p_G/\partial t$ only the component corresponding to $\tilde{p}_{00}$ is non-zero.) Thus the contribution to λ_p from the effective-medium part and from the finite wavelength ($O(z^2)$ term in (3.19)) can be shown to equal

$$\lambda_p^{\mathrm{e}} = \frac{\gamma}{\gamma^*}[1-\tfrac{1}{10}z^2]\,[j_0(z)+D_{00}\,h_0(z)]$$

$$= \frac{\gamma}{\gamma^*(1-\omega_r^2)}\left[1-\mathrm{i}zt_0-3\beta t_0\left\{\tfrac{1}{10}+\tfrac{1}{2}t_0\left(1+\frac{1}{\omega_r^2}\right)+t_0^2\right\}\right]. \quad (3.52)$$

Since $z^2 = 3\beta t_0$, we see that now the leading-order correction is $O(\beta^{\frac{1}{2}})$, and since this is a purely imaginary quantity, it implies an attenuation of the sound waves.

The other part, which accounts for the pairwise interactions, satisfies the remainder, i.e.

$$\nabla^2\hat{p}_1^{\mathrm{p}}+k^2\hat{p}_1^{\mathrm{p}}=\int_{S\geqslant 2R}\mathrm{d}V_2\,P_{\mathrm{c}}\int_{x'\in\partial V_2}\mathrm{d}S'\{-\mathrm{i}\omega\rho_{\mathrm{L}}\boldsymbol{n}'\cdot\hat{\boldsymbol{u}}_2\,\delta(\boldsymbol{x}-\boldsymbol{x}')$$

$$+(\hat{p}_{\mathrm{L}}-\hat{p}_{\mathrm{G}})\boldsymbol{n}'(\boldsymbol{x}')\cdot\nabla\delta(\boldsymbol{x}-\boldsymbol{x}')\}+\frac{3\beta t_0}{4\pi R^2}\int_{S>R}4\pi\delta(\boldsymbol{x}-\boldsymbol{x}_2)\,\hat{p}_1(\boldsymbol{x}_2)\,\mathrm{d}V_2. \quad (3.53)$$

Here $\boldsymbol{S}=\boldsymbol{x}_2-\boldsymbol{x}_1$ and S is the magnitude of $\boldsymbol{S}$. The boundary conditions are that $\hat{p}_1^{\mathrm{p}}$ satisfies (2.13) on the surface of the bubble $|\boldsymbol{x}-\boldsymbol{x}_1|=R$ and that $\hat{p}_1^{\mathrm{p}}\to 0$ as $|\boldsymbol{x}-\boldsymbol{x}_1|\to\infty$. Since P_{c} is $O(\beta)$, we need to determine the two-bubble problem only to $O(1)$ to obtain $\hat{p}_1^{\mathrm{p}}$ correct to $O(\beta)$. Similarly we can replace $\hat{p}_1$ on the right-hand side of the above equation by its $O(1)$ estimate.

The solution of the two-bubble problem can be obtained once again by the method of multipole expansions with the multipoles now located at $\boldsymbol{x}_1$ and $\boldsymbol{x}_2$. Thus we write, for $\boldsymbol{x}$ outside both bubbles,

$$\hat{p}_2=\hat{p}_{\mathrm{a}}\,\mathrm{e}^{-\mathrm{i}\boldsymbol{k}\cdot\boldsymbol{x}_1}\left[\mathrm{e}^{-\mathrm{i}\boldsymbol{k}\cdot\boldsymbol{s}}+\sum_{q=1}^{2}\sum_{n,m}A_{nm}^{q}\,\mathrm{Y}_n^m\left(\frac{\partial}{\partial s_1},\frac{\partial}{\partial s_2},\frac{\partial}{\partial s_3}\right)G(k|\boldsymbol{x}-\boldsymbol{x}_q|)\right]. \quad (3.54)$$

The details of the calculations of the strengths of multipoles A_{nm}^q are given in Appendix A. Here we note that since G is a fundamental solution of the Helmholtz equation, $\hat{p}_2$ has singularities at $\boldsymbol{x}_1$ and $\boldsymbol{x}_2$ as given by

$$\nabla^2\hat{p}_2+k^2\hat{p}_2=\hat{p}_{\mathrm{a}}\,\mathrm{e}^{-\mathrm{i}\boldsymbol{k}\cdot\boldsymbol{x}_1}\left[\sum_{q=1}^{2}\sum_{n,m}A_{nm}^{q}\,\mathrm{Y}_n^m\left(\frac{\partial}{\partial s_1},\frac{\partial}{\partial s_2},\frac{\partial}{\partial s_3}\right)(-4\pi\delta(\boldsymbol{x}-\boldsymbol{x}_q))\right]. \quad (3.55)$$

Returning now to the solution of $\hat{p}_1$, we note that the complete solution for $\hat{p}_1^{\mathrm{p}}$ can be obtained by first writing a particular solution due to the right-hand-side forcing in (3.53) as obtained by replacing $-4\pi\delta(\boldsymbol{x}-\boldsymbol{x}')$ on the right-hand side of that equation by $G(k|\boldsymbol{x}-\boldsymbol{x}'|)$ and then adding the solutions of the Helmholtz equations with singularities at $\boldsymbol{x}_1$ to satisfy the boundary conditions (2.13) on the surface of the bubble. However, since our interest is mainly in determining λ_p, we can bypass the latter step and determine λ_p directly from the behaviour of the particular solution near the centre of the bubble at $\boldsymbol{x}_1$. Thus, it can be readily shown from the calculations of §3.1, with a relative error of $O(z)$ (or $O(\beta^{\frac{1}{2}})$),

$$\hat{p}_{\mathrm{a}}\,\mathrm{e}^{-\mathrm{i}\boldsymbol{k}\cdot\boldsymbol{x}_1}\lambda_p^{\mathrm{p}}=\frac{\gamma}{\gamma^*(1-\omega_{\mathrm{r}}^2)}\hat{p}_{1,\mathrm{par}}^{\mathrm{p}}(\boldsymbol{x}=\boldsymbol{x}_1), \quad (3.56)$$

where $\hat{p}_{1,\mathrm{par}}^{\mathrm{p}}$ is the particular solution due to the right-hand side forcing in (3.53). Next, we note that, as far as the behaviour of $\hat{p}_{1,\mathrm{par}}^{\mathrm{p}}$ near $\boldsymbol{x}=\boldsymbol{x}_1$ is concerned, the distribution of fundamental singularities on the surface of the bubble at $\boldsymbol{x}_2$ in (3.53) must be equivalent to the series in higher-order multipoles at the centre of the bubble at $\boldsymbol{x}_2$ in (3.55) since both represent the same two-bubble interaction problem. Thus, replacing the terms inside the curly bracket in (3.53) by the right-hand side of (3.55) and then writing $G(kS)$ in place of $-4\pi\delta(\boldsymbol{x}_1-\boldsymbol{x}_2)$ to obtain the particular solution, we obtain the contribution to λ_p from the pairwise interactions part as

$$\lambda_p^{\mathrm{p}}=\frac{\gamma}{\gamma^*(1-\omega_{\mathrm{r}}^2)}\left[-\frac{3\beta t_0}{4\pi R^2}\int_{S>R}\mathrm{d}V_2\{\mathrm{e}^{-\mathrm{i}\boldsymbol{k}\cdot\boldsymbol{S}}+A_{00}\,G(kS)\}\,G(kS)\right.$$

$$\left.+\int_{S\geqslant 2R}\mathrm{d}V_2\,P_{\mathrm{c}}\sum_{n,m}A_{nm}^{2}\,\mathrm{Y}_n^m\,G(kS)\right], \quad (3.57)$$

where we have suppressed the differentiation arguments of Y_n^m for brevity. Note that only A_{00} from the single-bubble solution (cf. (3.3)) contributes to the $O(1)$ estimate of $\hat{p}_1$ as z is $O(\beta^{\frac{1}{2}})$. Now the summation in (3.57) can be replaced by the monopole at $\boldsymbol{x}_1$ by making use of the following relation derived in Appendix A (cf. (A 8)):

$$\sum_{n,m} A_{nm}^2 Y_n^m G(kS) = \frac{A_{00}^1}{Rt_0} - 1, \tag{3.58}$$

and, furthermore, as shown in Appendix A (cf. (A 17)), the term on the right-hand side of the above equation can be expressed as

$$\frac{A_{00}^1}{Rt_0} - 1 = Rt_0 G(kS) e^{-ik\cdot S} + R^2 t_0^2 (G(kS))^2 + R^3 t_0^3 (G(kS))^3 e^{-ik\cdot S} - \sum_{n=4}^{\infty} a_n \left(\frac{R}{S}\right)^n, \tag{3.59}$$

where the a_n correspond to the fourth- and higher-order reflections. Now $P_c \to P(\boldsymbol{x}_1) = \beta/V_b$ as $S \to \infty$ and hence we see that the contribution from the first two terms on the right-hand side of (3.59) cancel exactly the contribution from the integral of $\hat{p}_1$ in (3.57) resulting in an overall integrand that decays as $(G(kS))^3 e^{-ik\cdot S}$ as $S \to \infty$. If k is identically zero, then the resulting integral is not absolutely convergent. However, the presence of the term $e^{-ik\cdot S}$ makes it convergent for finite k. (It may be recalled that $k = z/R = O(\beta^{\frac{1}{2}}/R)$.)

We shall assume that P_c is given by the usual 'well-mixed' distribution according to which $P_c(S) = 0$ for $S < 2R$ and $P_c(S) = \beta/V_b$ for $S \geqslant 2R$. In this case we need to integrate $\hat{p}_1$ in (3.57) only over the exclusion region $R \leqslant S \leqslant 2R$ and we can use the expansion with $k \to 0$ for this purpose. Similarly, since the higher-order reflections decay as S^{-4} or faster, we need to evaluate a_n only for $k \to 0$. The only part where the finite value of k is important is the third term in the right-hand side of (3.59), which for small k can be evaluated from

$$\frac{1}{4\pi} \int_{S \geqslant 2R} \frac{e^{-3ikS} e^{-ik\cdot S}}{S^3} dV_2 = 1 - C - \ln(16) - \tfrac{1}{2}\ln(z^2) - \tfrac{1}{2}i\pi + O(z), \tag{3.60}$$

where $C = 0.577\,215\ldots$ is Euler's constant. Combining all terms, including the contribution from the effective medium part, we obtain the following expression for λ_p correct to $O(\beta)$:

$$\lambda_p = \frac{\gamma}{\gamma^*(1-\omega_r^2)} [1 - i(zt_0 + \tfrac{1}{2}\pi z^2 t_0^2) - \tfrac{3}{2} t_0^3 \beta \ln\beta - \beta\lambda_{p1}], \tag{3.61}$$

where

$$\lambda_{p1} = 3t_0 \left\{ \frac{8}{5} + \frac{t_0}{2}\left(3 + \frac{1}{\omega_r^2}\right) + t_0^2 (3.899\,11 + \tfrac{1}{2}\ln t_0) \right\} + 3 \sum_{n=4}^{\infty} a_n \frac{2^{3-n}}{n-3}, \tag{3.62}$$

with $t_0 = \omega_r^2/(1-\omega_r^2)$ and $z^2 = 3\beta t_0$. In the above expression for λ_{p1}, the contribution from the exclusion region is $\frac{3}{2} + t_0$, that from the finite wavelength is $\frac{1}{10}$, and the remainder is from the effective-medium part and the third- and higher-order reflections in the pairwise interaction of bubbles.

In summary, we see that the leading-order correction to λ_p is a purely imaginary quantity of $O(\beta^{\frac{1}{2}})$. As mentioned earlier, this contributes to the acoustic damping. The damping parameter b introduced in (3.39) now equals $\omega R/C_{ef}$ to the leading order (with $C_{ef}^{-2} = \beta\rho_L/[\gamma^* P_e(1-\omega_r^2)]$), instead of the commonly used estimate $\omega R/C_L$, and thus can be a quite significant damping mechanism, at least for $\omega_r < 1$. The leading-order correction to the phase speed, i.e. the real part of C_{ef}, is $O(\beta \ln\beta)$. This correction results from the third reflection in the two-bubble interaction.

There is a considerable resemblance between the calculations presented here and those in the problem of determining the permeability of random arrays of spheres (Howells 1974; Hinch 1977; Kim & Russel 1985*b*). In that problem, the disturbance flow due a particle placed in a uniform Stokes flow decays as $1/s$ near the particle and more rapidly, as $e^{-\alpha s}/s$ where $\alpha^2 R^2 = 9\beta/2$ is related to the inverse of permeability, at larger distances from the sphere due to what is known as the Brinkman screening. The force required to keep the particles fixed at their positions introduces a resistance term in the far-field description of the conditionally averaged velocity field which makes the conditionally averaged disturbances decay more rapidly at infinity than $1/s$ as predicted by the Stokes flow equations. Replacing the fluid medium around the test particle by an effective medium which satisfies the Brinkman equation produces the first correction to the permeability which is $O(\beta^{\frac{1}{2}})$, β being the volume fraction of the particles. It turns out that replacing the fluid by an effective medium actually accounts for the first two reflections in the two-particle problem. This is not so surprising when one realizes that the effective medium calculation in fact accounts for the change in properties of the medium as caused by the presence of other particles. The third reflection in the Stokes flow interaction of two particles is proportional to $O(R/S)^3$ and the straightforward integration of this diverges logarithmically for large distances. Therefore even here the fact that the two widely separated particles interact through the Brinkman medium and not the Stokes medium is important. This third reflection at large separations decays exponentially as $e^{-3\alpha S}/S^3$ and, accounting for the fact that $\alpha = O(\beta^{\frac{1}{2}})$, produces the $O(\beta \ln \beta)$ correction to the permeability.

In our problem, there is no such screening mechanism because α, which is proportional to ik, is a purely imaginary number. The effective medium now consists of a compressible medium with the compressibility determined by the amount of bubbles. The spherically scattered wave from the surface decays as e^{-iks}/s as opposed to a $1/s$ decay in an incompressible liquid. Once again this effective-medium calculation accounts for the first two reflections in the two-bubble problem. The third reflection, which decays as $e^{-3ikS - ik\cdot S}/S^3$ in the two-bubble interactions in a compressible medium, could be integrated to yield a finite value even in the absence of a screening mechanism because of the finite nature of the wavelength. The angular integration of $e^{-ik\cdot S}$ on the surface of a sphere of radius S yields $4\pi \sin kS/kS$ and thus, the third reflection actually gives rise to an integration in S that decays as $1/S^4$.

It is useful for the calculations in subsequent sections to summarize the essential steps used in the pairwise interactions calculations for determining λ_p to $O(\beta)$. These steps, which are very similar to the general method outlined by Acrivos & Chang (1986), involve the following. (i) Identifying the proper form of the conditionally averaged equations as $S \to \infty$. This was found from the requirement that the conditionally averaged fields must approach the unconditionally averaged fields to $O(\beta)$ (cf. (3.43), (3.44)). (ii) Solving for the effective part ($\hat{p}_1^e$) that satisfies the boundary conditions at infinity. This was done by replacing the governing equations with those satisfied by the averaged quantities in the effective medium. (iii) Subtracting the first two reflections (the first two terms on the right-hand side of (3.59)) from the two-bubble problem and then integrating the remainder over all possible positions of the second bubble with respect to the first. (iv) Adding contributions from the exclusion region ($R \leqslant S \leqslant 2R$) and the non-local effects such as those due to the finite value of the ratio of micro to macro lengthscales (finite kR). That the first two reflections from the two-bubble problem are automatically included in the effective medium calculation (step (ii)) is, in fact, a common feature

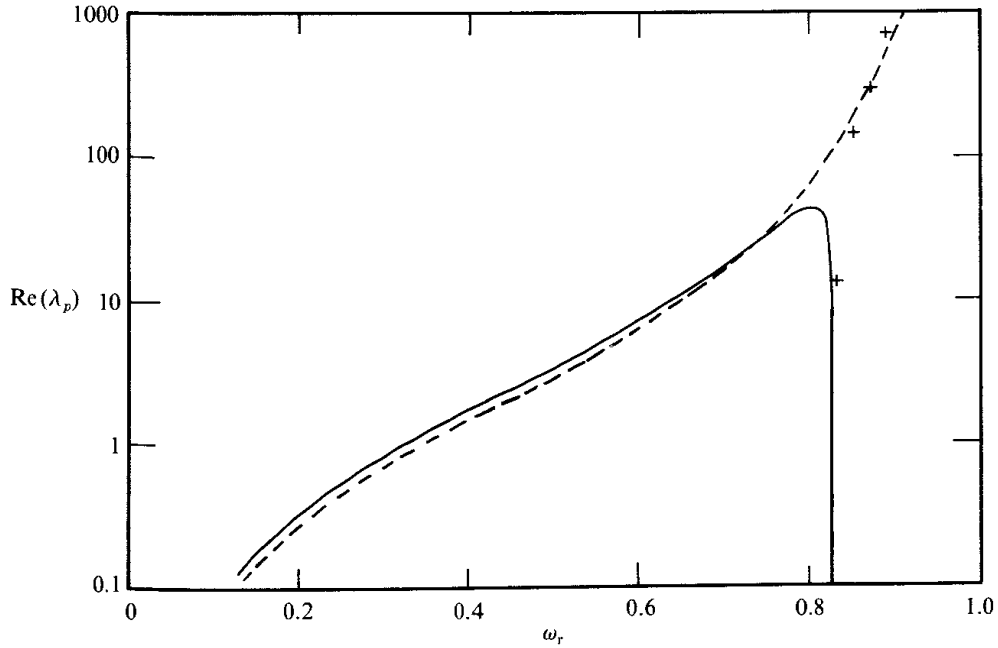

FIGURE 1. The real part of the $O(\beta)$ coefficient λ_{p1} as a function of ω_r for $\sigma^* = \infty$. The dashed curve is the contribution from the terms other than the fourth- and higher-order reflections (C_{ex}) and the solid curve is the overall value. The points indicated by + are obtained from the principal value of the integral for C_{ex} for $\omega_r > 0.828$.

in most calculations of this nature. Finally, in some problems it is possible to solve for an effective-medium part with the properties of the pure liquid for $R < S < 2R$ and the effective properties for $S \geqslant 2R$, in which case it is not necessary to evaluate the contribution from the exclusion region in (iv) (cf. §3.3).

In the work of Caflisch *et al.* (1985*a*, *b*) and Miksis & Ting (1986), the restrictions on ω_r and β were determined from the condition that the two lengthscales R and k_{ef}^{-1} must be widely separated so that the macroscopic description of the bubbly flows can be obtained from the leading-order homogenization. We see that such restrictions are not essential and that the results for a finite ratio of the two lengthscales can be just as easily determined using the method of ensemble averages. This, in fact, is also the advantage of the ensemble averaging technique over the volume averaging technique. Indeed, the ensemble averages approach has been applied quite successfully to studies involving non-local effects (Koch & Brady 1987; Shaqfeh 1988).

3.2.1. *Numerical results for* λ_{p1}

The solid curve in figure 1 shows the real part of λ_{p1} as a function of ω_r for $\sigma^* = \infty$, i.e. for the large-surface-tension case. (As noted in §2.1, σ^* is a function of ω_r for a fixed Weber number. For the purpose of discussion here, however, it is convenient to treat σ^* as a constant.) In this case the deformation of the bubbles from the spherical shape is zero. The $O(\beta \ln \beta)$ and $O(\beta)$ coefficients remain very small for ω_r up to about 0.4 and thus the expression given by Caflisch *et al.* (1985*b*) for $\omega_r \to 0$ is expected to yield very good estimates for the effective speed for $\omega_r < 0.4$ and small β. The coefficient λ_{p1} is positive for all values of ω_r except for a small range of frequencies near $\omega_r = 0.8280$, where the contribution from the last term in (3.62), which represents higher-order reflections, becomes important.

For $\sigma^* = \infty$, pairs of bubbles resonate in two different modes; one in which both bubbles undergo volume pulsations in phase with each other and the other in which

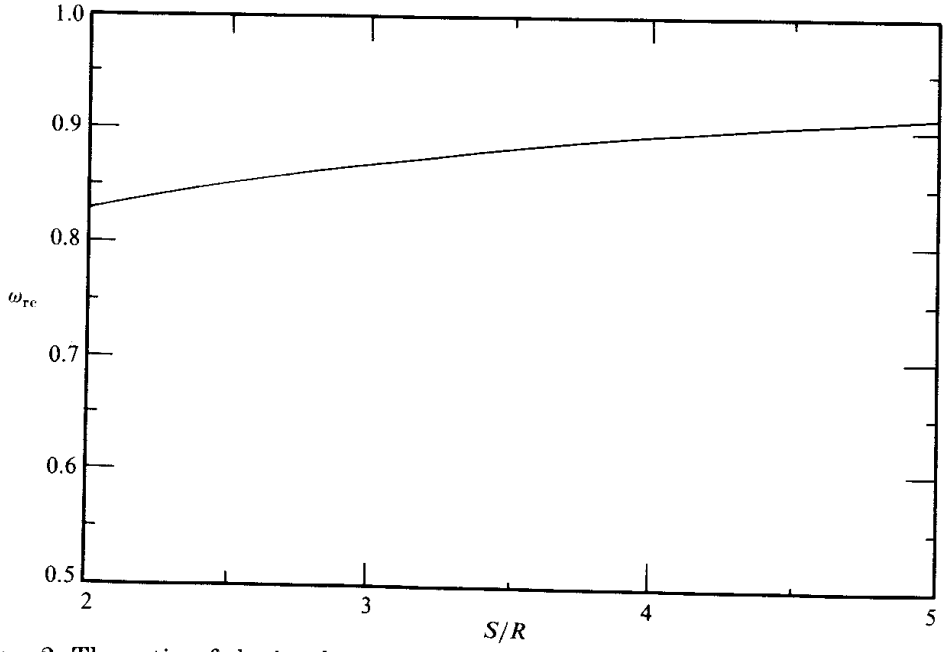

FIGURE 2. The ratio of the in-phase mode resonance frequency of a pair of bubbles separated by a distance S to the resonance frequency of isolated bubbles for $\sigma^* = \infty$.

the pulsations are out of phase (Scott 1981). The ambient pressure around the bubbles at $\boldsymbol{x}_1$ and $\boldsymbol{x}_2$ is proportional to $e^{-i\boldsymbol{k}\cdot\boldsymbol{x}_1}$ and $e^{-i\boldsymbol{k}\cdot\boldsymbol{x}_2}$ and hence the magnitude of the in-phase pulsation is proportional to the mean, $\frac{1}{2}(e^{-i\boldsymbol{k}\cdot\boldsymbol{x}_1}+e^{-i\boldsymbol{k}\cdot\boldsymbol{x}_2})$, and that of the out-of-phase pulsation is proportional to the difference $(e^{-i\boldsymbol{k}\cdot\boldsymbol{x}_1}-e^{-i\boldsymbol{k}\cdot\boldsymbol{x}_2})$ (see Appendix A). When $S = |\boldsymbol{x}_2-\boldsymbol{x}_1|$ is $O(R)$, the second mode is excited only by an $O(kR)$ or $O(\beta^{\frac{1}{2}})$ amount and therefore the contribution from this mode is of higher order. On the other hand, when kS is $O(1)$ both modes are excited but, since the two bubbles are then widely separated, both resonance frequencies are very close to the resonance frequency of the individual bubbles. Thus only the first mode of in-phase pulsations is important in the leading-order pairwise-interaction calculations. The resonance frequency for the pair of bubbles in this mode is smaller than the natural frequency of the individual bubbles.

Figure 2 shows the resonance frequency (for the in-phase mode) of a pair of bubbles, $\omega_{rc} = \omega_{reso,\,pair}/\omega_c$, as a function of their separation distance S for $\sigma^* = \infty$ and $k \to 0$. The minimum in ω_{rc} occurs for $S = 2R$, corresponding to a pair of touching bubbles, and equals 0.8280. Clearly, at this frequency the contribution from the higher-order reflections will become infinitely large and, therefore, let us examine the behaviour of λ_{p1} near this critical frequency. The series in (3.62) actually corresponds to A^1_{00} by means of (cf. (3.59) with $k = 0$)

$$C_{ex} \equiv 3\sum_{n=4}^{\infty} a_n \frac{2^{3-n}}{n-3} = 3\int_2^{\infty}\left\{1+\frac{t_0}{S'}+\frac{t_0^2}{S'^2}+\frac{t_0^3}{S'^3}-\frac{A^1_{00}}{t_0 R}\right\}S'^2\,dS', \tag{3.63}$$

where $S' = S/R$. As shown in Appendix A, A^1_{00} is given by

$$\frac{A^1_{00}}{t_0 R} = \frac{1}{1-t_0 f(S')}. \tag{3.64}$$

For $\sigma^* = \infty$, f is a monotonically decreasing function of S' with $f(2) = 0.4585$ and $f'(2) = -0.1914$. Thus, as the frequency is slowly increased, first a pair of touching bubbles will start resonating at a frequency ω_{rc} such that $t_{0c} = 1/f(2)$. For ω_r slightly

lower than ω_{rc}, the leading-order contribution to the integral in (3.63) arises from distances close to $2R$ and, hence, expanding the denominator of the term on the right-hand side of (3.64) as

$$1-t_0 f(S') = 1-\left[t_{0c}+(\omega_r-\omega_{rc})\frac{dt_0}{d\omega_r}(\omega_{rc})+\ldots\right][f(2)+(S'-2)f'(2)+\ldots]$$
$$= \text{const}\,(\omega_{rc}-\omega_r)-t_{0c}f'(2)(S'-2)+\ldots, \tag{3.65}$$

we see that the divergence of the integral in (3.63) is logarithmic, as given by

$$C_{ex} = B_1 \log(\omega_{rc}-\omega_r)+B_2, \quad 0<\omega_{rc}-\omega_r \leqslant 1, \tag{3.66}$$

where B_1 and B_2 are $O(1)$ constants with $B_1 = -12/(t_{0c}f'(2)) = 28.75$ for $\sigma^* = \infty$. The constant B_2 was estimated to equal 85 by comparing the above limiting form with the numerical results for ω_r up to about 0.81, for which the series in (3.63) was found to converge rapidly. It should be noted that the divergence at $\omega_r = \omega_c$ occurs strictly only in the absence of any damping mechanism. The damping due to viscous or non-adiabatic thermal effects that are usually present will eventually become important for sufficiently small values of $\omega_{rc}-\omega_r$, and, thereby, render λ_{p1} finite even for $\omega = \omega_{rc}$.

We now examine the behaviour of C_{ex} as ω_r is increased beyond ω_{rc}. The integral in (3.63) in this case is not absolutely convergent as the denominator of the term on the right-hand side of (3.64) always vanishes for some critical separation distance S'_c between the pair of bubbles with $2 < S'_c < \infty$. The strength of the monopole A^1_{00} at this critical separation distance becomes infinitely large and so at first it might appear that C_{ex} and hence λ_{p1} are infinite for $\omega_{rc} \leqslant \omega_r \leqslant 1$. This, however, is not the case as in fact $A^1_{00} \to \pm\infty$ on either side of this critical separation distance and this, in turn, has the effect of cancelling the large contributions from the pairs of almost resonating bubbles. Any mechanism which will act to dampen the pair of almost resonating bubbles will act equally on the pairs of bubbles with large positive and negative A^1_{00}, and hence the integral in (3.63) must be determined from its principal value in the Cauchy sense. To show this, let us suppose that the magnitude of a small damping term, due to the viscous or non-adiabatic thermal effects to be examined in §§4 and 5, equals Γ when the distance between the two bubbles is nearly equal to its critical distance S'_c, as determined from the relation $f(S'_c) = 1/t_0$. The denominator of the term on the right-hand side of (3.64) can be expanded near $S' = S'_c$ as $1-t_0[f(S'_c)+f'(S'_c)(S'-S'_c)+\ldots]+i\Gamma$, and therefore we write

$$\int_2^\infty \frac{A^1_{00}}{Rt_0}S'^2\,dS' = \int_2^\infty \left[\frac{A^1_{00}}{Rt_0}S'^2 - \frac{a(S')\,S'^2_c}{i\Gamma - t_0 f'(S'_c)(S'-S'_c)}\right]dS'$$
$$+\int_{S'_1}^{S'_2} \frac{S'^2_c\,dS'}{i\Gamma - t_0 f'(S'_c)(S'-S'_c)}, \tag{3.67}$$

where $a(S')$ equals unity for $S'_1 \leqslant S' \leqslant S'_2$ and zero otherwise, and S'_1 and S'_2 are arbitrary constants bounding S'_c, i.e. $S'_1 < S'_c < S'_2$. The integration of the second term on the right-hand side of the above equation yields

$$\frac{S'^2_c}{t_0 f'(S'_c)}\left[\pi i - \ln\frac{S'_2 - S'_c + i\Gamma/t_0 f'(S'_c)}{S'_c - S'_1 + i\Gamma/t_0 f'(S'_c)}\right]. \tag{3.68}$$

We can now ignore the small damping term in evaluating the logarithm in the above expression, and combine it with the first term on the right-hand side of (3.67) to

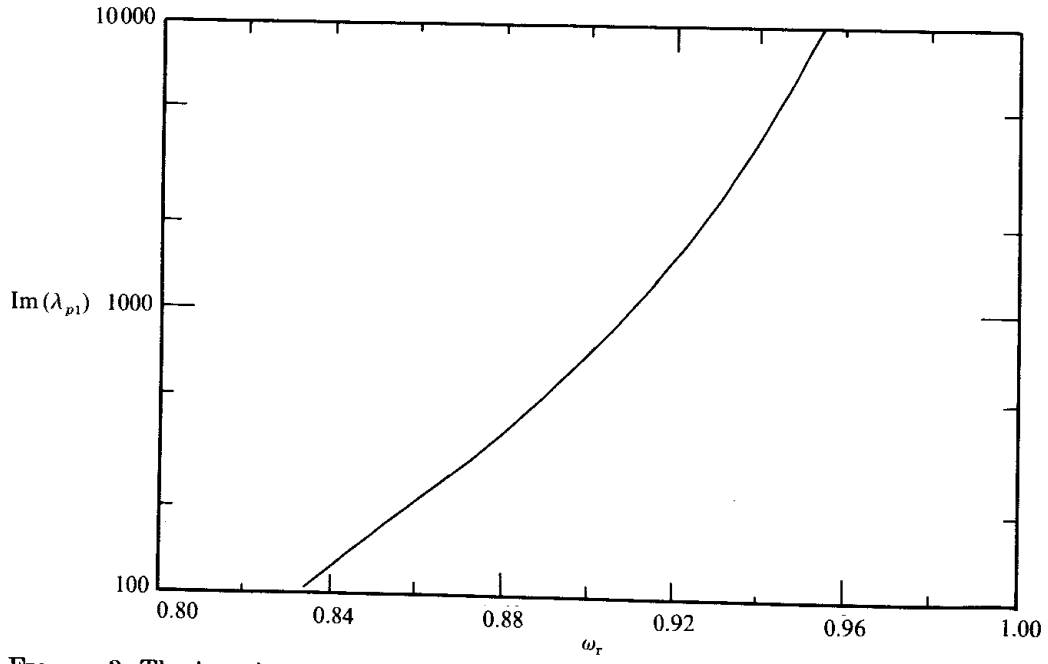

FIGURE 3. The imaginary part of λ_{p1} for $\omega_r > 0.828$ and $\sigma^* = \infty$ in the limit of small damping.

result in the principal value of the integral in (3.63). There is, however, now an extra term, equal to $-3i\pi S_c'^2/t_0 f'(S_c')$, that must be added to the principal value of the integral for $\omega > \omega_{rc}$. If $\Gamma \ll (\omega_r - \omega_{rc}) \ll 1$, then once again we find that the real part of λ_{p1} diverges logarithmically with $\omega_r - \omega_{rc}$ as in (3.66) except that now we must use the absolute value of $\omega_{rc} - \omega_r$ in that expression.

It is no longer possible to use the series in (3.63) to evaluate C_{ex} numerically for $\omega_r > 0.828$ as this series does not converge. We therefore determined A_{00}^1 by the method of direct substitution explained in Appendix A for several values of S' greater than 2 with increments of 0.01 up to S' equal to, say, 10. Then the precise S_c' at which A_{00}^1 changed its sign was estimated, and a term proportional to $1/(S'-S_c')$ was subtracted from each A_{00}^1 in its vicinity. The resulting coefficients were integrated numerically using Simpson's rule and the contribution from the term proportional to $1/(S'-S_c')$ was calculated separately and added. This procedure was repeated for different sizes of increments and the maximum value of S' until no significant change in C_{ex} was observed for the selected value of ω_r. The results of such numerical calculations for $\omega_r > 0.828$ are shown in figure 1 by pluses to distinguish them from the results for $\omega_r < 0.828$ indicated by the solid curve which were obtained by using the method of reflections. Note that this refers only to the real part of λ_{p1} for $\omega > 0.828$. The dotted line in figure 1 corresponds to the contribution to λ_{p1} from the terms other than C_{ex}, i.e. the terms from the effective medium, finite wavelength, and exclusion region. We see that these terms dominate over the contribution from the close pair interactions (C_{ex}) over most values of ω_r except near 0.828.

As mentioned earlier, the imaginary part of λ_{p1} is non-zero and equals $-3\pi S_c'^2/t_0 f'(S_c')$ for $\omega_r > 0.828$ even when the damping terms are very small. Since $S_c' \to \infty$ and $f'(S_c') \to 0$ as $\omega_r \to 1$, we see that the magnitude of the imaginary part is very large for $\omega_c \to 1$. The calculated values of this quantity are shown in figure 3. Since $f(S_c') = 1/t_0$ and $f(S') = 1/S' + O(S'^{-4})$, $\mathrm{Im}\,(\lambda_{p1}) \to 3\pi t_0^3$ as $\omega_r \to 1$. From (3.63) we see that $\mathrm{Re}\,(\lambda_{p1}) \to \frac{3}{2} t_0^3 \ln t_0$, so that both the real and imaginary parts of λ_{p1} become large as $\omega_r \to 1$.

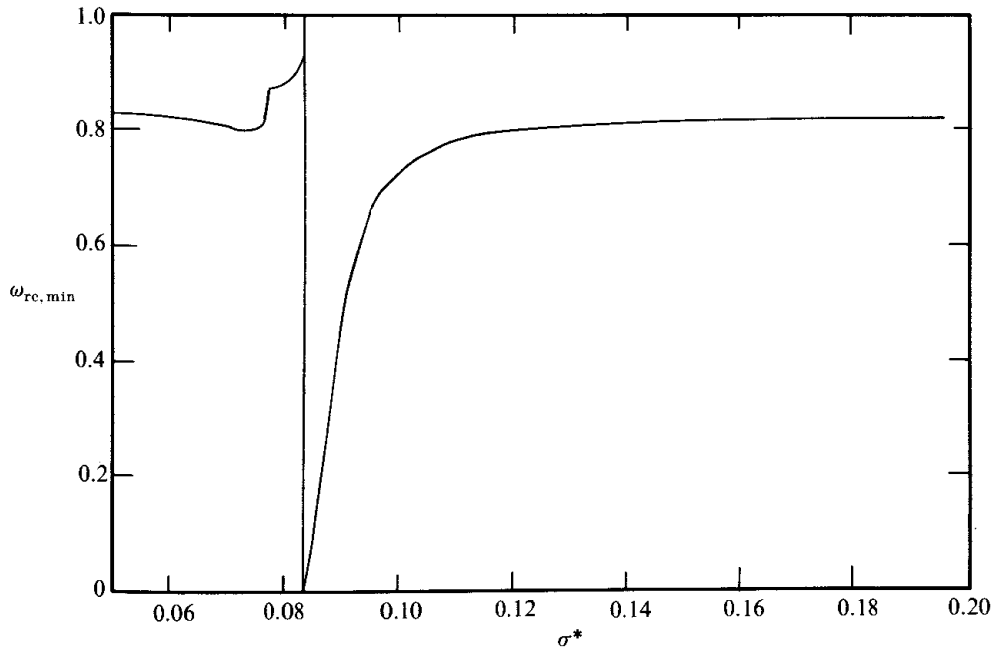

FIGURE 4. The ratio of minimum frequency for which a pair of bubbles resonants in the in-phase mode to the resonance frequency of isolated bubbles as a function of σ^*.

There is very little change in λ_{p1} as a function of ω_r as σ^* is decreased from infinity to about 0.15. For even smaller values of σ^*, however, there is a very rapid change in the behaviour of λ_{p1} in the vicinity of σ^* given by

$$\sigma_c^* = \frac{1}{(n^2-1)(n+2)}, \quad n = 2, 3, \ldots, \tag{3.69}$$

corresponding to the resonances in the P_n^m-mode shape deformation. Thus for finite surface tension there is an infinite number of modes in which pairs of bubbles resonate. In the vicinity of these critical values of the surface tension, resonance can occur even for very small values of ω_r. In figure 4 we have plotted the minimum in ω_{rc} among all the possible pairs of bubbles as a function of σ^*. For the range of values shown in this figure, the critical value of σ^* is $\frac{1}{12} = 0.08333\ldots$, corresponding $n = 2$ in (3.69). We see that as σ^* is slowly decreased from 0.2, ω_{rc} first decreases from about 0.8280 to zero at $\sigma^* = \frac{1}{12}$ and then suddenly jumps to unity for σ^* values slightly lower than $\frac{1}{12}$. The minimum in the resonance frequency occurs for nearly touching bubbles for $\sigma^* > \frac{1}{12}$, and for widely separated bubbles for σ^* slightly lower than $\frac{1}{12}$. As σ^* is further decreased, we find that first the separation distance for which the minimum in ω_{rc} occurs, decreases from ∞ to $2R$ as σ^* varies from $\frac{1}{12}$ to roughly about 0.077 and then once again the resonance of the pair of nearly touching bubbles determine ω_{rc} for smaller σ^*. Beyond this value of σ^*, ω_{rc} once again becomes constant until about $\sigma^* = \frac{1}{40} = 0.025$, whereby the P_3^m deformation begins to resonate and the same behaviour repeats except for the fact that the range over which the rapid changes in ω_{rc} now occurs becomes narrower.

Although the effect of surface tension in pairwise interactions described here is quite interesting, we find that its overall effect on λ_{p1} is not profound. As we decrease σ^* from ∞ to about 0.15, there is almost no change in λ_{p1} as a function of ω_r. Upon further decreasing σ^*, the frequency at which λ_{p1} diverges decreases in accordance with figure 4, but the range of frequency over which C_{ex} defined by (3.63) makes a significant contribution also becomes narrower. This is because $-f'(2)$ increases

rapidly as σ^* approaches $\frac{1}{12}$. For example, at σ^* equal to 0.1 and 0.09, $-f'(2)$ equals, respectively, 2.437 and 15.2. The corresponding values of B_1 and ω_{rc} are found to be respectively 2.462 and 0.7307 for $\sigma^* = 0.1$, and 0.3958 and 0.4763 for $\sigma^* = 0.09$. Furthermore, since t_0 is also small when ω_r is small, the magnitude of the imaginary part of λ_{p1} also decreases.

As concluding remarks to the calculations presented here, we recall that, as noted in §2.1, $\sigma^* = \sigma/(\rho_L R^3 \omega^2)$ can also be expressed, by means of (2.14), as $\sigma^* = \sigma/(3\gamma^* P_e R \omega_r^2)$. For P_e equal to 1 atm, $\sigma = 70$ dynes/cm, and $\omega_r^2 = 0.1$, σ^* is close to $\frac{1}{12}$ for bubbles having a radius of 0.3 mm, which is well within the range of practical applications and many experiments. Therefore we summarize the principal assumptions made in our calculations. We have assumed that all the bubbles are of equal size, there are no surface-active impurities in the mixture, deformations are small, the viscosity has a negligible effect, and the bubbles do not coalesce. The distribution in the size of the bubbles will not prevent the resonances due to shape deformation from occurring but ω_{rc} in that case will not jump rapidly from 0 to 1 as σ^* jumps across its critical values. The divergent nature of C_{ex} occurs only when the critical separation distance for the resonance of the pair of bubbles is close to $2R$. However, this can be significantly affected if a coalescence of the pair of nearly touching bubbles occurs as a result of the resonance, although the experimental observations often do not show evidence of significant coalescence. Finally, it may be noted that while the effect of the usual monopole resonance for an isolated bubble is felt over a fairly large range of frequencies, say $0.6 < \omega_r < 1$, the shape deformation resonance effects are felt only over a very narrow range of frequencies for a given gas–liquid mixture because of their weak logarithmic divergence. The damping terms usually present due to a finite viscosity and non-adiabatic thermal effects are likely to be the most important ones in preventing these logarithmic divergences from occurring, resulting in a much smoother response of the bubbly liquid as a function of frequency over these critical values of surface tension. Indeed, the numerical calculations for λ_p including the viscous and thermal dampings and for bubbles with diameters of about 5 mm carried out in §5 seem to show almost no effect of these shape-induced resonances.

3.3. *Determination of λ_v to $O(\beta)$ for small ω_r*

The estimates for λ_p correct to $O(\beta)$ and for $\lambda_{\sigma m}$ and λ_v to $O(1)$ obtained so far allow us to estimate C_{ef}^{-2} correct to $O(\beta^2)$ when the compressibility of the liquid can be neglected, i.e. when $k_L^2 R^2 \ll \beta\omega_r^2/(1-\omega_r^2)$. Since $\lambda_p \to \gamma/\gamma^*$ as $\omega_r \to 0$, for all values of β, it is possible to determine C_{ef}^{-2} correct to $O(\beta^3)$ by calculating $\lambda_{\sigma m}$ and λ_v correct only to $O(\beta)$ when ω_r is small. Since ω_r is indeed small in many practical situations, we shall determine in this section the $O(\beta)$ correction to λ_v for $\omega_r \to 0$. Also, since $k_L^2 R^2$ is typically very small, we shall assume that the liquid is essentially incompressible.

In §3.1 we found that the coefficient $\lambda_{\sigma m}$ equals $4\sigma^* t_0$ or, equivalently, $4/(3We\gamma^*(1-\omega_r^2))$, so that if we treat σ^* as an $O(1)$ quantity, then $\lambda_{\sigma m} \to 0$ as $\omega_r \to 0$. It should be noted that for an air–water system at ordinary temperatures and pressures We is approximately equal to $R \times 10^4$, R being in cm, and hence $\lambda_{\sigma m}$ is less than 0.1 whenever R is greater than 10^{-3} cm. In other words, the numerical value of $\lambda_{\sigma m}$ is small for most practical situations. Consequently, it is unimportant to evaluate the $O(\beta)$ correction to $\lambda_{\sigma m}$. On the other hand, the effect of surface tension through shape deformation of the bubbles is likely to be quite important and therefore we shall treat σ^* as an $O(1)$ quantity even though $\omega_r \to 0$.

To determine λ_v, we must solve once again (3.49), but instead of determining the

pressure inside the bubble at $\boldsymbol{x}_1$, we must now determine the acceleration of the bubble relative to the mixture. The condition that $\hat{p}_1$ must approach $\hat{p}_0$ as $|\boldsymbol{x}-\boldsymbol{x}_1| \to \infty$ can be expressed now as

$$\hat{p}_1 = \text{const} + \boldsymbol{E}\cdot\boldsymbol{s}, \quad s = |\boldsymbol{x}-\boldsymbol{x}_1| \to \infty, \tag{3.70}$$

since the pressure disturbances decay rapidly enough and the wavelength of the mixture is large. Here the constant equals $\hat{p}_a e^{-i\boldsymbol{k}\cdot\boldsymbol{x}_1}$ and $\boldsymbol{E} = -i\boldsymbol{k}\hat{p}_a e^{-i\boldsymbol{k}\cdot\boldsymbol{x}_1}$. Although the liquid acceleration is small, of $O(k)$, the ratio of the bubble to liquid accelerations remains finite and can be determined by treating $\boldsymbol{E}$ an $O(1)$ constant. For small ω_r, the radial oscillations of the bubble vanish and so the temporal variations in the pressure represented by the constant term in (3.70) do not cause any relative acceleration of the bubble. Consequently, we can set the constant in (3.70) to zero. Now $\hat{p}_1$ satisfies the Laplace equation outside the bubble with the boundary conditions at the bubble surface given by (2.13), and has a constant gradient at infinity. The solution of this problem has been determined by van Wijngaarden (1976) and Jeffrey (1973). In fact, the problem as posed above is exactly the same as the one examined by van Wijngaarden who used the volume averaging technique due to Batchelor (1974) and obtained the $O(\beta)$ correction to λ_v for $\sigma^* = \infty$. In a later article (Biesheuvel & van Wijngaarden 1984), it was suggested that the numerical coefficient of this $O(\beta)$ correction was in error. Jeffrey (1973) has examined an analogous problem of determining the effective thermal conductivity k^* of a composite consisting of spherical particles of thermal conductivity k_2 dispersed randomly in a matrix of thermal conductivity k_1. The pressure and velocity in the present problem are analogous to the temperature and heat flux in the problem examined by Jeffrey. The boundary conditions at the surface of the spheres, however, are generally different in the two problems. Only when $k_2/k_1 = \infty$ and $\sigma^* = 0$ do the two problems become identical. In fact, it can be readily shown that there is an exact relationship between λ_v and k^* in this case for all values of β:

$$\lambda_v(\sigma^* = 0) = \frac{k^* - k_1}{\beta k^*} \quad \left(\frac{k_2}{k_1} = \infty\right). \tag{3.71}$$

Since the calculations of λ_v for the complete range of σ^* have not been reported in the literature and since there was some uncertainty about the accuracy of the coefficient of $O(\beta)$ as reported by van Wijngaarden (1976), we have re-examined this problem using Hinch's ensemble averaging technique. The strength of the monopole A^1_{00} in (3.55) now vanishes and the components of the dipole strength (A^1_{1m}) now determine λ_v. Let us express the dipole strength of the bubble at $\boldsymbol{x}_1$ by a vector $\boldsymbol{A}^1$ as

$$\boldsymbol{A}^1\cdot\boldsymbol{\nabla} \equiv \sum_{m=-1}^{1} A^1_{1m}\, Y_1^m\left(\frac{\partial}{\partial s_1}, \frac{\partial}{\partial s_2}, \frac{\partial}{\partial s_3}\right). \tag{3.72}$$

Now the procedure to determine the $O(\beta)$ correction is essentially the same as that described by steps (i)–(iv) in §3.2. The velocity of the bubble at $\boldsymbol{x}_1$ is calculated from the behaviour of the particular part of $\boldsymbol{\nabla}\hat{p}_1$ evaluated at the centre of the bubble by means of

$$-i\omega\rho_L \boldsymbol{u}_1 = 3\boldsymbol{\nabla}\hat{p}_{1,\,\mathrm{par}}(\boldsymbol{x}_1). \tag{3.73}$$

There are two contributions to $\hat{p}_{1,\,\mathrm{par}}$. The first one, which is similar to that from the effective-medium part in §3.2, corresponds to a uniform distribution of dipoles of

strength $\boldsymbol{A}^0 = \boldsymbol{E}R^3$ for $S' \geqslant 2$, and its contribution to $\nabla\hat{p}_{1,\mathrm{par}}$ can be shown readily to equal $\boldsymbol{E}(1+\beta)$. The second part, which arises from the pairwise interactions, is given by

$$\nabla\hat{p}^{\mathrm{p}}_{1,\mathrm{par}} = \int_{S\geqslant 2R} \mathrm{d}V_2 P_{\mathrm{c}}\left[\sum_{nm} A^2_{nm}\, \mathrm{Y}^m_n \nabla\frac{1}{|\boldsymbol{x}-\boldsymbol{x}_2|} - \boldsymbol{A}^0\cdot\nabla\nabla\frac{1}{|\boldsymbol{x}-\boldsymbol{x}_2|}\right]_{x=x_1}. \tag{3.74}$$

Once again, it can be shown from the details of the two-bubble problem that the quantity inside the square brackets on the right-hand side of the above equation is exactly equal to the dipole strength of the bubble at $\boldsymbol{x}_1$ minus the first two reflections in the pairwise interactions. Now from Jeffrey's (1973) solution for the Laplace field around two spheres we can express the dipole strength of the sphere at $\boldsymbol{x}_1$ as

$$\frac{\boldsymbol{A}^1}{R^3} = g_{11}\boldsymbol{E} - \boldsymbol{E}\cdot\frac{\boldsymbol{S}'\boldsymbol{S}'}{S'^2}(g_{01}+g_{11}), \tag{3.75}$$

where g_{01} and g_{11} are scalar functions of S' and σ^*. Combining the contributions from both the effective-medium part and the pairwise interactions, and making use of the fact that for $We \approx \infty$

$$\hat{\boldsymbol{u}}_0 = (1+3\beta)\boldsymbol{E}, \tag{3.76}$$

it can be shown that the ratio of the acceleration of the bubble to that of the mixture is given by

$$\lambda_v = 3[1+\lambda_{v1}\beta] = 3\left[1+\beta\left\{-2+\int_2^\infty (2g_{11}-g_{01}-3)\,S'^2\,\mathrm{d}S'\right\}\right]. \tag{3.77}$$

The evaluation of g_{01} and g_{11} is similar to that in the Jeffrey's paper except that β_n which were defined in terms of k_2/k_1 in that paper are now defined in terms of σ^* by means of

$$\beta_n = \frac{1+n\sigma^*[n(n+1)-2]}{1-(n+1)\,\sigma^*[n(n+1)-2]}. \tag{3.78}$$

Note that for the special case of $\sigma^* = 0$, the above expression reduces to $\beta_n = 1$ for all n, which is also the case for $k_2/k_1 = \infty$, and this, in turn, suggests the aforementioned connection between λ_v and k^* (cf. (3.71)). The quantity $2g_{11}-g_{01}-3$ in (3.77) can be expanded in inverse powers of S' as in Jeffrey (1973). The leading-order term as $S' \to \infty$ is $O(S'^{-6})$ corresponding to the third term in the expansion of $\boldsymbol{A}^1/R^3$, and the integral in (3.77) can be expressed as

$$\int_2^\infty (2g_{11}-g_{01}-3)\,S'^2\,\mathrm{d}S' = \sum_{p=6}^{\infty}\int_2^\infty \frac{b_p}{S'^p}S'^2\,\mathrm{d}S' = \sum_{p=6}^{\infty}\frac{b_p 2^{3-p}}{p-3}. \tag{3.79}$$

The first few coefficients of the above series are given by

$$b_6 = 6;\quad b_7 = 0;\quad b_8 = 15\beta_2;\quad b_9 = 6, \tag{3.80}$$

where use has been made of the fact that $\beta_1 = 1$ for all σ^*.

The convergence of the series in the above expression was found to be generally slow, and up to about 60 terms were needed in determining the $O(\beta)$ coefficient for the two extreme values of σ^* of 0 to ∞. For $\sigma^* = \infty$, this coefficient approached -1.846, which is in agreement with the value -1.85 reported by van Wijngaarden

(1976) in his original study. Thus we believe that the remark made by this author in his later work (Biesheuvel & van Wijngaarden 1984) must be ignored. (In a more recent study, Biesheuvel & Spoelstra (1989) have also quoted the coefficient to equal -1.85, thus confirming the validity of the original result.)

For $\sigma^* = 0$, the $O(\beta)$ coefficient equals -1.50, which is in agreement with the result reported by Jeffrey (1973) after making use of (3.71). (For $k_2/k_1 = \infty$, Jeffrey gave $k^*/k_1 = 1+3\beta+4.51\beta^2$.)

3.3.1. *Resonance effects in λ_v for finite surface tensions*

We now discuss the dependence of the $O(\beta)$ coefficient of λ_v on intermediate values of σ^*. In particular, it is of interest to examine the influence of the shape-dependent resonances. Note that, as mentioned earlier, although we are interested in the present section in situations where ω_r is small compared to unity, we may still have $\sigma^* = \sigma/(\rho_L R^3\omega^2)$ small enough that these shape-dependent resonances occur even for small ω_r. As an illustration of the effect of these resonances, let us examine the case when σ^* is nearly equal to $\frac{1}{12}$ corresponding to the P_2^m-mode resonance (cf. (3.69)). Let $\epsilon = \sigma^* - \frac{1}{12}$ be a small quantity. We note from (3.78) that $\beta_2 \to \pm\infty$ as $\epsilon \to \pm 0$, and therefore it is clear that the series in (3.79) will diverge as $\epsilon \to 0$. An analysis of the equations that arise in the two-sphere interactions shows that for, small ϵ,

$$g_{11} = 1 - \frac{1}{S'^3}\left[1 + \frac{3}{(\frac{36}{5}\epsilon S'^5 - 4)}\right] + O(S'^{-6}), \tag{3.81}$$

$$g_{01} = -1 - \frac{1}{S'^3}\left[2 - \frac{3}{(\frac{12}{5}\epsilon S'^5 + 2)}\right] + O(S'^{-6}). \tag{3.82}$$

Thus we see that the coefficients of $O(S'^{-3})$ (the second reflection) in g_{11} and g_{01} depend on $\epsilon S'^5$. The magnitude of this reflection in the inner resonance region ($2 \leqslant S' < \epsilon^{-\frac{1}{5}}$) is quite different from its value for a pair of widely separated bubbles. In other words, the magnitude of this reflection remains quite different from that used in determining the contribution from the effective-medium part. Since the series in (3.79) diverges for small ϵ, we must evaluate the integral in (3.79) directly by evaluating g_{01} and g_{11} numerically as a function of S' using the method of direct substitution described in Appendix A. Separating the contributions in (3.79) that decay slowly when ϵ is small from the remainder we write

$$\int_2^\infty \frac{\mathrm{d}S'}{S}\left[\frac{-\frac{3}{2}}{\frac{6}{5}\epsilon S'^5 + 1} + \frac{\frac{3}{2}}{1 - \frac{9}{5}\epsilon S'^5}\right] + \int_2^\infty S'^2\,\mathrm{d}S'(2g_{11}^r - g_{10}^r), \tag{3.83}$$

where g_{11}^r and g_{01}^r are the remainders that decay uniformly as S'^{-6} as $\epsilon \to 0$. Now we note that although the contribution from each term in the first integral in (3.83) taken separately does not converge, their combination does and hence this integral approaches a constant as $\epsilon \to 0$. Consequently, the $O(\beta)$ correction to λ_v is finite even when $\epsilon = 0$. The detailed numerical calculations using the Simpson's rule for integration yielded the $O(\beta)$ correction to λ_v to be -2.10 for $\epsilon = 0$.

The above discussion applies to the other critical values of σ^* (cf. (3.69)) also, so that we conclude that λ_v is finite at $\sigma^* = \sigma_c^*$. While there is no divergence at $\epsilon = 0$, we find that the calculation of λ_{v1} for finite ϵ is not so straightforward and that, in fact, there are other values of σ^* for which λ_{v1} diverges. The difficulty arises from the fact that the denominator in (3.81) diverges for $\epsilon S'^5 = \frac{5}{9}$ implying that, at this

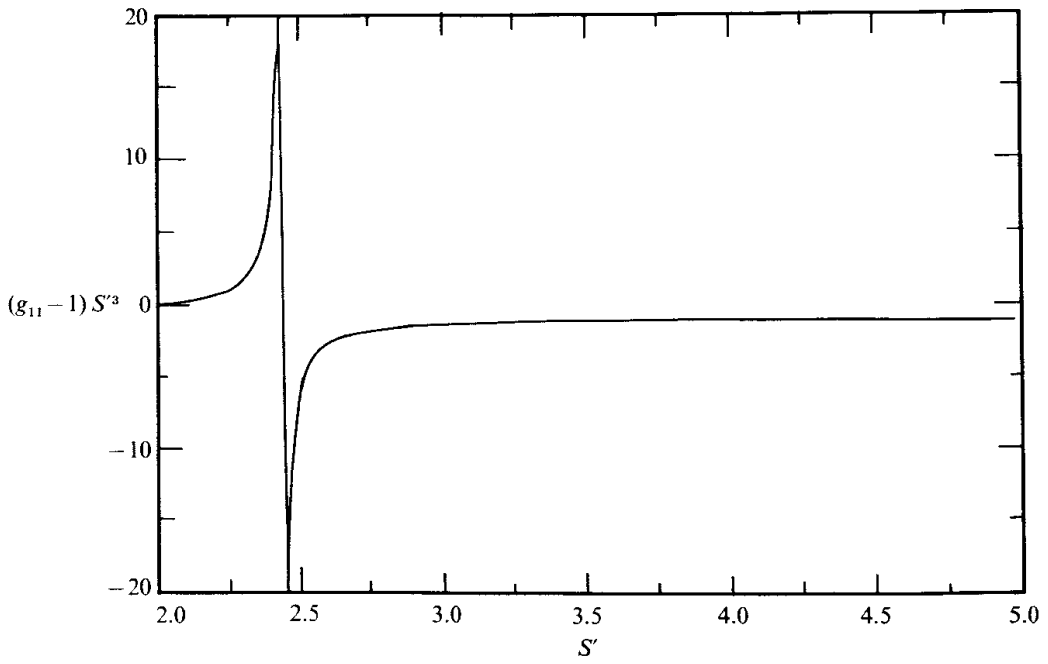

FIGURE 5. The quantity $(g_{11}-1)S'^3$ as a function of $S' = S/R$ for a pair of bubbles at $\epsilon = \sigma^* - \frac{1}{12} = 0.01$ and small ω_r.

separation distance between the pair of bubbles (provided that $S' \geqslant 2$), $g_{11} \to \pm\infty$. Although the expression for g_{11} given by (3.81) is valid only asymptotically for large S' and small ϵ, we note that the higher-order terms only change the precise S' at which g_{11} diverges. For example, figure 5 shows $(g_{11}-1)S'^3$ as a function of S' for $\epsilon = 0.01$ as determined numerically by solving the two-sphere problem by the method of direct substitution for various S' using a sufficiently large number of multipoles. It is seen that the divergence occurs at $S' \approx 2.4$, while $\epsilon S'^5 = \frac{5}{9}$ yields $S' = 2.23$. Thus, for ϵ-values which give the divergence of g_{11} for some S' greater than 2, there is a difficulty in evaluating the λ_{v1}. Since at such critical values of S' the function g_{11} changes its value from $+\infty$ to $-\infty$, we note that the contribution from the large positive values of g_{11} will roughly cancel that from the large negative values, resulting in a finite contribution. In other words, we must once again evaluate the principal value of the integral in (3.79) when g_{11} diverges for some S' greater than 2. For one critical value of ϵ, however, the divergence in g_{11} will occur precisely at $S' = 2$ and for ϵ-values close to that critical value we must observe a logarithmic divergence of λ_{v1}. Thus, for example, we find that

$$\lambda_{v1} = 0.14 \ln|\sigma^* - \sigma^*_{\text{crit}}| - 1.73, \quad \sigma^*_{\text{crit}} \approx 0.109. \tag{3.84}$$

Here the constants 0.109 and 0.14 are evaluated from the divergent nature of g_{11} near $\sigma^* = \sigma^*_{\text{crit}}$ and the constant 1.73 is evaluated by comparing the numerical results for λ_{v1} for $\sigma^* > 0.109$ with the leading order in (3.84).

Similarly, the denominator in the term on the right-hand side of (3.82) becomes zero for some S' for negative values of ϵ and, consequently, once again there will be a logarithmic divergence in λ_{v1} near a negative value of ϵ. The detailed calculations show that this occurs at $\epsilon = -0.0208$ or at $\sigma^* = 0.0625$. While $\lambda_{v1} \to -\infty$ as $\sigma^* \to 0.109$, we find that $\lambda_{v1} \to +\infty$ as $\sigma^* \to 0.0625$. Thus, although λ_{v1} is finite exactly at $\sigma^* = \sigma^*_c$ given by (3.69), it diverges at two values of σ^* in the vicinity of this critical value. This behaviour is also observed near other critical values of σ^* with each σ^*_c

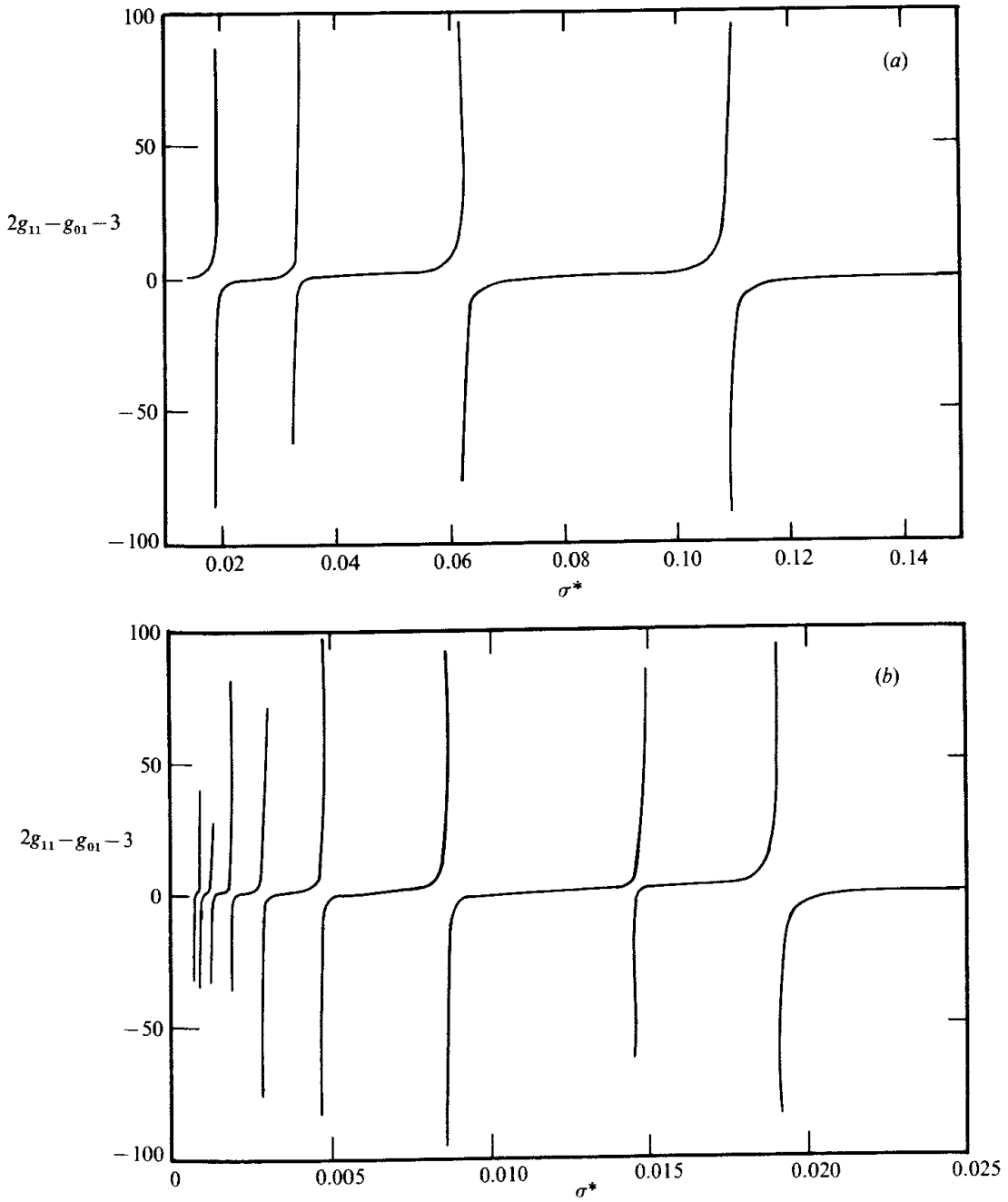

FIGURE 6(*a*, *b*). The quantity $2g_{11}-g_{01}-3$ at the surface of the bubble as a function of $\sigma^*(\omega_r = 0)$.

in (3.69) giving a pair of values of σ^* for which λ_{v1} diverges. This can be shown by evaluating the quantity $2g_{11}-g_{01}-3$ at $S' = 2$ as a function of σ^*. This quantity, as shown in figure 6, goes through $\pm\infty$ near each critical σ_c^*. The calculations have been carried out for σ^* values up to about 0.0005 in figure 6(*b*) and it appears from these calculations that the range of ϵ-values for each critical σ_c^* over which the influence of a particular P_n^m-mode resonance is felt, becomes narrower at a sufficiently fast rate for larger n so that there is no overlap of the resonance range for one n with that corresponding to the other n. In other words, it appears that λ_{v1} goes through an infinite number of discontinuities in the limit $\sigma^* \to 0$.

From the above discussion it is clear that for σ^* values near each critical σ_c^* given by (3.69) there will always be a pair of bubbles that resonates due to shape

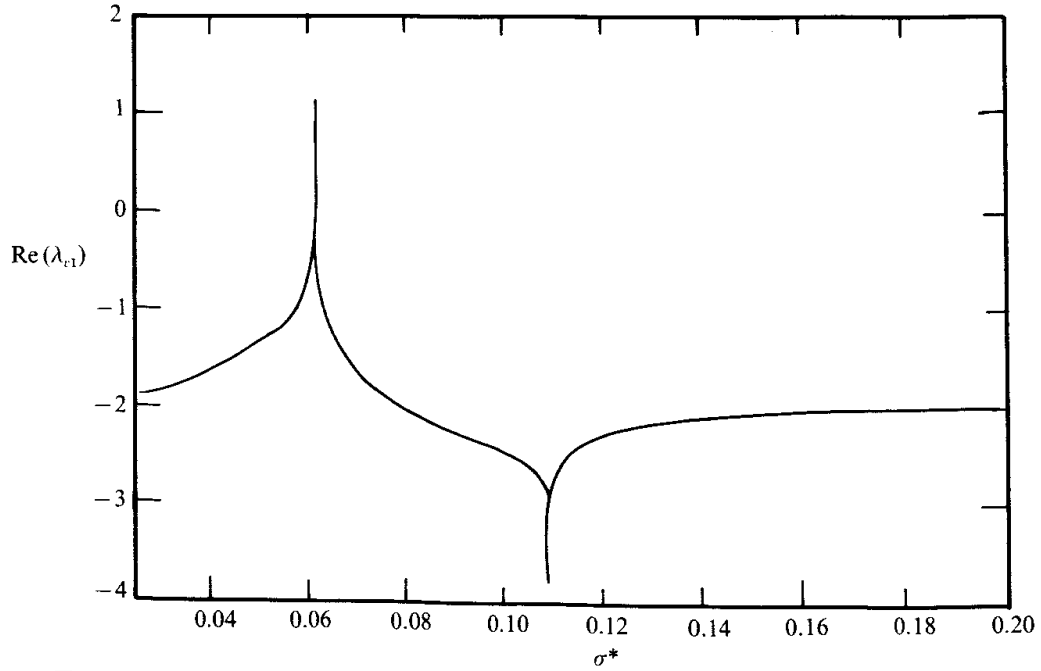

FIGURE 7. The real part of the $O(\beta)$ coefficient of λ_v as a function of σ^* for small ω_r.

deformations and λ_{v1} is indeterminate in the absence of any damping mechanism. In the presence of slight damping, however, the contribution from the nearly resonating pairs will cancel and λ_{v1} can then be determined by evaluating the principal value of the integral in (3.77) as in §3.2.1. The results are shown in figure 7. The peaks near each critical σ^* becomes narrower as we decrease σ^* from about 0.12 to 0. The approximate values of σ^* at which λ_{v1} diverges are 0.109 and 0.0621, corresponding to $\sigma_c^* = \frac{1}{12} = 0.0833\ldots$ for the P_2-mode resonance, and at 0.0328 and 0.01898 for $\sigma_c^* = \frac{1}{40} = 0.025$ or the P_3^m-mode resonance. The results for σ^* in the range 0.0621–0.109 and 0.01898–0.0328 were, of course, determined from the principal value of the integral in (3.77). Since the series in (3.79) does not converge even when σ^* is outside these ranges, all the calculations shown in figure 7 were made by the direct substitution method.

As in the case of λ_{p1}, an imaginary contribution also arises for λ_{v1} for a range of σ^* values around each σ_c^* whenever it is required to evaluate the principal value of the integral. Thus an attenuation of $O(1)$ arises from pairwise interactions even when ω_r is small. (Of course, at sufficiently small ω_r, σ^* will eventually exceed 0.109 for a fixed We and below such frequencies there will be no attenuation due to shape deformations.) When the damping term is small, the imaginary part of λ_{v1} can be determined easily from S_c', at which the resonance occurs, and the derivative of $(S'-S_c')(2g_{11}-g_{01}-3)$ at S_c'. The results for σ^* in the range 0.062–0.109 are shown in figure 8. As $\sigma^* \to \frac{1}{12}$, resonance occurs for widely separated bubbles and the asymptotic expressions for g_{11} and g_{01} as given by (3.81) and (3.82) become applicable. From these expressions it is easy to show that $\mathrm{Im}\,(\lambda_{v1}) \to \pm 3\pi/10$ as $\epsilon = \sigma - \frac{1}{12} \to \pm 0$. In other words, this quantity goes through a jump discontinuity at $\sigma^* = \frac{1}{12}$. Thus the result $\lambda_{v1} = -2.10$ at $\epsilon = 0$ mentioned earlier is actually correct if we take the imaginary part to equal the mean of its limiting values for $\epsilon \to \pm 0$.

We also find that $\mathrm{Im}\,(\lambda_{v1})$ remains finite as $\sigma^* \to 0.109_-$ and $\sigma^* \to 0.062_+$ since the derivatives of $(S'-2)(2g_{11}-g_{01}-3)$ remain finite at these critical values corresponding to the resonance of pairs of touching bubbles.

Finally, it may be noted that the above discussion for $\mathrm{Im}\,(\lambda_{v1})$ applies strictly in

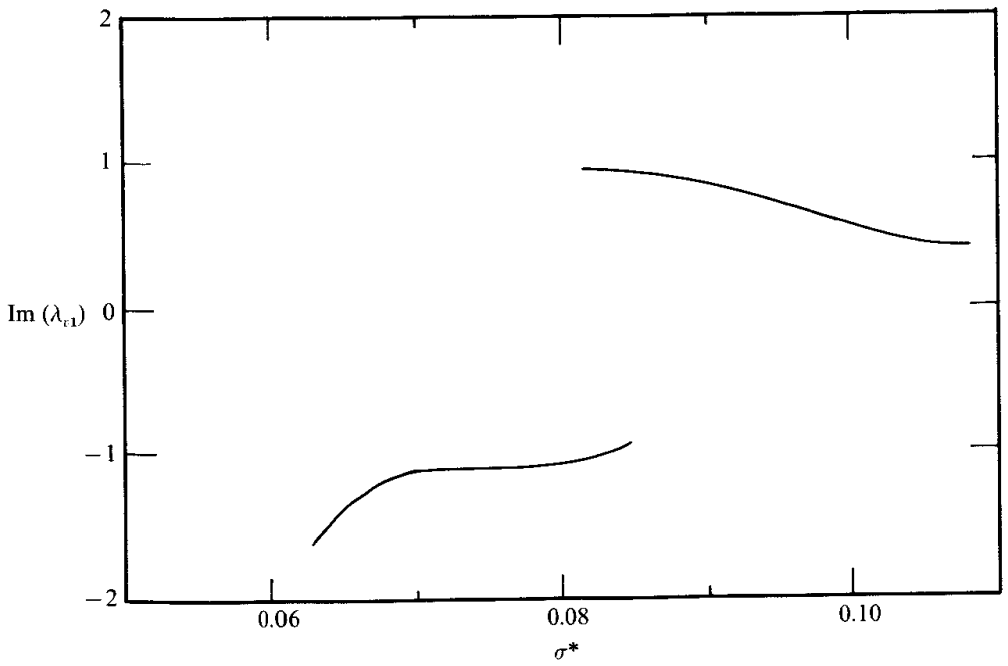

FIGURE 8. The imaginary part of the $O(\beta)$ coefficient of λ_v as a function of σ^* for small ω_r.

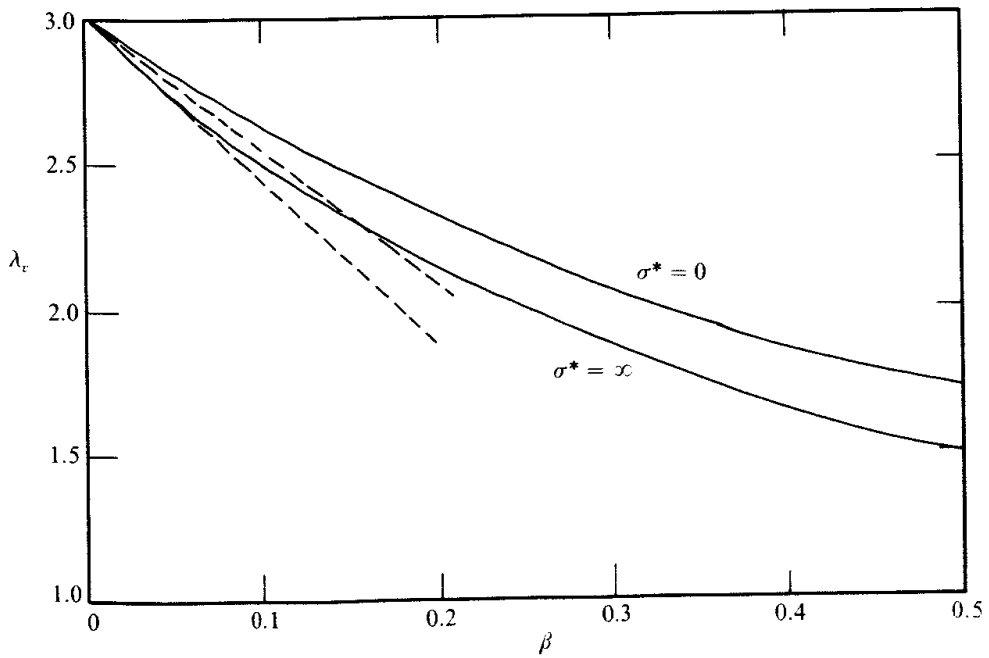

FIGURE 9. λ_v as a function of β for $\sigma^* = \infty$ and small ω_r. The solid curves are the results of large-scale numerical simulations using 16 bubbles randomly placed within a unit cell and the dashed curves are due to the $O(\beta)$ theories for σ^* equal to 0 and ∞. The results of simulations for $\sigma^* = \infty$ are taken from Sangani *et al.* (1991) and those for $\sigma^* = 0$ are obtained from the results of effective thermal conductivity presented by Sangani & Yao (1988) by making use of (3.71).

the limit of small damping. If we fix the damping to an arbitrary but small value, then the behaviour of Im (λ_{v1}) will, of course, be affected eventually by the exact value of the damping for σ^* sufficiently close to 0.062, $\frac{1}{12}$, and 0.109. We shall address this question again in §4 where we explicitly take into account the damping due to small viscosity.

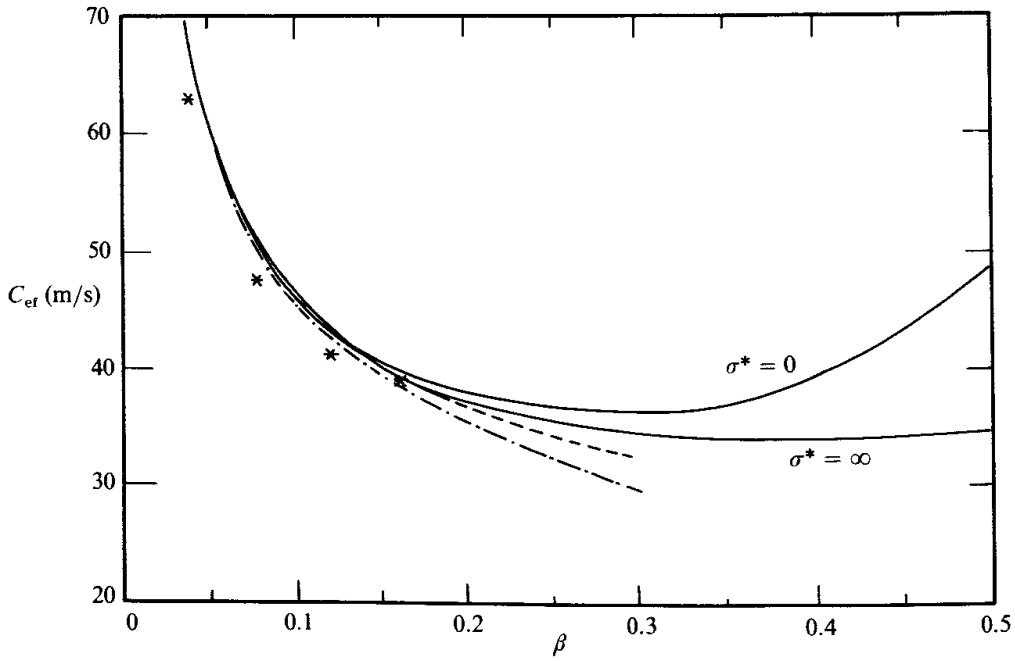

FIGURE 10. Effective speed of sound as a function of β for small ω_r. The experimental data of Micaelli (1982) are denoted by stars; the broken curves are due to the $O(\beta^3)$ theory; and the solid curves are calculated from the numerical values of λ_v taken from the simulations of Sangani *et al.* (1991) and Sangani & Yao (1988).

3.3.2. *Comparison with the numerical and experimental results*

Using the methods of computing multiparticle interactions now available it is possible to compute λ_v directly by a large-scale simulation involving a sufficiently large number of randomly placed bubbles. The corresponding calculations for the determination of the effective conductivity were made by Sangani & Yao (1988). Using the method outlined there, Sangani *et al.* (1991) have recently determined λ_v for selected values of σ^* and β. Their results with $\sigma^* = \infty$ are shown in figure 9. The corresponding results for $\sigma^* = 0$ as obtained from the numerical results for effective conductivity with $k_2/k_1 = \infty$ as given by Sangani & Yao and using (3.71) are also shown. The comparison of these direct numerical simulations with the asymptotic expressions for λ_v obtained here shows that the latter yield reasonable estimates of λ_v up to about $\beta = 0.2$.

In figure 10 we have compared the speed of sound calculated by substituting the above estimates of λ_v in

$$C_{ef}^{-2} = \frac{\beta\rho_L}{\gamma^* P_e}(1-\beta\lambda_v), \tag{3.85}$$

with the experimental values reported by Micaelli (1982). (Actually the data were taken from Caflisch *et al.* (1985*b*) who have reproduced them from the original work of Micaelli.) In these experiments, P_e was about 1.12 bar, the radius of the bubbles was about 2 mm, and the frequencies ν were in the range of 20–80 Hz (1 Hz $= 2\pi$ s^{-1}). Of course, $\rho_L = 1$ g/cm^3 and $\gamma^* \approx 1.4$. If we take $\sigma = 70$ dynes/cm, then σ^* is in the range 0.55–0.03 and ω_r is in the range 0.012–0.05. We see that the agreement between the theoretical expressions derived here with $\sigma^* = \infty$ and $\omega_r = 0$ and the experimental data is very good for β-values up to about 0.15 (beyond which experimental data are not available). In addition, we have also shown the estimates of C_{ef} as obtained from the results of direct numerical simulations of multiparticle

interactions for λ_v given in figure 9. In the absence of coalescence or other nonlinear effects, λ_v determined from these numerical simulations are expected to yield estimates of C_{ef} that are valid even when β is not small (ω_r must, of course, be small and σ^* values above 0.109 for their validity). From these estimates, it is evident that the speed of sound does not vary significantly in the low-frequency regime for β-values in the range of about 0.1 to 0.5. In this range, the compressibility of the mixture increases roughly by a factor of 5 but the decrease in the relative acceleration of the bubble reduces the factor $1-\lambda_v\beta$ by roughly the same amount, resulting in a nearly constant effective speed of sound over a wide range of β.

Finally, we note that although our theory, which ignored the damping due to finite viscosity or thermal effects, suggested that λ_v should become very sensitive to the variations in σ^* when the latter is smaller than 0.15, there does not seem to be any evidence of the resonance effects in the experimental data of Micaelli (1982).

3.3.3. *Effects of buoyancy*

In the calculations presented so far we have ignored the effects of viscosity, surface-active impurities, buoyancy, and nonlinearities due to finite-amplitude deformations and coalescence. The effect of slight viscosity and non-adiabatic changes will be discussed in the following two sections. Here we discuss briefly the effect of buoyancy as its effect is relevant to the discussion of experimental data reported by Micaelli.

Buoyancy can affect our results in a number of ways. These include its effect on the shape of the bubbles, the conditional pair probability density function P_c, the distribution of surface-active impurities on the surface of the bubbles, and the generation of the base flow around each bubble, which, in turn, interacts with the flow due to acoustics. The bubbles in Micaelli's experiments were 2 mm in radius and the deformation of bubbles of this size rising under gravity is generally significant. Here, however, we shall concentrate only on the effect of flow generated due to buoyancy. Thus, we shall assume that surface-active impurities are absent and that the bubbles rise under the influence of buoyancy keeping their shape nearly spherical.

If we denote the base flow and the pressure distribution generated due to the rise of the bubbles by $(\boldsymbol{v}, q)$, ignore the compressibility of the liquid and nonlinear effects, and take $We \approx \infty$, then the momentum and continuity equations reduce to

$$\rho_L(1-g)\,[\mathrm{i}\omega\hat{\boldsymbol{u}} + \boldsymbol{\nabla}\cdot(\hat{\boldsymbol{u}}\boldsymbol{v} + (\hat{\boldsymbol{u}}\boldsymbol{v})^+)] + \boldsymbol{\nabla}\hat{p} = 0, \tag{3.86}$$

$$\frac{g}{\gamma P_e}(\mathrm{i}\omega\hat{p} + \boldsymbol{v}\cdot\boldsymbol{\nabla}\hat{p} + \boldsymbol{u}\cdot\boldsymbol{\nabla}\hat{q}) + \boldsymbol{\nabla}\cdot\hat{\boldsymbol{u}} = 0, \tag{3.87}$$

where g, as before, is the generalized function whose value is unity inside the gas bubbles and zero outside, and $\hat{\boldsymbol{u}}$ and $\hat{p}$ are the amplitudes of the velocity and pressure fluctuations due to sound waves. If the average rise velocity of the bubbles is V, then the relative magnitude of the second term inside the square brackets in (3.86) compared to the first term in that equation is $O(V/R\omega)$, which can be large depending upon R and ω. If we assume that V is determined by the balance of buoyancy and viscous drag (drag $= 12\pi\mu VR$, where μ is the viscosity of the liquid) under conditions of nearly potential flow, then for the conditions under which Micaelli's experiments were conducted, i.e. $R = 2$ mm and $\omega = 125$–$500\ \mathrm{s}^{-1}$, $V/R\omega$ is about 10. Thus there is no reason *a priori* to believe that the buoyancy had a negligible effect on the effective speed of the sound measured by Micaelli. The details of the analysis are presented in

Appendix B where we show that the primary effect of the buoyancy at $O(\beta)$ is to reduce the resonance frequency of the bubbles. Thus the factor $(1-\omega_r^2)$ is now replaced by $(1-(1+B^2)\omega_r^2)$. With ω_r of approximately 0.03, this corresponds to a correction factor of about 10%. The $O(\beta)$ coefficient of λ_v will also vary with B but its determination as a function of B will not be pursued here.

4. Viscosity effects

In §3 we found that the resonance due to a pair of bubbles occurs at frequencies lower than the natural frequency of the bubbles and leads to infinite estimates of λ_p and λ_v at frequencies other than the natural frequencies. Near such resonance frequencies, however, the damping due to viscosity can play an important role and hence we now analyse the effect of viscosity on the ensemble-averaged equations and the estimates of λ_p and λ_v. We shall continue to assume that the compressibility of the liquid may be regarded as negligible. To simplify the calculations, we shall also assume that the viscosity of the gas is negligible. We therefore write the viscous stress in the medium as

$$\boldsymbol{\tau} = \mu(1-g)\,[\boldsymbol{\nabla u} + (\boldsymbol{\nabla u})^+ - \tfrac{2}{3}\boldsymbol{I}\boldsymbol{\nabla}\cdot\boldsymbol{u}], \tag{4.1}$$

where μ is the viscosity of the liquid and $\boldsymbol{I}$ is the unit tensor. Note that since the liquid is regarded as incompressible and since the viscosity of the gas is assumed to be negligible, we can alternatively express $\boldsymbol{\tau}$ without the last term on the right-hand side of (4.1). Both expressions are equivalent and yield the same final result upon taking ensemble averages. The average viscous stress is given by

$$\boldsymbol{\tau}_0 = \mu[\boldsymbol{\nabla u}_0 + (\boldsymbol{\nabla u}_0)^+ - \tfrac{2}{3}\boldsymbol{I}\boldsymbol{\nabla}\cdot\boldsymbol{u}_0] - \frac{\beta\mu}{V_b}\int_{s\leqslant R}[\boldsymbol{\nabla u}_1 + (\boldsymbol{\nabla u}_1)^+ - \tfrac{2}{3}\boldsymbol{I}\boldsymbol{\nabla}\cdot\boldsymbol{u}_1]\,\mathrm{d}V_1. \tag{4.2}$$

Inside the bubble, $\boldsymbol{u}_1$ is still given by $\boldsymbol{\nabla}\varphi_1$, with φ_1 given by (3.34), so that it can be readily seen that the integral on the right-hand side of (4.2) is $O(E_{20})$ (cf. (3.34)), which is $O(k^2)$. Neglecting this small term, the ensemble-averaged continuity and momentum equations are now given by

$$\frac{\beta\lambda_p}{\gamma P_e}\frac{\partial p_0}{\partial t} + \boldsymbol{\nabla}\cdot\boldsymbol{u}_0 = 0, \tag{4.3}$$

$$\rho_L(1-\lambda_v\beta)\frac{\partial \boldsymbol{u}_0}{\partial t} + \boldsymbol{\nabla}p_0 - \mu(\nabla^2\boldsymbol{u}_0 + \tfrac{1}{3}\boldsymbol{\nabla}\boldsymbol{\nabla}\cdot\boldsymbol{u}_0) = 0, \tag{4.4}$$

where λ_p and λ_v are now functions of viscosity and we have neglected $\lambda_{\sigma m}$ as $We \approx \infty$. Eliminating $\boldsymbol{u}_0$ from the above equations, we see that p_0 satisfies the wave equation and that the dispersion relation is now given by

$$\frac{k^2}{\omega^2} = (1-\lambda_v\beta)\frac{\beta\rho_L\lambda_p}{\gamma P_e}\left[1 + \mathrm{i}\frac{4\mu\beta\omega\lambda_p}{3\gamma P_e}\right]^{-1}. \tag{4.5}$$

It should be noted that the term $\boldsymbol{\nabla}\boldsymbol{\nabla}\cdot\boldsymbol{u}_0$ in (4.4), which resulted from keeping the term $\boldsymbol{\nabla}\cdot\boldsymbol{u}$ in (4.1), is actually an $O(\beta)$ quantity as can be seen from (4.3). If we had chosen to estimate the viscous stress by its alternative expression without the $\boldsymbol{\nabla}\cdot\boldsymbol{u}$ term in (4.1), then we would have found the term containing the integral over the volume of

the bubble in (4.2) to be proportional to the pressure inside the gas bubble, and then evaluating that integral in terms of λ_p would have given exactly the same expression as (4.4) derived here.

4.1. *Viscous corrections to the $O(1)$ estimates of λ_p and λ_v*

We now determine the corrections to the $O(1)$ estimates of λ_p and λ_v when the viscosity of the liquid is not negligible. Neglecting the two-bubble interaction terms, the conditionally averaged continuity and momentum equations with one bubble fixed at $\boldsymbol{x}_1$ satisfy, for $\boldsymbol{x}$ outside the bubble,

$$\boldsymbol{\nabla}\cdot\hat{\boldsymbol{u}}_1 = 0, \tag{4.6}$$

$$(\mathrm{i}\omega\rho_{\mathrm{L}} - \mu\nabla^2)\,\hat{\boldsymbol{u}}_1 + \boldsymbol{\nabla}\hat{p}_1 = 0. \tag{4.7}$$

We shall assume that there are no surface-active impurities at the bubble surface so that the tangential stress there is zero. The solution of these equations yield estimates of λ_p and λ_v as

$$\lambda_p = \frac{\gamma}{\gamma^*[1-\omega_{\mathrm{r}}^2(1-4\mathrm{i}\mu^*)]}, \tag{4.8}$$

$$\lambda_v = \frac{1+\alpha R+\frac{1}{2}\alpha^2R^2+\frac{1}{6}\alpha^3R^3}{1+\alpha R+\frac{1}{6}\alpha^2R^2+\frac{1}{18}\alpha^3R^3}, \quad \alpha^2R^2 = \mathrm{i}\frac{\omega R^2\rho_{\mathrm{L}}}{\mu} = \frac{\mathrm{i}}{\mu^*}, \tag{4.9}$$

where $\mu^* = \mu/(\omega R^2\rho_{\mathrm{L}})$ is the non-dimensional viscosity of the liquid. It may be noted that λ_v approaches unity in the limit $\mu^*\to\infty$, corresponding to no relative acceleration of the bubble with respect to the mixture for very viscous fluids, and to $3+36\mathrm{i}\mu^*$ for small μ^* or nearly inviscid flows. Miksis & Ting (1987) have examined the viscous effects for very small ω_{r} and k in which case, once again, $\lambda_p\to\gamma/\gamma^*$ for all values of β and the dispersion relation (4.5) to $O(\beta^2)$ can be determined solely from the $O(1)$ estimate of λ_v obtained here. These authors considered a more general case by including the finite viscosity of the gas, but their results agree with those derived here upon setting the gas viscosity to zero.

4.2. *Viscous corrections to the $O(\beta)$ estimates of λ_p and λ_v*

The viscous corrections obtained in the previous section are valid for arbitrary values of the non-dimensional viscosity μ^*. We are now interested in determining the corrections for higher-order terms in β when μ^* is small. It is customary to employ the energy dissipation method to estimate the small viscosity corrections, as was done by Levich (1962), who used it to estimate the viscous drag force on a single bubble. Using this method, for example, it is easy to show that, for a single bubble, $\lambda_v\to 3+36\mathrm{i}\mu^*+O(\mu^{*\frac{3}{2}})$, which is in accordance with the analysis of the previous section. The presence of slight viscosity is only important very close to the surface of the bubble where the tangential stress must be zero (Batchelor 1967). The potential flow approximation, which is very accurate for most regions of the flow, yields a non-zero estimate of the tangential stress at the surface of the bubble so that a modification to the stress components is needed near the surface of the bubble. This slight modification, however, makes a negligible contribution to the overall dissipation, which can thus be evaluated from the potential flow approximation.

For the case of a pair of two bubbles which are simultaneously undergoing volume and displacement oscillations and for the case of finite surface tension, it is difficult

to use the dissipation method, and so we devise a different method for estimating directly the viscous drag on the individual bubbles. The method presented here is also useful in calculations involving more than two bubbles as the dissipation method in that case cannot be used to estimate the viscous drag on the individual bubbles. A method for directly evaluating the viscous drag has also been presented recently by Kang & Leal (1988) who used it to study the deformation of bubbles under an axisymmetric straining flow.

Let us start by examining the interaction of two bubbles placed in a viscous liquid. The velocity and pressure satisfying (4.6) and (4.7) for this problem can be determined from (see, for example, Kim & Russel 1985*a* who solved a similar problem involving an interaction of two spheres in a Brinkman medium):

$$\hat{\boldsymbol{u}} = \frac{-1}{\mathrm{i}\omega\rho_{\mathrm{L}}}\nabla\hat{p} + \sum_{q=1}^{2}\{\nabla\times\nabla\times[(\boldsymbol{x}-\boldsymbol{x}_q)\hat{\boldsymbol{\Phi}}_q] + \nabla\times[(\boldsymbol{x}-\boldsymbol{x}_q)\hat{\chi}_q]\}, \tag{4.10}$$

with the pressure field $\hat{p}$, poloidal field $\hat{\boldsymbol{\Phi}}_q$, and toroidal field $\hat{\chi}_q$ satisfying

$$\nabla^2\hat{p} = 0, \quad \nabla^2\hat{\boldsymbol{\Phi}}_q = \alpha^2\hat{\boldsymbol{\Phi}}_q, \quad \nabla^2\hat{\chi}_q = \alpha^2\hat{\chi}_q. \tag{4.11}$$

Here we have dropped the subscript 2 (for the two-bubble conditional fields) on the velocity and pressure fields for brevity. The conditionally averaged $\hat{p}_2$ actually satisfies the Helmholtz equation instead of the Laplace equation shown here but, as we shall see presently, the calculations presented here are needed only for determining the higher-order reflections in the two-bubble interaction problem, and the Laplace equation provides adequate accuracy for estimating these higher-order reflections. Now the poloidal and toroidal fields can be expanded around the centre of each bubble in terms of modified spherical Bessel functions k_n (Abramowitz & Stegun 1972) as

$$\hat{\boldsymbol{\Phi}}_q = \sum_{n=0}^{\infty}\sum_{m=-n}^{n} b_{nm}^q\, k_n(\alpha s_q)\, P_n^m(\cos\theta)\,\mathrm{e}^{\mathrm{i}m\phi}, \tag{4.12}$$

$$\hat{\chi}_q = \sum_{n=0}^{\infty}\sum_{m=-n}^{n} c_{nm}^q\, k_n(\alpha s_q)\, P_n^m(\cos\theta)\,\mathrm{e}^{\mathrm{i}m\phi}, \tag{4.13}$$

where s_q is the radial distance measured from the centre of the bubble at $\boldsymbol{x}_q$. The coefficients b_{nm}^q and c_{nm}^q together with the coefficients in the expansion of $\hat{p}$ in spherical harmonics can then be determined from the boundary conditions on the surface of each bubble after making use of the appropriate addition theorems for the modified spherical Bessel functions or numerically by a collocation technique, as was done by Kim & Russel (1985*a*). The analysis for the case of small viscosity (large α), however, is considerably simpler as we can then make use of the fact that the functions k_n decay exponentially and hence the poloidal and toroidal fields of one bubble do not influence the velocity field near the surface of the other bubble (unless, of course, the two bubbles are nearly in contact). In other words, these fields for each bubble are important only in thin boundary layers surrounding each bubble. Since the pressure, on the other hand, satisfies the Laplace equation, its variations occur on a lengthscale comparable with the separation distance between the bubbles. Thus we expand the pressure field in a regular perturbation series in powers of $\mu^{*\frac{1}{2}}$ as

$$\hat{p} = \hat{p}^0 + \mu^{*\frac{1}{2}}\hat{p}^1 + \mu^*\hat{p}^2 + \ldots. \tag{4.14}$$

Further details of the calculations are given in Appendix A where we show that $\hat{p}^1$

vanishes for a bubble surface free of surface-active impurities and that the boundary conditions for $\hat{p}^0$ and $\hat{p}^2$ on the surface of the bubbles are given by

$$\hat{p}^0_{nm} + f(n) R \frac{\partial \hat{p}^0_{nm}}{\partial s} = 0, \tag{4.15}$$

$$\hat{p}^2_{nm} + f(n) R \frac{\partial \hat{p}^2_{nm}}{\partial s} = 2\mathrm{i}\left[R^2 \frac{\partial \hat{p}^0_{nm}}{\partial s^2} + n(n+1) f(n) \left(\hat{p}^0_{nm} - R \frac{\partial \hat{p}^0_{nm}}{\partial s}\right)\right], \tag{4.16}$$

where $f(0) = 1/\omega_r^2$ and $f(n) = \sigma^*[n(n+1)-2]$ for $n \geqslant 1$. Here $\hat{p}_{nm}$ is related to the expansion of $\hat{p}$ near the bubble at $\boldsymbol{x}_q$ by means of

$$\hat{p} = \sum_{n=0}^{\infty} \sum_{m=-n}^{n} \hat{p}_{nm}(s) P_n^m(\cos\theta) \, \mathrm{e}^{\mathrm{i}m\phi}. \tag{4.17}$$

It is easily seen that the boundary conditions (4.15) for $\hat{p}^0$ are the same as given by (2.13) for the potential flow approximation. Thus the scheme for calculating the viscous correction consists of first solving for the potential flow approximation for a pair of bubbles and then evaluating the right-hand side of (4.16) to determine the boundary conditions for the viscous correction to the pressure field.

We now determine the viscous correction to $O(\beta)$ terms in λ_p. The calculation, as before, consists of determining the contributions from the effective-medium and pairwise-interaction parts separately. The effective-medium part for the pressure satisfies as before (cf. (3.51)) the Helmholtz equation except that now k^2 is given by

$$k^2 R^2 = z^2 = \frac{3\beta\omega_r^2}{1-\omega_r^2(1-4\mathrm{i}\mu^*)} \equiv 3\beta t_v. \tag{4.18}$$

We are only interested in the spherically symmetric part of the pressure distribution around the bubble at $\boldsymbol{x}_1$ in determining λ_p^e. This part is unaffected by the poloidal and the toroidal fields and so the contribution to the normal stress from the radial flow near the surface of the bubble can be easily evaluated and is valid for arbitrary values of μ^*. The viscosity to be used in evaluating the normal stress at the surface is that of the pure liquid and not the effective viscosity of the mixture. The contributions from the effective medium and the finite wavelength can be calculated by replacing t_0 in (3.52) by t_v. An extra term equal to $-2\mathrm{i}\mu^*$ now arises due to the different normal stress condition. Similarly, the calculation for the pairwise interactions can also be carried out and the resulting expression for λ_p is

$$\lambda_p = \frac{\gamma t_v}{\gamma^* \omega_r^2}[1 - \mathrm{i}zt_v(1+\tfrac{1}{2}\pi z t_v) - \tfrac{3}{2}t_v^3 \beta \ln\beta - \beta\lambda_{p1}] \tag{4.19}$$

with λ_{p1} given by

$$\lambda_{p1} = 3t_v\left[\tfrac{8}{5} + \tfrac{1}{2}t_v\left(3 + \frac{1}{\omega_r^2}\right) + t_v^2(3.899\,11 + \tfrac{1}{2}\ln t_v) - 2\mathrm{i}\mu^*\right] + C_{ex}. \tag{4.20}$$

Here C_{ex} is the contribution from the fourth and higher-order reflections in the two-bubble problem that can be expressed as $C_{ex} = C_{ex}^0 + \mathrm{i}\mu^* C_{ex}^2$, with C_{ex}^0 being the same as that obtained from the potential flow approximation in §3 (cf. (3.63)) and C_{ex}^2 the correction due to small μ^*.

It may be noted that in evaluating all the terms in (4.19) and (4.20), except for the evaluation of the higher-order reflections (C_{ex}), the flow near each bubble may be approximated as radial. For all of these radial flow terms, the toroidal and poloidal

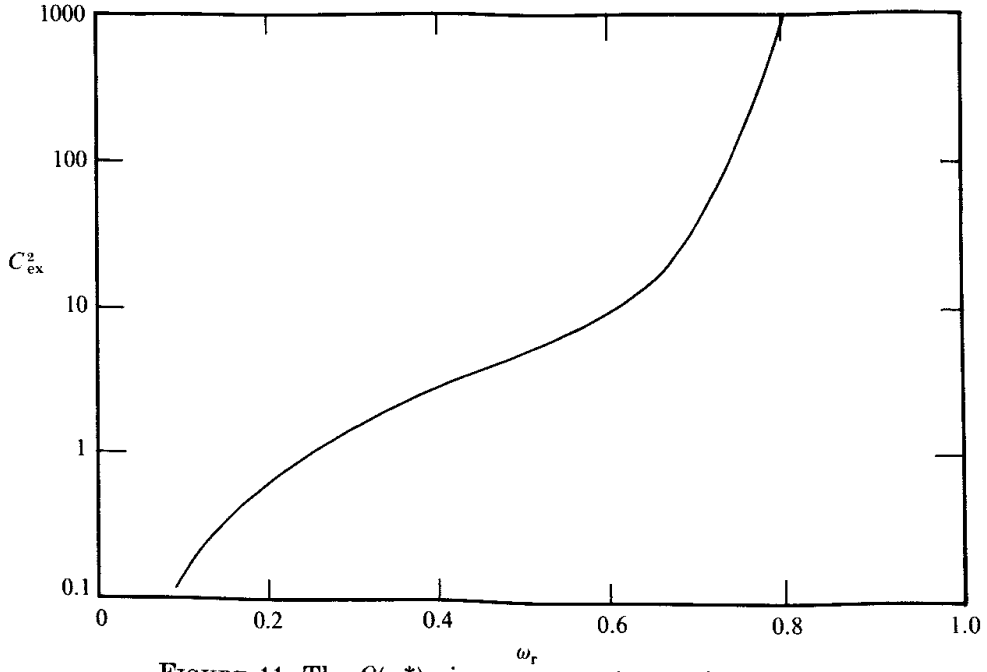

FIGURE 11. The $O(\mu^*)$ viscous correction to C_{ex} for $\sigma^* = \infty$.

fields do not contribute. Thus they are all exact for arbitrary values of μ^* and the approximation of small viscosity is used only in evaluating C_{ex}. Also since these reflections decay as $1/S^4$ or faster, we can approximate the Helmholtz equation for $\hat{p}_2$ by the Laplace equation and this justifies our ignoring the $k^2\hat{p}_2$ term in (4.11).

4.2.1. *Numerical results for the viscous correction to the $O(\beta)$ coefficient of λ_p*

To calculate the viscous correction to C_{ex}, t_v and A_{00}^1 are first expanded for small μ^* as

$$t_v = \frac{\omega_r^2}{1-\omega_r^2+4i\mu^*\omega_r^2} = t_0 - 4it_0^2\mu^* + O(\mu^{*2}), \tag{4.21}$$

$$A_{00}^1 = A_{00}^{0,1} + i\mu^* A_{00}^{2,1} + \ldots, \tag{4.22}$$

and substituted in the expression for C_{ex} to obtain

$$C_{ex} = C_{ex}^0 + i\mu^* C_{ex}^2 + O(\mu^{*\frac{3}{2}}) = 3\int_{S'=2}^{\infty} \left\{1 + \frac{t_v}{S'} + \frac{t_v^2}{S'^2} + \frac{t_v^3}{S'^3} - \frac{A_{00}^1}{Rt_v}\right\} S'^2\, dS'$$

$$= C_{ex}^0 - 3i\mu^* \int_{S'=2}^{\infty} \left\{\frac{4t_0^2}{S'} + \frac{8t_0^3}{S'^2} + \frac{12t_0^4}{S'^3} + \frac{4A_{00}^{0,1}}{R} + \frac{A_{00}^{2,1}}{Rt_0}\right\} S'^2\, dS', \tag{4.23}$$

where C_{ex}^0 is the same as the potential flow contribution calculated in §3. Now C_{ex}^2 can be calculated either by the method of successive approximations, in which both $A_{00}^{0,1}$ and $A_{00}^{2,1}$ are expanded in inverse powers of S' and each term then analytically integrated to yield a series expansion for C_{ex}^0 and C_{ex}^2, or by the method of direct substitution in which both $A_{00}^{0,1}$ and $A_{00}^{2,1}$ are evaluated directly for each S' separately and then the integration carried out numerically using Simpson's rule. The method of successive approximations converged rapidly for ω_r less than 0.8 and the results for $\sigma^* = \infty$ are shown in figure 11. The viscous correction to C_{ex} increases rapidly beyond ω_r of approximately 0.6, and, in fact, diverges as ω_r approaches 0.828, corresponding to a pair of nearly touching bubbles at their resonance frequency. This, however, does not imply that λ_p diverges in the presence of viscosity. In fact, we expect the viscosity to act as a damping mechanism, and thus to yield a finite estimate of λ_p at all frequencies. The difficulty arises here because we are trying

to evaluate the viscosity correction as a regular perturbation over the inviscid estimate of λ_p. To obtain therefore a finite estimate of λ_p for $0 < \omega_{rc} - \omega_r \ll 1$, with $\omega_{rc} = 0.828$, we must retain the viscous correction to A^1_{00} in the denominator, i.e. write A^1_{00}/Rt_v as

$$\frac{A_{00}}{Rt_v} = \frac{1}{1 - t_v f(S')}$$

$$= \frac{1 - \omega_r^2(1 - 4i\mu^*)}{1 - \omega_r^2(1 - 4i\mu^*) - \omega_r^2[f_0 + if_2\mu^* + (f_0' + i\mu^* f_2')(S' - 2)]}, \tag{4.24}$$

where $f(S') = f_0(S') + i\mu^* f_2(S')$, and f_0, f_2, f_0', etc. are evaluated at $S' = 2$. Now the leading-order terms in the denominator of the term on the far right of the above equation can be expressed as $1 - \omega_r^2[1 + f_0(2)] = 2\Delta/\omega_{rc}$, where $\Delta \equiv \omega_{rc} - \omega_r$, so that the integral in (4.23) diverges logarithmically for small μ^* and Δ at the lower limit $S' = 2$ as

$$C_{ex} = \frac{-12 f_0}{f_0'} \ln\left[i(4 + f_2)\mu^* + \frac{2\Delta}{\omega_{rc}^3}\right] + \text{const.} \tag{4.25}$$

The constant $-12 f_0/f_0'$ is same as B_1 in (3.66) and equals 28.75 for $\sigma^* = \infty$. Thus we see that C_{ex} and hence λ_p are finite even at $\Delta = 0$ when the viscosity is finite. It is also clear from the above calculation that if we treat the viscosity as a small term and expand A_{00}/Rt_v for small viscosity first and then evaluate each term separately, then each of the terms in the expansion will diverge at $\Delta = 0$. The results presented in figure 11 are thus useful only for ω_r much smaller than 0.828.

The difficulty becomes more severe for $\omega_r > 0.828$ for which there is always a pair of bubbles having a separation distance between $2R$ and ∞ that resonates. As seen in §3, there is an $O(1)$ imaginary contribution to C_{ex} even when $\mu^* \to 0$ in this case that results upon using the principal value of the integral in evaluating C_{ex}. To evaluate the $O(\mu^*)$ correction, the expression similar to (3.68) must now be expanded to $O(\mu^*)$ (or $O(\Gamma)$ in (3.68)) and the appropriate corrections must be made to the integrand in (4.23) to subtract its singularity, which is now proportional to $1/(S' - S_c')^2$. Such calculations, however, have a limited utility as this $O(\mu^*)$ correction will again diverge as $\omega_r \to 0.828$, and therefore we shall not present these results.

Since it is not possible to obtain $O(1)$ and $O(\mu^*)$ estimates of C_{ex} that are uniformly valid for the complete range of ω_r, it is perhaps best to evaluate C_{ex} directly for selected values of μ^*. The procedure for evaluating such viscous corrections to λ_p is to first evaluate A^1_{00} numerically for selected values of μ^* and S' and then to compute the integral in (4.23) numerically. It is important in this calculation to keep the term that corresponds to the viscous correction to A^1_{00}/Rt_v in the denominator. Thus after determining $A^{0,1}_{00}$ and $A^{2,1}_{00}$ for each S' for a selected value of ω_r, the integrand in (4.23) is expressed as

$$1 + \frac{t_v}{S'} + \frac{t_v^2}{S'^2} + \frac{t_v^3}{S'^3} - \frac{A^1_{00}}{Rt_v} \equiv I_0 - i\mu^* I_2 + \ldots \approx \left[\frac{1}{I_0} + i\mu^* \frac{I_2}{I_0^2}\right]^{-1}. \tag{4.26}$$

where I_0 and I_2 are the coefficients of $O(1)$ and $O(\mu^*)$ terms in the expansion of the term on the far left of the above equation and are related to $A^{0,1}_{00}$ and $A^{2,1}_{00}$. Note that although both I_0 and I_2 taken individually diverge at $\omega_r = 0.828$, the term on the far right of the above expression remains finite.

The estimates of C_{ex} for small but finite μ^* obtained by the above procedure are shown in figures 12 and 13. Note that $\mu^* = \mu/(\omega R^2 \rho_L)$ can be expressed as μ_c^*/ω_r,

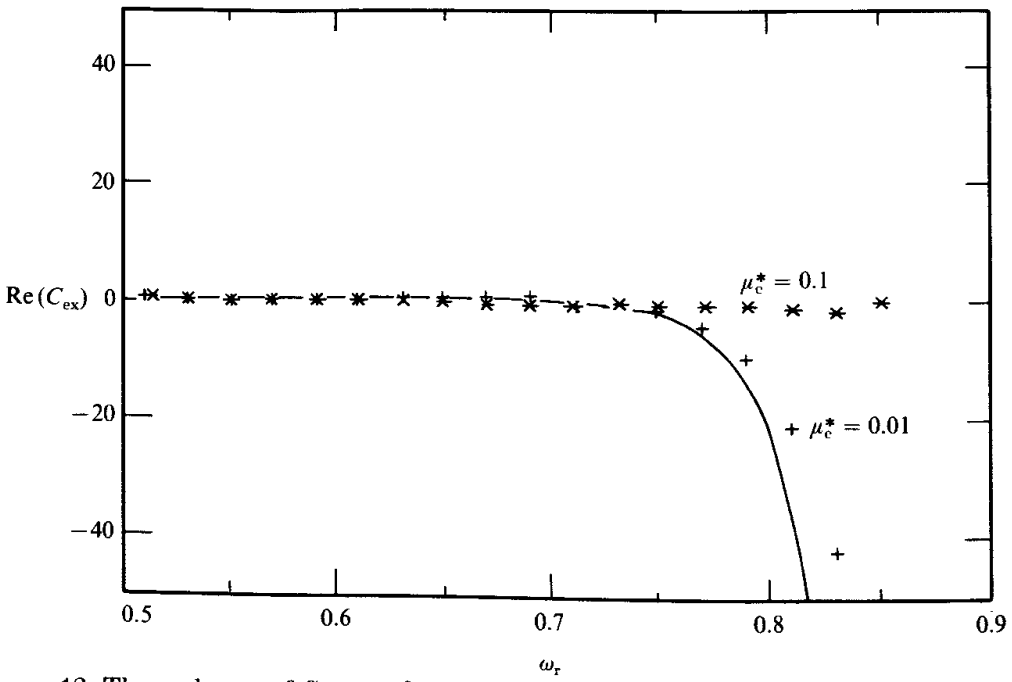

FIGURE 12. The real part of C_{ex} as a function of ω_r for $\sigma^* = \infty$. The solid curve corresponds to the calculations of §3 with $\mu_c^* = 0$ and pluses and stars correspond to those for finite values of μ_c^*.

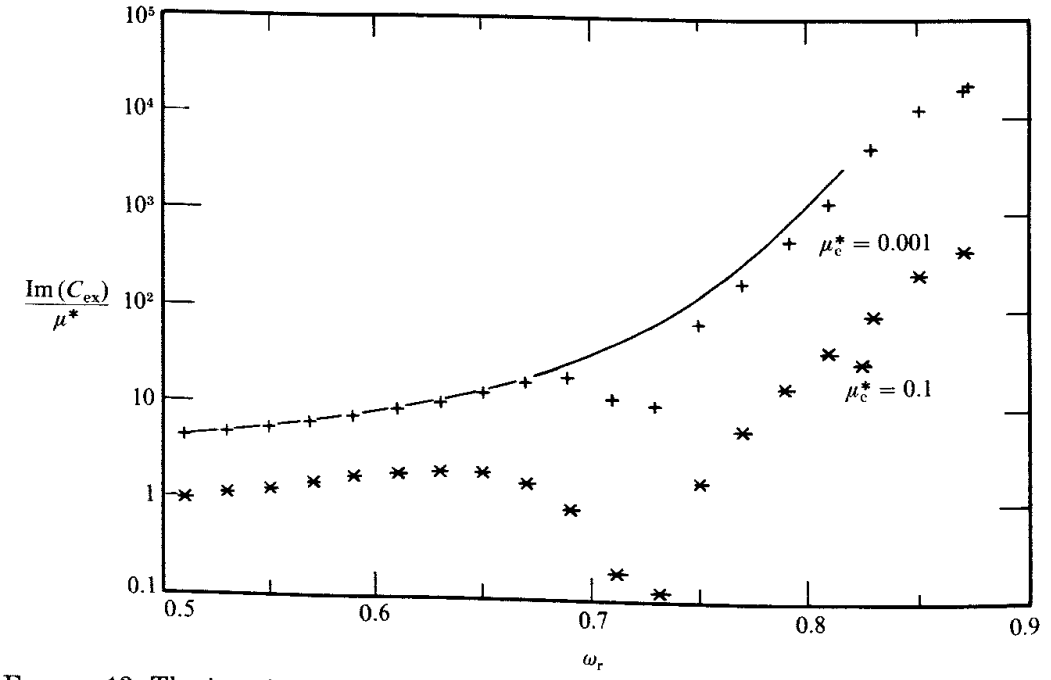

FIGURE 13. The imaginary part of C_{ex}/μ^* as a function of ω_r for $\sigma^* = \infty$. The solid curve is the asymptotic result for small μ_c^* and pluses and stars are with small finite values of μ_c^*.

where $\mu_c^* = \mu/(3\gamma^*\rho_L R^2 P_e)^{\frac{1}{2}}$ is the non-dimensional viscosity based on the natural frequency of the bubbles. For an air–water system at atmospheric pressure μ_c^* roughly equals $10^{-3}/(2R)$, R being in mm, so that μ_c^* is in the range 0.1–0.001 for bubbles with radii in the range 0.005–0.5 mm. The solid curves in figures 12 and 13 are obtained by the method of successive approximations for $\mu^* \to 0$ whereas the stars and pluses are obtained by the direct substitution method for various values of μ_c^*. We see that the results for $\mu_c^* = 0.001$, which correspond to bubbles with radius of about 0.5 mm, have been approximated quite well by the asymptotic results for small μ_c^*. On the other hand, the damping is quite significant for $\mu^* = 0.1$. We see

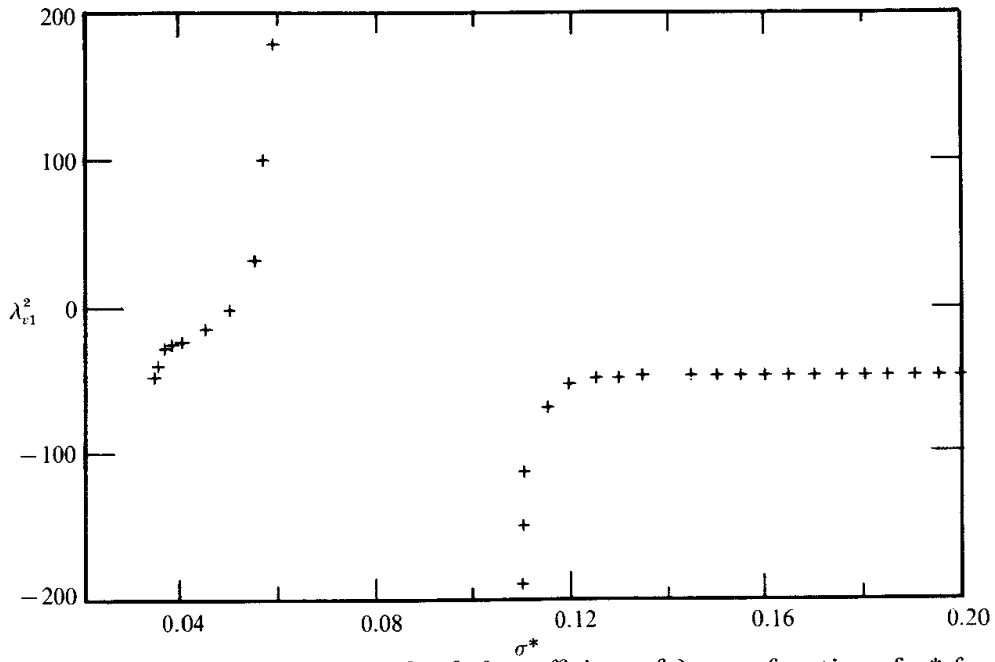

FIGURE 14. The $O(\mu^*)$ correction to the $O(\beta)$ coefficient of λ_v as a function of σ^* for small ω_r. This correction diverges for a range of σ^* values around each critical σ_c^*.

that there is a substantial decrease in C_{ex} and hence λ_p for ω_r near 0.828 even in the presence of viscous damping for bubbles that are greater than say 0.5 mm.

4.3. *The viscous correction to the $O(\beta)$ estimate of λ_v*

When ω_r is small, we can determine the effective speed and attenuation to $O(\beta^3)$ simply by determining λ_v correct to $O(\beta)$, and therefore in this section we shall present the results for the viscous correction to the $O(\beta)$ coefficient in λ_v. Following the same procedure as in §3.3, we can show that λ_v is given by

$$\lambda_v = 3+36\mathrm{i}\mu^*+3\beta\left\{-2(1+24\mathrm{i}\mu^*)+\int_2^\infty [2g_{11}-g_{01}-3(1+12\mathrm{i}\mu^*)]S'^2\,\mathrm{d}S'\right\}$$
$$= 3[1+12\mathrm{i}\mu^*+\beta(\lambda_{v1}^0+\mathrm{i}\mu^*\lambda_{v1}^2)], \tag{4.27}$$

where g_{11} and g_{01} are now functions of μ^* in addition to S' and σ^*. The potential flow approximation yields the results for λ_{v1}^0 which were presented in §3.3 and the first correction due to viscosity is given by λ_{v1}^2, which is determined by expanding g_{01} and g_{11} in a power series of $\mu^{*\frac{1}{2}}$. Detailed numerical calculations gave λ_{v1}^2 equal to -38 and -18 for σ^* equal to ∞ and 0. The calculation for the case of $\sigma^*=0$ was slightly difficult computationally as the pair of nearly touching bubbles made a significant contribution to the overall value of the coefficient. The pressure distribution on the surface of the bubbles becomes uniform when $\sigma^*\to 0$. It can be shown that the viscous dissipation in the gap between nearly touching bubbles is very large in this case and that the dipole strengths of the bubbles (or, equivalently, g_{01}) become $O(1/((S'-2)^2\ln(S'-2))$ as $S'\to 2$. The presence of the logarithmic term is important in making the overall integral in (4.27) convergent, but it also makes the exact determination of the coefficient λ_{v1}^2 somewhat difficult. We estimate that the result $\lambda_{v1}^2=-18$ is therefore correct only to within $\pm 10\%$.

The variation of λ_{v1}^2 for intermediate values of σ^* is not gradual as in the case of λ_{v1}^0 owing to the shape-dependent resonances. The results for σ^* in the range 0.04–0.20 are shown in figure 14. There is no significant change in λ_{v1}^2 as σ^* is varied from ∞ to about 0.12. Upon further decreasing σ^*, however, λ_{v1}^2 decreases rapidly

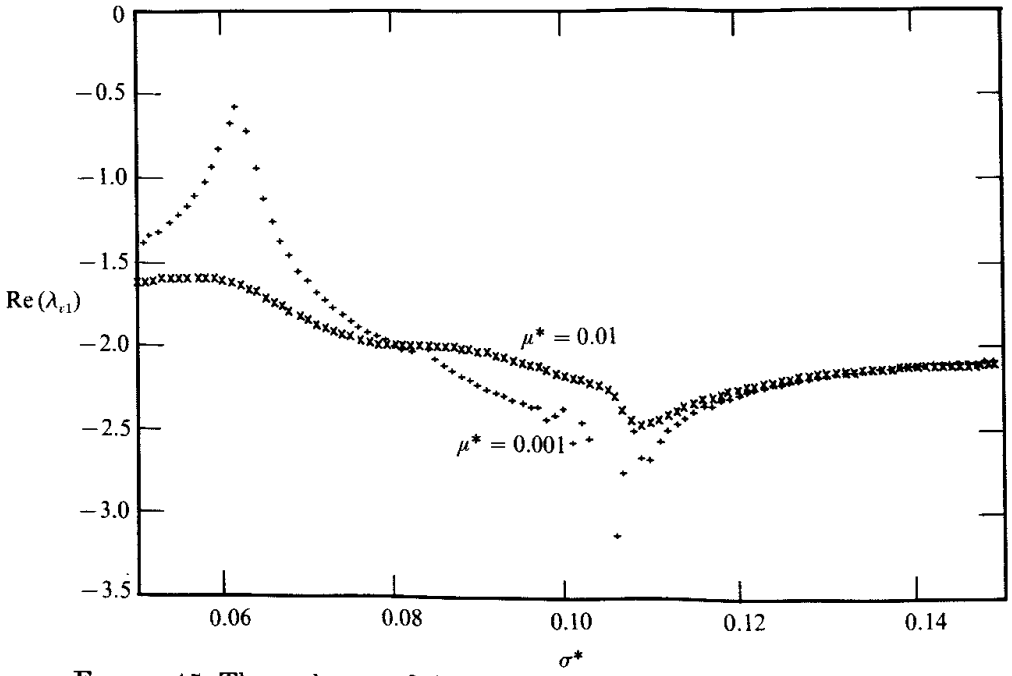

FIGURE 15. The real part of the $O(\beta)$ coefficient of λ_v as a function of σ^* and μ^*.

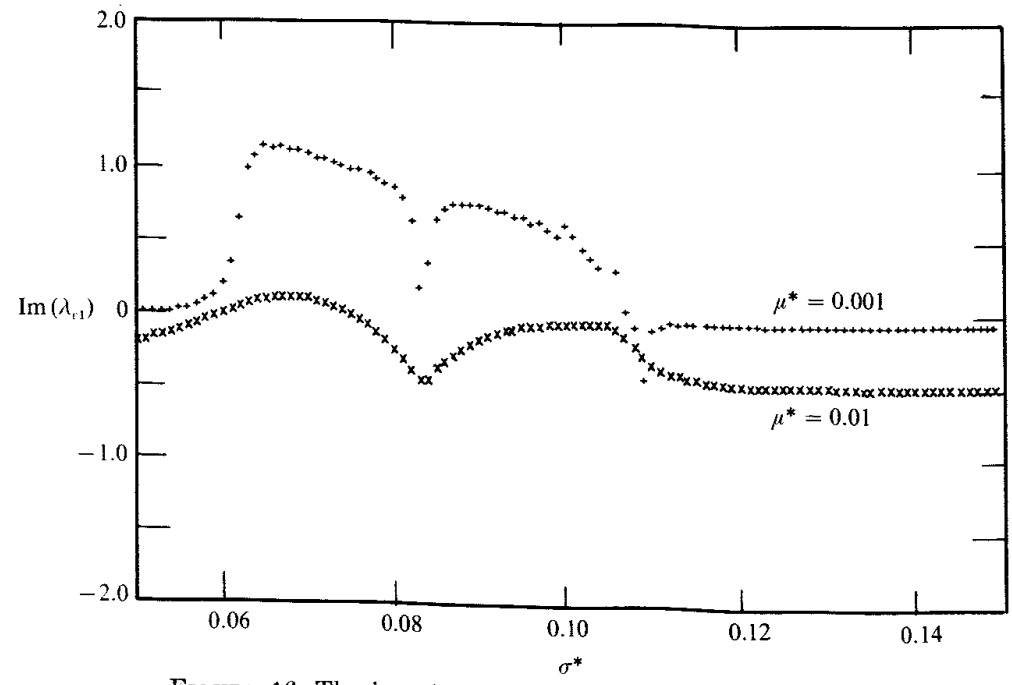

FIGURE 16. The imaginary part of λ_{v1} as a function of σ^* and μ^*.

and diverges at $\sigma^* = 0.109$, corresponding to the pair of touching bubbles resonating with a P_2-mode deformation. Thus, once again, it is not possible to obtain a uniformly valid $O(\mu^*)$ correction to λ_{v1} for the complete range of σ^* and, as in the case of λ_{p1}, it is probably best to estimate λ_{v1} by the direct substitution method for selected values of μ^*. The results of such computations for μ^* equal to 0.01 and 0.001 are shown in figures 15 and 16. From these calculations we see that for bubbles of size greater than about 1 mm, the viscous damping is small and therefore the influence of shape-dependent resonances on λ_{v1} can be quite significant.

We have examined in this section the viscous effects for the case when the surface-active impurities do not significantly alter the nature of the interface between the gas

and liquid. For small bubbles, the surface-active impurities usually present in gas–liquid mixtures will have the effect of making the interface appear rigid, and, instead of the zero tangential stress boundary condition used here, we must apply the no-slip boundary condition at the bubble surface. The corrections to λ_p and λ_v are then $O(\mu^{*\frac{1}{2}})$. Once again, the method presented here can be applied with a slight modification to determine the viscous corrections in this case, but we shall not pursue these calculations here. More detailed calculations of the viscous effect including the multi-bubble interactions in non-dilute bubbly liquids are presented in Sangani *et al.* (1991) in which calculations are also made for the case of bubbles satisfying the no-slip boundary condition.

It may be noted that the viscous damping is the most significant attenuation mechanism when ω_r is small. This is because the acoustic radiation damping is proportional to the effective wavenumber which becomes vanishingly small in the limit of small ω_r and the thermal effects, being dependent on the volume oscillations of the bubbles, also become unimportant at small ω_r. Thus the attenuation of sound waves at small frequencies can be determined simply from the imaginary part of λ_v as determined from the viscous effects.

5. Thermal effects and attenuation

In this section we wish to determine the attenuation of sound waves by including the pairwise interactions of bubbles in our analysis and then compare it with the experimental data available in the literature. Since the attenuation due to non-adiabatic thermal effects is significant for many of the experimental data presented in the literature, we shall first present briefly an analysis to include the thermal effects. Our interest is mostly in comparing the attenuation data for frequencies comparable with the natural frequency of the bubbles. Of course, close to resonance the nonlinear effects due to finite deformation of bubbles or coalescence may also become important but we shall not account for these effects here. Our calculations can be expected to apply when the intensity of sound waves is small and the damping due to various mechanisms is of sufficiently large magnitude to keep the deformations relatively small.

5.1. *Thermal effects*

While the energy changes during sound wave propagation in a single-phase medium can be regarded as adiabatic to a very good approximation, they are not so in the case of gas–liquid mixtures. This is because there is a net exchange of energy between the two phases during each cycle of the volume oscillations of the bubbles owing to the different surface areas of the bubbles at their maximum and minimum radii. Since the thermal diffusivity of the liquid is typically much greater than that of the gas (the ratio being about 10^3 for the air–water system), the temperature variations in the liquid are negligible compared to those inside the gas bubbles. We shall therefore take $\hat{T}$, the amplitude of the temperature variation, to equal zero in the liquid. Thermal effects are important then only in determining the density derivative $\partial\rho/\partial t$ inside the gas bubbles. To include these, we must first solve the energy and continuity equations inside the gas bubbles and then evaluate the density derivative to be used in taking the ensemble average of the continuity equation (cf. (2.1)). The analysis of thermal effects at the $O(\beta)$ approximation to $C_{\rm ef}^2$ has been given by a number of investigators in the past (see, for example, Miksis & Ting 1987*b*; Prosperetti 1984). Miksis & Ting used the homogenization method and derived an expression for the effective speed and attenuation by including the thermal effects in

both liquid and gas phases. The thermal conductivity of the liquid is usually large and therefore we shall assume the liquid temperature to remain unchanged. This yields the problem of including the thermal effects in pairwise interactions as particularly simple as one needs to solve for the temperature field only within one bubble, and in what follows, we shall adopt the approach taken by Prosperetti (1984) to do this.

The linearized energy equation for a compressible fluid is given by

$$c_p \frac{\partial}{\partial t}(\rho T) + \frac{T}{\rho}\left(\frac{\partial \rho}{\partial T}\right)_p \frac{\partial p}{\partial t} + c_p \rho T \boldsymbol{\nabla}\cdot\boldsymbol{u} = k\nabla^2 T, \tag{5.1}$$

where T is the absolute temperature, c_p is the constant-pressure specific heat of the gas, and k is the thermal conductivity of the gas. Now we follow Prosperetti (1984), and eliminate the $\boldsymbol{\nabla}\cdot\boldsymbol{u}$ term in the above equation by combining it with the continuity equation (cf. (2.1)) to obtain

$$\rho c_p \frac{\partial T}{\partial t} - \frac{\partial p}{\partial t} = k\nabla^2 T, \tag{5.2}$$

where we have used the relation $(\partial\rho/\partial T)_p = -\rho/T$ for an ideal gas. Since the pressure inside the gas is a function of time alone, the above equation can be readily integrated, and, using the boundary condition that $\hat{T} = 0$ at the surface of the bubble, we obtain

$$\hat{T} = \frac{\hat{p}}{\rho c_p}\left[1 - \frac{R}{s}\frac{\sinh\,(\mathrm{i}s^2/R^2k^*)^{\frac{1}{2}}}{\sinh\,(\mathrm{i}/k^*)^{\frac{1}{2}}}\right], \quad k^* = \frac{k/(\rho c_p)_g}{\omega R^2}, \tag{5.3}$$

where k^* is the non-dimensional thermal conductivity of the gas and s is the distance measured from the centre of the bubble. Thus we see that the uniform pressure within the gas bubble gives rise to a purely radial or spherically symmetric temperature distribution within the bubble. Now, upon multiplying the continuity equation (2.1) with $\rho T c_p$, combining it with the energy equation (5.1), and making use of the relation $c_p \rho T = \gamma P_e/(\gamma - 1)$ for ideal gases, we obtain

$$\frac{1}{\gamma P_e}\frac{\partial p}{\partial t} - \frac{\gamma - 1}{\gamma P_e} k\nabla^2 T + \boldsymbol{\nabla}\cdot\boldsymbol{u} = 0. \tag{5.4}$$

Upon integrating the above equation we obtain the velocity field inside the gas bubble as

$$\boldsymbol{u} + \frac{\mathrm{i}\omega \hat{p}_g \boldsymbol{s}}{\gamma P_e 3} = \frac{\gamma - 1}{\gamma P_e} k\boldsymbol{\nabla}\hat{T} + \boldsymbol{u}', \tag{5.5}$$

where $\hat{p}_g$ is the amplitude of the pressure variation inside the bubble and $\boldsymbol{u}'$ is the spherically non-symmetric part of the velocity field within the gas bubble. Since the temperature is a function of s alone, it influences only the spherically symmetric part of the velocity field. In other words, the non-adiabatic effects only influence the boundary condition for the spherically symmetric part of the pressure and velocity fields on the surface of the bubbles. Introducing a complex quantity $\mathscr{H}$ as given by

$$\mathscr{H} = 3\gamma[1 - 3(\gamma - 1)\,\mathrm{i}k^*\{(\mathrm{i}/k^*)^{\frac{1}{2}}\coth\,(\mathrm{i}/k^*)^{\frac{1}{2}} - 1\}]^{-1}, \tag{5.6}$$

and denoting the spherically symmetric part of the velocity field by u_{r00}, we obtain, by combining (5.3) and (5.5),

$$\frac{u_{r00}}{R} = -\frac{\mathrm{i}\omega \hat{p}_g}{\mathscr{H} P_e}. \tag{5.7}$$

We note that $\mathscr{H}$ is a real quantity in the two limits of small and high frequencies and equals 3 and 3γ, corresponding, respectively, to the isothermal and adiabatic changes. Now since the spherically symmetric part of the velocity in the incompressible liquid near the surface of the bubble can be taken as A/s^2 and the pressure as $\hat{p} = \hat{p}_a + i\omega\rho_L A/s$, $\hat{p}_a$ being the amplitude of the pressure variation in the absence of the bubble and A being equal to $u_{r00}R^2$, the spherically symmetric part of the normal stress boundary condition at the bubble surface can be expressed as

$$\hat{p}_a + \left[\frac{i\omega\rho_L}{R} + \frac{4\mu}{R^3}\right]A = \hat{p}_g\left[1 - \frac{2\sigma}{R\mathscr{H}P_e}\right]. \tag{5.8}$$

Now taking the ensemble average of the continuity equation (2.1), evaluating the integral of the density derivative over the volume of the bubble from the surface integral of $\boldsymbol{u}\cdot\boldsymbol{n}$, and comparing the resulting averaged equation with $\lambda_p \beta i\omega\hat{p}_0/(\gamma P_e) + \nabla\cdot\hat{\boldsymbol{u}}_0 = 0$, we find that λ_p to the leading order in β is now given by

$$\lambda_p = \frac{\gamma}{\gamma^*}\frac{\omega_c^2}{\omega_{ct}^2 - \omega^2(1 - ib)}, \tag{5.9}$$

where the ω_{ct}, the resonant frequency including the non-adiabatic effects, and the damping parameter b are given by

$$\omega_{ct}^2 = \frac{3\gamma P_e}{\rho_L R^2}\left[\frac{\mathscr{H}_R}{3\gamma} - \frac{2\sigma}{3R\gamma P_e}\right], \tag{5.10}$$

$$b = 4\mu^* + \frac{P_e\mathscr{H}_I}{\rho_L R^2\omega^2}. \tag{5.11}$$

Here $\mathscr{H}_R$ and $\mathscr{H}_I$ denote, respectively, the real and imaginary parts of $\mathscr{H}$ (cf. (5.6)). Since non-adiabatic effects only influence the spherically symmetric part of the velocity near the surface of each bubble, λ_v is unaffected and thus the effective speed can now be evaluated by making use of (2.29), (3.37), and (5.9).

The determination of the $O(\beta)$ correction to λ_p accounting for viscous and non-adiabatic changes is now straightforward. Although the pressure inside the gas bubble is uniform, the density derivative is not, owing to non-uniform temperatures. Thus the finite wavelength contribution is different from previous calculations and (3.19) must be used to evaluate it. The resulting expression is

$$\lambda_p = \frac{\gamma t_*}{\gamma^*\omega_r^2}[1 - izt_*(1 + \tfrac{1}{2}\pi z t_*) - \tfrac{3}{2}t_*^3\beta\ln\beta - \lambda_{p1}\beta], \tag{5.12}$$

$$\lambda_{p1} = 3t_*\left[\frac{3}{2} + \frac{\mathscr{H}}{30\gamma} + \mathscr{H}\mathscr{H}_1\frac{\gamma - 1}{\gamma} + \tfrac{1}{2}t_*\left(3 + \frac{1}{\omega_{r*}^2}\right) - 2i\mu^* + t_*^2(3.899\,11 + \tfrac{1}{2}\ln t_*)\right] + C_{ex}, \tag{5.13}$$

where

$$t_* = \frac{\omega_{rt}^2}{1 - \omega_{rt}^2(1 - ib)}. \tag{5.14}$$

$$\omega_{rt}^2 = \omega^2/\omega_{ct}^2, \quad \omega_{r*}^2 = \omega^2/\omega_{c*}^2. \tag{5.15}$$

$$\mathscr{H}_1 = k^{*2}\left[1 + \frac{i}{2k^*} - \left\{\left(\frac{i}{k^*}\right)^{\frac{1}{2}} + \frac{1}{6}\left(\frac{i}{k^*}\right)^{\frac{3}{2}}\right\}\coth\left(\frac{i}{k^*}\right)^{\frac{1}{2}}\right]. \tag{5.16}$$

ω_{c*} is a complex quantity defined by

$$\omega_{c*}^2 = \frac{3\gamma P_e}{\rho_L R^2}\left[\frac{\mathscr{H}}{3\gamma} - \frac{2\sigma}{3R\gamma P_e}\right] = \omega_{ct}^2 + \frac{i\mathscr{H}_I P_e}{\rho_L R^2}, \tag{5.17}$$

and C_{ex} is the contribution from the fourth- and higher-order reflections in the two-bubble interaction problem, i.e.

$$C_{ex} = 3\int_2^\infty \left\{1 + \frac{t_*}{S'} + \frac{t_*^2}{S'^2} + \frac{t_*^3}{S'^3} - \frac{A_{00}^1}{Rt_*}\right\} S'^2\, dS'. \tag{5.18}$$

As in the case of calculations for the corrections due to the viscous effects, we can once again evaluate C_{ex} by expanding A_{00}^1 for small viscous and non-adiabatic ($\mathscr{H}_I P_e/(\rho_L \omega^2 R^2)$) terms, but the utility of such expansions will be limited as they will diverge as $\omega_{rt} \to 0.828$. It is therefore best to evaluate C_{ex} directly for selected values of the physical parameters (k^*, μ^*, ω_{rt}, etc.) by first evaluating A_{00}^1 as a function of S' and then numerically integrating (5.18). We shall do this in the next section.

5.2. *Comparison with experiments*

Data on the phase speed and attenuation of sound waves in bubbly liquids have been presented by a number of investigators (Carstensen & Foldy 1947; Silberman 1957; Fox, Curley & Larson 1955; Kol'tsova *et al.* 1979; Ruggles, Scarton & Lahey 1986). Most of these data are for very low volume fractions of gas, typically less than 0.01, except for those reported by Ruggles *et al.* (1986) who presented the results for β up to about 0.2. An extensive comparison between the leading-order theory for bubbly liquids that takes into account the interaction between a single bubble and the mixture, such as those due to Foldy, with the experimental data has been made by a number of investigators. (See, for instance, the review article by van Wijngaarden 1972; Ruggles *et al.* 1986; and Commander & Prosperetti 1989.) The agreement between the leading-order theory and experiments is generally good for frequencies small compared to the resonance frequency. At frequencies close to resonance, however, the theory predicts attenuation which is generally 4–6 times greater than the measured attenuation even for β-values as low as 0.005. Recently, Commander & Prosperetti (1989) have made a very careful analysis of the data and examined the possible effects of the size distribution of the bubbles, the hydrostatic head, etc., and found that none of these factors can be responsible for such a large discrepancy between the experiments and theory. These investigators offered an explanation that the contribution due to the pairwise interaction between the bubbles, which was not included in the leading-order theory, may be quite significant near the resonance frequency even for such low values of β. It should be noted that accurate measurements near the resonance frequency with a uniform size distribution of bubbles are quite difficult, but it is generally believed that they are accurate to within about 50%. Finally, the disagreement between theory and experiments generally persists for larger frequencies and, for instance, a discrepancy by a factor of 2–3 exists even at frequencies as high as five times the resonance frequency.

In view of the above discussion it is important to see if the theory presented here, which includes the pairwise interactions of bubbles, can reduce the discrepancy between theory and experiments at frequencies close to and above the resonance frequency. Moreover, the only experimental data at relatively high volume fractions have been presented by Ruggles *et al.* (1986) as mentioned earlier, but their data is only for low frequencies where the existing theories had already been shown to agree

with the experiments to within 10%, and, therefore, a comparison of the $O(\beta^2)$ theory presented here with their data would be uninteresting. We therefore focus on the data for attenuation presented by Silberman (1957), which are also probably the most reliable in terms of uniformity of the size distribution of bubbles. The largest volume fraction considered by this investigator was 0.01 and we shall compare the theory and experiments only for this particular value of β.

The data on attenuation are usually reported in dB per unit length, which is related to the imaginary part of the effective wavenumber by

$$A = (20\log_{10} e)\, v = (8.68589)\, v, \tag{5.19}$$

where v is related to z by means of

$$\frac{z}{R} = \frac{\omega}{C_{\mathrm{ef}}} = u - \mathrm{i}v. \tag{5.20}$$

The radius of the bubbles in Silberman's experiments was about 0.26 cm. The corresponding resonance frequency is estimated to equal about 1.25 kHz. Since we wish to compare various theories with the experimental data, let us briefly summarize the various expressions obtained so far.

In our theory there are three principal mechanisms that make the effective wavenumber a complex quantity when ω_{r} is less than unity: viscous, thermal, and acoustic. For a single bubble the relative importance of these are estimated from

$$b_{\mathrm{v}} = \frac{4\mu}{\rho_{\mathrm{L}} R^2 \omega} = 4\mu^*, \quad b_{\mathrm{t}} = \frac{P_{\mathrm{e}} \mathscr{H}_{\mathrm{I}}}{\rho_{\mathrm{L}} R^2 \omega^2}, \quad b_{\mathrm{a}} = \frac{\omega R}{C_{\mathrm{L}}}, \tag{5.21}$$

where b_{v}, b_{t}, and b_{a} correspond, respectively, to the viscous, thermal and acoustic damping. The relative magnitudes of these three damping mechanisms for the experimental conditions of Silberman are shown in figure 17. The thermal damping is most significant at low frequencies but becomes of the same order of magnitude as, or lower than, the acoustic damping beyond the resonance frequency. We also see that the viscous damping for the frequency range of interest is negligible. (For smaller bubbles and larger frequencies, however, all three mechanisms can be significant.)

The above discussion applies mostly to $\omega_{\mathrm{r}} < 1$. As mentioned in the Introduction, C_{ef} and hence z are complex even in the absence of viscous, thermal, or acoustic radiation effects when the frequency is greater than the natural frequency of bubbles owing to the negative apparent compressibility of the bubbles at frequencies greater than their natural frequencies. As seen from the Foldy's expression (1.1), the compressibility of the liquid will eventually become important at sufficiently large frequencies and C_{ef} becomes real at high frequencies. The balance of the two compressibilities occurs at $\omega_{\mathrm{r}} \approx (\beta\rho_{\mathrm{L}} C_{\mathrm{L}}^2/\gamma P_{\mathrm{e}})^{\frac{1}{2}}$, which for an air–water system with $\beta = 0.01$ occurs at ω_{r} of about 10 (or a frequency of about 12 kHz for bubbles of 0.26 cm).

We now summarize the various expressions for determining the attenuation. The leading-order Foldy theory, which takes into account the interaction of a single bubble with the wave, gives

$$z^2 = z_{\mathrm{L}}^2 + 3\beta \frac{\omega^2}{\omega_{\mathrm{ct}}^2 - \omega^2[1 - \mathrm{i}(b_{\mathrm{v}} + b_{\mathrm{t}} + b_{\mathrm{a}})]}, \tag{5.22}$$

where $z_{\mathrm{L}} = \omega R/C_{\mathrm{L}}$ is the wavenumber based on pure liquid speed. The contribution

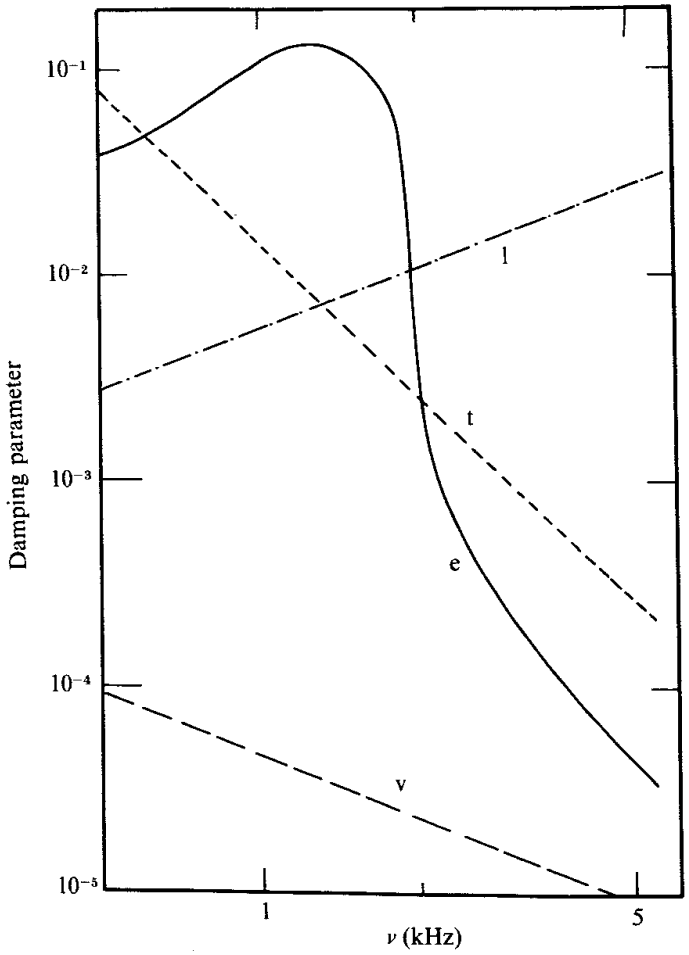

FIGURE 17. Relative magnitudes of the viscous (v) damping, the acoustic radiation damping based on the speed of sound in pure liquid (l), the acoustic radiation damping based on the effective speed in the medium (e), and the thermal (t) damping for the experimental conditions of Silberman (1957).

from the finite compressibility of the liquid is important at large ω_r and therefore we shall include the z_L^2 in our calculations. (As mentioned above, the two terms on the right-hand side of the above equation are comparable in magnitude for $\omega_r \approx 10$ for $\beta = 0.01$.)

At the next approximation, z^2 correct to $O(\beta^{\frac{3}{2}})$ is given by

$$z^2 = z_L^2 + \frac{3\beta\omega_{rt}^2}{1-\omega_{rt}^2(1-ib)}[1 - izt_* + O(\beta \ln \beta)] \approx z_L^2 + \frac{3\beta\omega_{rt}^2}{1-\omega_{rt}^2(1-ib-iz)}, \quad (5.23)$$

where $b = b_v + b_t$. In other words, the acoustic damping based on the pure-liquid wavenumber is replaced by the effective-medium wavenumber. In the above expression z on the right-hand side must be actually evaluated from the $O(\beta)$ theory as given by (5.22). However, the difference between the $O(\beta)$ and $O(\beta^{\frac{3}{2}})$ estimates of z^2 can be quite significant near resonance and therefore it is perhaps more accurate to solve for z from (5.23) in a self-consistent manner. The predictions of these $O(\beta)$ and $O(\beta^{\frac{3}{2}})$ theories are shown in figure 18 by the dashed and dashed-and-dot lines, respectively. The experimental data of Silberman are shown by stars. We note that the measured values of attenuation in dB/cm at about 1 and 1.4 kHz are about 1.3 and 4.3, respectively. The corresponding values predicted by the $O(\beta)$ theory are about 0.27 and 12.1, and those from the $O(\beta^{\frac{3}{2}})$ theory are about 1.3 and 7.9, respectively. In fact, very close to resonance (1.25 kHz), the $O(\beta)$ theory yields an

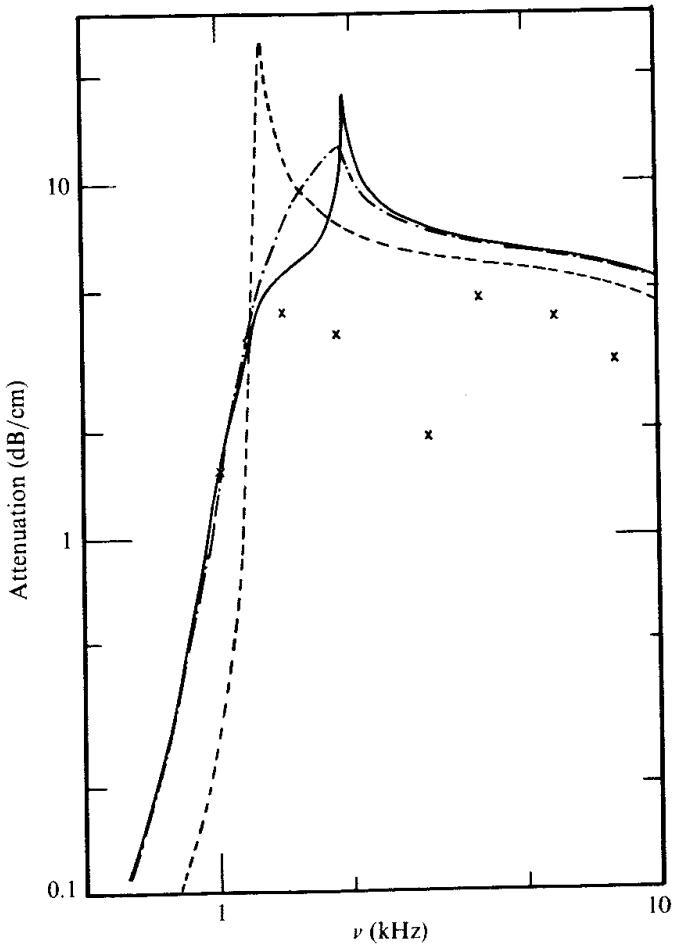

FIGURE 18. The attenuation of sound waves as a function of frequency for $\beta = 0.01$. The experimental data of Silberman (1957) are indicated by stars, the solid curve is due to the $O(\beta^2)$ theory, the dot-and-dash curve to the $O(\beta^{\frac{3}{2}})$ theory, and the dashed curve to the $O(\beta)$ theory.

estimate of A equal to about 25 dB/cm, compared with an estimate of about 5.6 dB/cm from the $O(\beta^{\frac{3}{2}})$ theory. Although the experimental value at this frequency is not reported, it appears from figure 18 that it is likely to agree very well with the prediction of the $O(\beta^{\frac{3}{2}})$ theory. Thus we see that the $O(\beta^{\frac{3}{2}})$ theory, with z estimated in the self-consistent manner, gives estimates of attenuation that are in excellent agreement for frequencies close to the natural frequency of bubbles, and this confirms our observation that one must estimate the acoustic radiation damping based on the effective speed of sound in the medium and not on the speed in pure liquid.

The acoustic damping based on the effective speed in the medium equals Re (z) and the magnitude of this relative to the other three damping mechanisms can be seen from figure 17. Below the natural frequency of bubbles, the acoustic damping based on the effective speed is an order of magnitude greater than that based on the speed in the pure liquid. In fact, close to resonance, even the thermal damping is an order of magnitude smaller than the effective-speed-based acoustic damping. On the other hand, at higher frequencies, while the acoustic damping based on the speed of sound in pure liquid continues to increase, we see that the effective-speed-based damping decreases with increasing frequencies. This is because once ω_{rt} exceeds 1, the real part of z^2 becomes negative and consequently z becomes a nearly imaginary quantity. Thus, for $\omega_{rt} > 1$, z does not contribute much to damping. Instead it shifts the resonance frequency of the mixture. Of course, at sufficiently large frequencies, the

term z_L^2 will eventually become larger than the $O(\beta)$ term and the effective-speed-based damping will then once again increase with the frequency. For $\beta = 0.01$, this happens only for frequencies greater than about 12 kHz. As seen in figure 18, the attenuation predicted by the $O(\beta^{\frac{3}{2}})$ theory peaks at about 2 kHz ($\omega_{rt} \approx 1.6$), and the agreement between the theory and experiments is quite poor for such frequencies.

Now we proceed to compare the data with the $O(\beta^2)$ theory which yielded

$$z^2 = z_L^2 + 3\beta\lambda_p \frac{\omega_r^2 \gamma^*}{\gamma}[1-(\lambda_v+\lambda_{\sigma m}+4i\mu^*\omega_r^2\lambda_p)\beta], \tag{5.24}$$

where $\lambda_v = 3+36i\mu^*$, $\lambda_{\sigma m} = 4\sigma^* t_*$, and λ_p correct to $O(\beta)$ is given by (5.12). The straightforward substitution of these coefficients into (5.24) yields rather poor estimates of attenuation and, in fact, yields negative values for some frequencies. Therefore we must recast the above expression in a different form while still maintaining its accuracy to $O(\beta^2)$. The difficulty arises mainly because the expression for λ_p contains terms that are proportional to t_*^2 and t_*^3 which become very large for frequencies above the natural frequency of the bubbles. To suppress the relative importance of these terms we write the $O(\beta^2)$ correction as modifying the attenuation. Thus we write

$$z^2 = z_L^2 + \frac{3\beta\omega_{rt}^2}{1-\omega_{rt}^2[1-i(b_v+b_t+b_{ef})]} \tag{5.25}$$

and expand the above expression for small b_{ef} so that the resulting expression is the same as that given by (5.24) correct to $O(\beta^2)$. Writing $b_{ef} = z+b_p$ and expanding (5.25) we find that

$$1-it_*(z+b_p)-t_*^2(z+b_p)^2 = 1-izt_*(1+\tfrac{1}{2}\pi z t_*)-\beta[\tfrac{3}{2}t_*^3\ln\beta+\lambda_{p1} + \lambda_v+\lambda_{\sigma m}+4i\mu^* t_*\gamma/\gamma^*]. \tag{5.26}$$

Thus b_p is $O(\beta\ln\beta)$ and we obtain

$$b_p = \frac{\beta\lambda^* - t_*^2 z^2}{it_* + 2zt_*^2}, \tag{5.27}$$

where λ^* is the term inside the square bracket on the right-hand side of (5.26). Note that if we regard z as an $O(\beta^{\frac{1}{2}})$ quantity, the the term $2zt_*^2$ in the denominator of the term on the right-hand side of the above equation is small compared to it_* and should therefore be dropped. However, since t_*^2 and z near resonance are not small, we retain this term in the expression. (For bubbles of radius 0.26 cm and an attenuation of about 5 dB/cm, the imaginary part of z is about 0.2.) Similarly, we replace t_* in the calculation of λ^* by t_e as given by

$$t_e = \frac{\omega_{rt}^2}{1-\omega_{rt}^2[1-i(b_v+b_t+z)]}, \tag{5.28}$$

to reflect the fact that while z is an $O(\beta^{\frac{1}{2}})$ quantity, its effect for frequencies close to resonance can be substantial. Finally, we express the $\ln\beta$ and terms that appeared from the effective medium and finite wavelength in terms of z (using $z^2 = 3\beta t_*$) and retain the explicit dependence of the remaining terms in terms of β to write

$$\lambda^* = \frac{z^2}{\beta}\left[\frac{\mathscr{H}}{30\gamma}+\frac{\gamma-1}{\gamma}\mathscr{H}\mathscr{H}_1+\tfrac{1}{2}t_e\left(1+\frac{1}{\omega_{r*}^2}\right)+t_e^2(3.3498+\ln(iz))-2\mu^*\right] + 3+i\mu^*(36+4t_e\gamma/\gamma^*)+4\sigma^* t_e+3t_e(1.5+t_e)+C_{ex}. \tag{5.29}$$

here $\ln(\mathrm{i}z)$ is to be calculated from

$$\ln(\mathrm{i}z) = \tfrac{1}{2}\ln[R^2(u^2+v^2)] + \mathrm{i}\tan^{-1}(u/v). \tag{5.30}$$

As in the case of the $O(\beta^{\frac{3}{2}})$ theory, z may be now determined in a self-consistent manner from (5.25), (5.27), and (5.29) but the estimates obtained in this manner were not good and hence we used z determined from the $O(\beta^{\frac{3}{2}})$ theory first and then used its value to evaluate the right-hand side of (5.25) and thereby to determine the $O(\beta^2)$ estimate of z^2. The values of attenuation determined in this manner are shown in figure 18 by solid curves. At slightly above the resonance frequency, $\nu = 1.4$ kHz, this theory gave attenuation of about 5.4 dB/cm compared to 7.9 and 12 as given by $O(\beta^{\frac{3}{2}})$ and $O(\beta)$ theories respectively. The measured value is about 4.3 and thus we see that the $O(\beta^2)$ theory gives better estimates for frequencies close to natural frequency of the bubbles. On the other hand, as in the case of the $O(\beta^{\frac{3}{2}})$ theory, the predicted values at frequencies above 2 kHz ($\omega_{\mathrm{rt}} \approx 1.6$) seem to give poor estimates of attenuation.

Finally, it may be noted that although the number of rearrangements we have made to arrive at (5.25) with the various quantities in it evaluated as given by (5.27)–(5.30) seems to be the most natural way of recasting the original expression for z^2 correct to $O(\beta^2)$, we have also attempted to recast the original expression (5.24) in a number of other ways, always keeping its accuracy to $O(\beta^2)$, but none of these expressions predicted attenuation values that were in very good agreement with the experimental data over the complete range of frequencies. Thus it appears that the problem of predicting attenuation of sound waves at frequencies above the natural frequency of the bubbles still remains unsolved.

Most of this work was carried out at The Johns Hopkins University while the author was on sabbatical leave from Syracuse University. The author is most grateful to Professor Andrea Prosperetti for his hospitality, his keen interest in the work, and for many valuable discussions. The author is also grateful to Mr Vinod Kamath for the critical reading of the previous version of this manuscript and for valuable suggestions.

This work was supported by the Department of Energy under Grants DE-FG02-89ER 14043 and DE-FG02-90ER 14136.

Appendix A. Details of the two-bubble interaction problem

A.1. *The inviscid case*

For brevity, let us choose $\hat{p}_{\mathrm{a}}\,\mathrm{e}^{-\mathrm{i}\boldsymbol{k}\cdot\boldsymbol{x}_1} = 1$. Then the pressure field in the liquid is given by

$$\hat{p} = \mathrm{e}^{-\mathrm{i}\boldsymbol{k}\cdot\boldsymbol{s}} + \sum_{q=1}^{2}\sum_{n,m} A^q_{nm}\,\mathrm{Y}^m_n\left(\frac{\partial}{\partial s_1}, \frac{\partial}{\partial s_2}, \frac{\partial}{\partial s_3}\right) G(k|\boldsymbol{x}-\boldsymbol{x}_q|), \tag{A 1}$$

where $\boldsymbol{s} = \boldsymbol{x}-\boldsymbol{x}_1$. Now since $\hat{p}$ satisfies the Helmholtz equation, it can also be expanded in spherical Bessel functions around the centre of each bubble. Thus the expansion around the centre of bubble at $\boldsymbol{x}_q$ can be expressed as

$$\hat{p}^q = \sum_{n,m} [C^q_{nm} j_n(ks^q) + D^q_{nm} h_n(ks^q)]\,P^m_n\,\mathrm{e}^{\mathrm{i}m\phi}, \tag{A 2}$$

where s^q is measured from $\boldsymbol{x}_q$. Since the coefficients of the regular Bessel functions (j_n) must be related to the regular part of $\hat{p}_2$ at $\boldsymbol{x}_q$, and the coefficients of the singular Bessel functions (h_n) to the singular part, we can obtain the relation between the

coefficients in (A 1) to the coefficients in (A 2). Using the general theorems for integration and differentiation given in Hobson (1931), we obtain

$$C_{nm}^{q} = \frac{2(2n+1)}{(1+\delta_{m0})}\frac{(n-m)!}{(n+m)!}\left(\frac{1}{k}\right)^{n} \mathrm{Y}_n^m\left(\frac{\partial}{\partial s_1}, \frac{\partial}{\partial s_2}, \frac{\partial}{\partial s_3}\right)\hat{p}^r(\boldsymbol{s}_q), \tag{A 3}$$

$$D_{nm}^{q} = \mathrm{i}(-k)^{n+1} A_{nm}^{q}. \tag{A 4}$$

Now the boundary conditions (2.13) can be applied readily to the expansion (A 2), and (A 3) and (A 4) then yield the following relationship among A_{nm}^{q}:

$$A_{nm}^{q} = t_{nm} R^{2n+1}\left[(-\mathrm{i})^n \mathrm{Y}_n^m(k_1, k_2, k_3)\, \mathrm{e}^{-\mathrm{i}\boldsymbol{k}\cdot\boldsymbol{s}_q} + \sum_{r,s} A_{rs}^{3-q}\, \mathrm{Y}_n^m\, \mathrm{Y}_r^s\, G(k|\boldsymbol{x}-\boldsymbol{x}_{3-q}|)\right], \tag{A 5}$$

where $\mathrm{Y}_n^m\, \mathrm{Y}_r^s = \mathrm{Y}_n^m(\partial/\partial s_1, \partial/\partial s_2, \partial/\partial s_3)\, \mathrm{Y}_r^s(\partial/\partial s_1, \partial/\partial s_2, \partial/\partial s_3)$ is a differential operator of rank $n+r$ and t_{nm} are given by

$$t_{00} = -\frac{\mathrm{i}}{z}\frac{\omega_r^2 j_0(z) + z j_0'(z)}{\omega_r^2 h_0(z) + z h_0'(z)}, \quad z = kR, \tag{A 6}$$

$$t_{nm} = \frac{2(\mathrm{i})^{n-1}(2n+1)(n-m)!}{(1+\delta_{m0})(n+m)!\, z^{2n+1}}\frac{j_n(z) - \sigma^* z j_n'(z)\,[2-n(n+1)]}{h_n(z) - \sigma^* z h_n'(z)\,[2-n(n+1)]}. \tag{A 7}$$

Note that for $q = 1$ and $n = m = 0$ (A 5) reduces to

$$\frac{A_{00}^{1}}{R t_{00}} = 1 + \sum_{n,m} A_{nm}^{2}\, \mathrm{Y}_n^m\, G(kS), \tag{A 8}$$

which was used in the main text (cf. (3.58)). Now the above set of infinite linear equations in the unknowns A_{nm}^{q} can be truncated to a finite number of equations in a finite number of unknowns, and the resulting equations can be solved either asymptotically when the separation distance S is large and the effective wavenumber k is small or by the method of direct substitution for selected values of S and k. Both methods were used in the study and so we shall describe them briefly, but first we note that we are primarily interested in solving the above set of equations when k, being of $O(\beta^{\frac{1}{2}})$, is small. Since S, on the other hand, can be arbitrarily large, we retain k in evaluating $G(kS)$ in the above equations but take the limit $k \to 0$ in the remaining terms. To leading order, t_{nm} are given by

$$t_{00} = t_0 = \frac{\omega_{\mathrm{r}}^2}{1-\omega_{\mathrm{r}}^2}, \tag{A 9}$$

$$t_{nm} = \frac{2(n-m)!\,(-1)^{n+1}}{(1+\delta_{m0})(n+m)!\,[(2n-1)!!]^2}\frac{1-n[2-n(n+1)]\,\sigma^*}{1-(n+1)\,[2-n(n+1)]\,\sigma^*}. \tag{A 10}$$

Let us first determine the solution of the problem when S is large. The equations for the first few coefficients are given by

$$A_{00}^{1} = R t_0\left[1 + A_{00}^{2} G(kS) + A_{10}^{2}\frac{\partial}{\partial s_1} G(kS) + \ldots\right], \tag{A 11}$$

$$A_{00}^{2} = R t_0\left[\mathrm{e}^{-\mathrm{i}\boldsymbol{k}\cdot\boldsymbol{S}} + A_{00}^{1} G(kS) + A_{10}^{1}\frac{\partial}{\partial s_1} G(kS) + \ldots\right], \tag{A 12}$$

$$A_{10}^{1} = R^3 t_{10}\left[-\mathrm{i}k_1 + A_{00}^{2}\frac{\partial}{\partial s_1} G(kS) + \ldots\right], \tag{A 13}$$

$$A_{10}^{2} = R^3 t_{10}\left[-\mathrm{i}k_1\, \mathrm{e}^{-\mathrm{i}\boldsymbol{k}\cdot\boldsymbol{S}} - A_{00}^{1}\frac{\partial}{\partial s_1} G(kS) + \ldots\right]. \tag{A 14}$$

These can be readily solved to obtain

$$A_{10}^1 = O\left(kR^3, \frac{R^4}{S^2}\right), \tag{A 15}$$

$$A_{00}^1 = Rt_0\left[1 + Rt_0\, G(kS)\{e^{-ik\cdot S} + A_{00}^1\, G(kS)\} + O\left(\frac{kR^3}{S^2}, \frac{R^4}{S^4}\right)\right], \tag{A 16}$$

so that as $k \to 0$

$$\frac{A_{00}^1}{Rt_0} = \frac{1 + Rt_0\, G\, e^{-ik\cdot S}}{1-(Rt_0\, G)^2} = 1 + Rt_0\, G\, e^{-ik\cdot S} + R^2 t_0^2 G^2 + R^3 t_0^3 G^3\, e^{-ik\cdot S} + O\left(\frac{R}{S}\right)^4, \tag{A 17}$$

where $G = G(kS)$. The above expression with the higher-order terms explicitly written were used in the main text (cf. (3.59)). The remainder of this Appendix is devoted to the determination of these higher-order terms and to the method of calculating the viscous correction.

Since the higher-order terms decay rapidly enough, we are only interested in these terms when kS is small. Consequently, we can further simplify the calculations by solving the Laplace equation, instead of the Helmholtz equation for $\hat{p}_2$, subject to the boundary condition that $\hat{p}_2 \to 1$ as $s \to \infty$. Replacing $G(kS)$ by $1/S$ now, redefining the differential operator, and noting that the problem in this inner region ($R \leqslant S \ll 1/k$) is independent of the orientation of the vector $\boldsymbol{S}$, we write

$$\hat{p} = 1 + \sum_{n,q} A_n^q \left(\frac{\partial}{\partial s_1}\right)^n \frac{1}{|\boldsymbol{s} - \boldsymbol{s}_q|}, \tag{A 18}$$

where we have chosen the two bubbles to lie on the s_1 axis. Because of the symmetry about the s_1 axis, the problem has now become axisymmetric, so that only the coefficients A_{nm} with $m = 0$ are non-zero. Also since $\nabla^2(1/s) = 0$, only the first term in the expansion of the differential operator Y_n^m is needed and thus the differentiation of the basic singularity G has become relatively simple. Now, from symmetry it is easy to see that $A_n^1 = (-1)^n A_n^2 = A_n$, and the relationship among the coefficients A_n reduces to

$$A_n = t_0 R\delta_{n0} + \frac{t_n R^{2n+1}}{(n!)^2} \sum_{p=0}^{\infty} (-1)^{n+p} \frac{(n+p)!}{S^{n+p+1}} A_p, \tag{A 19}$$

where t_n are defined by

$$t_n = \frac{\sigma^* n[2-n(n+1)]-1}{\sigma^*(n+1)[2-n(n+1)]+1}, \quad n \geqslant 1. \tag{A 20}$$

Now the standard procedure for calculating the higher-order reflections by the asymptotic method is to expand A_n in powers of R/S (for selected values of σ^* and ω_r) and then to solve (A 19) for each power in R/S. Since we would like to evaluate the reflections as accurately as possible, even near the resonance frequency, we modify this procedure slightly. Specifically, since the strength of the monopole A_0 is expected to become vary large near the resonance frequency, we first solve for A_n/A_0 in the series of R/S. Thus, writing

$$A_n' = \frac{A_n}{A_0} = R^n \sum_q b_{nq} \left(\frac{R}{S}\right)^q, \tag{A 21}$$

and substituting in (A 19) for $n \geqslant 1$, we obtain the following recursion relation among the coefficients b_{nq}:

$$b_{nq} = \frac{t_n}{(n!)^2} \sum_p (-1)^{n+p} (n+p)!\, b_{p,q-n-p-1}, \tag{A 22}$$

with $b_{0q} = \delta_{0q}$, and $b_{nq} = 0$ for $q \leqslant 0$ and $n \neq 0$. Now the coefficients b_{nq} can be readily computed for selected values of σ^*, and A_0 can be subsequently evaluated for various ω_r using (A 19) with $n = 0$, which yields

$$\frac{A_0}{Rt_0} = \frac{1}{1 - t_0 f(S/R)}, \tag{A 23}$$

where

$$f\left(\frac{S}{R}\right) = \sum_{p,q} (-1)^p p!\, b_{pq} \left(\frac{R}{S}\right)^{p+q+1} \equiv \sum_n C_n \left(\frac{R}{S}\right)^n. \tag{A 24}$$

The resonance frequency for the pair of bubbles separated by a distance S can then be obtained from the relation $1/t_{0,\mathrm{crit}} = \sum C_n (R/S)^n$. The first few C_n are listed below:

$$C_1 = 1; \quad C_2 = C_3 = 0; \quad C_4 = t_1 = -1; \quad C_5 = 0; \quad C_6 = t_2. \tag{A 25}$$

Thus we obtain the following expansion for A_0 valid in the inner incompressible region ($kS \ll 1$):

$$\frac{A_0}{Rt_0} = 1 + t_0 \frac{R}{S} + t_0^2 \left(\frac{R}{S}\right)^2 + t_0^3 \left(\frac{R}{S}\right)^3 + \ldots, \tag{A 26}$$

which agrees with the uniformly valid solution derived earlier (cf. (A 17)). Finally, the coefficients a_n used in the main text were obtained by taking the inverse of the series for A_0. This series converges quickly when ω_r is not too close to the critical value for the pair of bubbles. The method of direct substitution was used whenever the series for a_n did not converge. In this method, the system of equations given by (A 19) were first truncated to $n \leqslant N$, and the resulting equations were solved directly for selected values of S/R. The calculations were then repeated for larger values of N until A_0 converged to a desired level of accuracy.

A.2. *Resonances of pairs of bubbles*

It is interesting to discuss the resonance nature of a pair of bubbles. At resonance frequencies, the strength of monopoles for the two bubbles become infinitely large. If the bubbles are widely separated then we can use (A 17) to determine these frequencies. Thus we find that the denominator in this equation vanishes for $t_0 = \pm 1/(RG)$. Since t_0 is a real quantity, we must disregard the imaginary part of G in determining the resonance frequencies. (The imaginary part, of course, contributes to the acoustic radiation damping.) Thus, for large S, we find the resonance frequencies of the pair of bubbles to be given by $\omega_r = 1 \pm R \cos kS/(2S)$. When kS is $O(1)$, these frequencies are only $O(kR)$ different from the natural frequency of the individual bubbles. On the other hand, the resonance frequencies of the pair of bubbles with S comparable with R are substantially different from the natural frequency but (A 23) derived here seems to suggest that there is only one resonance frequency (given by $t_0 = 1/f(S/R)$) for such pairs. There is, of course, another resonance frequency but this did not appear in our calculations because in the inner incompressible region $kS \ll 1$ this resonance does not contribute at the leading order. To show this, let us consider a slightly more general case in which $\hat{p}_2 \to p_\infty(s)$ as

$s\to\infty$. Then writing $A^1_{n0}=A_n+B_n$ and $A^2_{n0}=(-1)^n(A_n-B_n)$, it is easy to show that A_n and B_n satisfy

$$A_n=\frac{p_\infty(0)+p_\infty(\boldsymbol{S})}{2}t_0R\delta_{n0}+\frac{t_nR^{2n+1}}{(n!)^2}\sum_{p=0}^{\infty}(-1)^{n+p}\frac{(n+p)!}{S^{n+p+1}}A_p, \tag{A 27}$$

$$B_n=\frac{p_\infty(0)-p_\infty(\boldsymbol{S})}{2}t_0R\delta_{n0}-\frac{t_nR^{2n+1}}{(n!)^2}\sum_{p=0}^{\infty}(-1)^{n+p}\frac{(n+p)!}{S^{n+p+1}}B_p. \tag{A 28}$$

Note that the A_n correspond to the strengths of multipoles for the two bubbles resonating in phase with each other, while the B_n correspond to those resonating out of phase with each other. Now (A 27) and (A 28) can be solved readily to obtain

$$\frac{A_0}{Rt_0}=\frac{p_\infty(0)+p_\infty(\boldsymbol{S})}{2[1-t_0f(S/R)]}, \tag{A 29}$$

$$\frac{B_0}{Rt_0}=\frac{p_\infty(0)-p_\infty(\boldsymbol{S})}{2[1+t_0g(S/R)]}, \tag{A 30}$$

where $f(S/R)$ is the same function as given by (A 24) and $g(S/R)$ can be shown to equal

$$g\left(\frac{S}{R}\right)=\frac{R}{S}+\frac{R^4}{S^4}-\frac{t_2R^6}{S^6}+\ldots. \tag{A 31}$$

Now if we choose $p_\infty(\boldsymbol{s})\equiv e^{-ikx_1}$, then we see that the coefficient B_0 is proportional to kS_1 and hence small compared to A_0. Thus only the in-phase resonance of the pair of bubbles is important at the leading order in kR.

A.3. *The viscous corrections*

The components of the velocity in the spherical polar coordinates centred at $\boldsymbol{x}_1$ can be written from (4.10) as

$$u_s=-\frac{1}{i\omega\rho_L}\frac{\partial p}{\partial s}-\frac{1}{s\sin\theta}\frac{\partial}{\partial\theta}\left(\sin\theta\frac{\partial\Phi}{\partial\theta}\right)-\frac{1}{s\sin^2\theta}\frac{\partial^2\Phi}{\partial\phi^2}, \tag{A 32}$$

$$u_\theta=-\frac{1}{i\omega\rho_L}\frac{\partial p}{s\partial\theta}+\frac{1}{s}\frac{\partial}{\partial s}\left(s\frac{\partial\Phi}{\partial\theta}\right)+\frac{1}{s\sin\theta}\frac{\partial\chi}{\partial\phi}, \tag{A 33}$$

$$u_\phi=-\frac{1}{i\omega\rho_L}\frac{\partial p}{s\sin\theta\partial\phi}+\frac{1}{s\sin\theta}\frac{\partial}{\partial s}\left(s\frac{\partial\Phi}{\partial\phi}\right)-\frac{1}{s}\frac{\partial\chi}{\partial\theta}, \tag{A 34}$$

where we have dropped the subscripts on Φ and χ and the hat on p for brevity. The tangential stress components are given by

$$\tau_{s\theta}=\mu\left[\frac{\partial u_\theta}{\partial s}-\frac{u_\theta}{s}+\frac{1}{s}\frac{\partial u_s}{\partial\theta}\right], \tag{A 35}$$

$$\tau_{s\phi}=\mu\left[\frac{\partial u_\phi}{\partial s}-\frac{u_\phi}{s}+\frac{1}{s\sin\theta}\frac{\partial u_s}{\partial\phi}\right]. \tag{A 36}$$

Now to satisfy the boundary condition of zero tangential stress at the surface of the bubble, we note that since Φ and χ decay rapidly when α is large, we can replace the functions $k_n(\alpha s)$ in (4.12) and (4.13) by their leading-order terms as $e^{\alpha(R-s)}$. By comparing the magnitude of various terms that appear in the boundary conditions.

we find that $\Phi = O(\alpha^{-2}) = O(\mu^*)$ and $\chi = O(\mu^{*\frac{3}{2}})$. Since the radial derivatives of Φ can be large, we need to retain these terms in determining $\partial u_\theta/\partial s$ and $\partial u_\phi/\partial s$ in the tangential stress components. Thus, for example, we have

$$\frac{\partial u_\theta}{\partial s} = -\frac{1}{\mathrm{i}\omega\rho_{\mathrm{L}}}\frac{\partial}{\partial s}\left(\frac{1}{s}\frac{\partial p^0}{\partial \theta}\right)+\frac{\partial^3 \Phi}{\partial s^2\,\partial\theta}+O(\mu^{*\frac{1}{2}}). \tag{A 37}$$

Now the remaining terms in $\tau_{s\theta}$ in (A 35) can be evaluated to $O(1)$ by neglecting Φ and χ and then the application of the boundary condition $\tau_{s\theta} = 0$ yields

$$\Phi = \frac{-2}{\mathrm{i}\omega\rho_{\mathrm{L}}\alpha^2R^2}\left[p^0 - R\frac{\partial p^0}{\partial s}\right]\mathrm{e}^{\mathrm{i}\alpha(R-s)}+O(\alpha^{-3}). \tag{A 38}$$

The boundary condition $\tau_{s\phi} = 0$ at $s = R$ is also satisfied to $O(1)$ with the above expression for Φ and therefore the toroidal field χ does not contribute to this leading-order analysis. Now the normal stress balance at $s = R$ gives

$$p = p_{\mathrm{g}} + (2\eta + \nabla_{\mathrm{s}}^2\eta)\,\sigma + 2\mu\frac{\partial u_r}{\partial s}, \tag{A 39}$$

where p_{g} is the amplitude of the pressure variation inside the gas bubble. Substituting (A 38) into (A 32) we obtain

$$u_s = -\frac{1}{\mathrm{i}\omega\rho_{\mathrm{L}}}\frac{\partial p}{\partial s}+\frac{2}{\mathrm{i}\omega\rho_{\mathrm{L}}\alpha^2R^2s}\nabla_{\mathrm{s}}^2\left(p^0 - R\frac{\partial p^0}{\partial s}\right)\mathrm{e}^{\alpha(R-s)}. \tag{A 40}$$

Decomposing the velocity and pressure fields in Legendre polynomials and combining the kinematic and normal stress conditions we obtain

$$p_{nm} = p_{\mathrm{g}}\,\delta_{n0}\,\delta_{m0} + \sigma[2 - n(n+1)]\frac{u_{s,\,nm}}{\mathrm{i}\omega}+2\mu\left(\frac{\partial u_s}{\partial s}\right)_{nm}. \tag{A 41}$$

Since the velocity derivative in the above equation is multiplied by μ, the leading-order approximation for the normal stress balance is simply the inviscid approximation

$$p^0_{nm} + f(n)\,R\left(\frac{\partial p^0}{\partial s}\right)_{nm} = 0, \tag{A 42}$$

with $f(0) = 1/\omega_{\mathrm{r}}^2$ and $f(n) = \sigma^*[n(n+1)-2]$ for $n \geqslant 1$. At the next order, which is $O(\mu^*)$, the velocity to be used in the kinematic boundary condition is modified due to the poloidal field as given by (A 38) but, since the normal derivative of u_s is multiplied by μ, only the leading-order estimate of the velocity as determined from the potential flow approximation is needed in its evaluation. The resulting boundary condition at the surface of the bubble therefore becomes

$$p^2_{nm} + f(n)\,R\left(\frac{\partial p^2}{\partial s}\right)_{nm} = 2\mathrm{i}\left[R^2\frac{\partial^2 p^0}{\partial s^2}+f(n)\,n(n+1)\left(p^0 - R\frac{\partial p^0}{\partial s}\right)\right]_{nm}, \tag{A 43}$$

where the derivatives of p_{nm} are evaluated at $s = R$. The above condition then yields the $O(\mu^*)$ boundary condition for the viscous correction to pressure and its normal derivatives at the surface of the bubble. Thus, once again, p^2 is expressed in terms of multipoles at the centre of each bubble and then expanded in spherical harmonics around each bubble as in the inviscid case. The only difference is that now the relation between the coefficients of the growing and decaying harmonics is established

through the use of (A 43). We shall omit further details now but quote some of the important results. If we write $A_{00}^1 = A_0 + i\mu^* A_0^v$, where A_0 is obtained from the potential flow approximation (cf. (A 23)) and A_0^v is the viscous correction then

$$\frac{A_0^v}{R} = -4t_0^2\left[1+3t_0\frac{R}{S}+7t_0^2\frac{R^2}{S^2}+21t_0^3\frac{R^3}{S^3}+\ldots\right]. \tag{A 44}$$

The functions g_{11} and g_{01} that appear in the calculation of λ_v may also be determined by the methods described here. In particular, the method of successive approximations yield

$$g_{11} = \left[1-\frac{R^3}{S^3}+\frac{R^6}{S^6}+\ldots\right]+12i\mu^*\left[1-\frac{3R^3}{S^3}+\frac{7R^6}{S^6}+\ldots\right], \tag{A 45}$$

$$g_{01} = \left[-1-\frac{2R^3}{S^3}-\frac{4R^6}{S^6}+\ldots\right]+12i\mu^*\left[-1-\frac{6R^3}{S^3}-\frac{28R^6}{S^6}+\ldots\right]. \tag{A 46}$$

Appendix B. The effect of buoyancy

We shall assume that the gas–liquid mixture is contained in a large vessel so that $\boldsymbol{v}_0 = 0$, $(g\boldsymbol{v})_0 = \beta\boldsymbol{V}$, and $\{(1-g)\,\boldsymbol{v}\}_0 = -\beta\boldsymbol{V}$. The base flow due to buoyancy is assumed to be unaffected by the acoustics and given by the potential flow around the bubbles. Thus we assume that outside the bubble at $\boldsymbol{x}_1, \boldsymbol{v}_1$ is given by

$$\boldsymbol{v}_1 = \boldsymbol{\nabla}\psi, \quad \psi = \tfrac{1}{2}R^3\boldsymbol{V}\cdot\boldsymbol{\nabla}s^{-1}, \tag{B 1}$$

and that the density of the gas is negligible, in which case the pressure inside the gas is uniform. Now we proceed to evaluate the ensemble average of various terms in (3.86) and (3.87). The convective term in (3.87) yields

$$\begin{aligned}\{(1-g)\,\boldsymbol{\nabla}\cdot(\hat{\boldsymbol{u}}\boldsymbol{v}+(\hat{\boldsymbol{u}}\boldsymbol{v})^+)\}_0 &= \{(1-g)\,(\boldsymbol{v}\cdot\boldsymbol{\nabla}\hat{\boldsymbol{u}}+\hat{\boldsymbol{u}}\cdot\boldsymbol{\nabla}\boldsymbol{v})\}_0\\ &= -\beta\boldsymbol{V}\cdot\boldsymbol{\nabla}\hat{\boldsymbol{u}}_0+\{(1-g)\,(\boldsymbol{v}\cdot\boldsymbol{\nabla}\hat{\boldsymbol{u}}'+\hat{\boldsymbol{u}}'\cdot\boldsymbol{\nabla}\boldsymbol{v})\}_0,\end{aligned} \tag{B 2}$$

where $\hat{\boldsymbol{u}}' = \hat{\boldsymbol{u}}-\hat{\boldsymbol{u}}_0$. In obtaining the last equality in (B 2), we have made use of the facts that $\{(1-g)\,\boldsymbol{v}\}_0 = -\beta\boldsymbol{V}$ and $\{(1-g)\,\boldsymbol{\nabla}\boldsymbol{v}\}_0 = 0$. Now since the viscosity effects have been neglected, $\boldsymbol{u}+\boldsymbol{v}$ satisfies the potential flow equations, and we can express the disturbance velocity in terms of a velocity potential, i.e. $\hat{\boldsymbol{u}}' = \boldsymbol{\nabla}\varphi'$. The last term in (B 2) then simplifies to

$$\begin{aligned}\{(1-g)\,(\boldsymbol{v}\cdot\boldsymbol{\nabla}\hat{\boldsymbol{u}}'+\hat{\boldsymbol{u}}'\cdot\boldsymbol{\nabla}\boldsymbol{v})\}_0 &= \{(1-g)\,\boldsymbol{\nabla}(\boldsymbol{\nabla}\psi\cdot\boldsymbol{\nabla}\varphi')\}_0\\ &= -\frac{\beta}{V_b}\int_{s=R}\boldsymbol{n}(\boldsymbol{\nabla}\psi\cdot\boldsymbol{\nabla}\varphi')_1\,\mathrm{d}S,\end{aligned} \tag{B 3}$$

where we have used the divergence theorem to convert the volume integral in the averaging to the area integral on the surface of the bubble at $\boldsymbol{x}_1$. The quantity $\boldsymbol{\nabla}(\boldsymbol{\nabla}\psi\cdot\boldsymbol{\nabla}\varphi')$ decays as R^6/s^6 and hence the integral at infinity does not contribute to the average. The ensemble averages of the remaining terms are straightforward and the resulting averaged momentum and continuity equations are given by

$$i\omega\rho_L(\hat{\boldsymbol{u}}_0-\beta\hat{\boldsymbol{u}}_g)-\rho_L\,\boldsymbol{V}\cdot\boldsymbol{\nabla}\hat{\boldsymbol{u}}_0+\boldsymbol{\nabla}\hat{p}_0 = \frac{\beta\rho_L}{V_b}\int_{s=R}\boldsymbol{n}(\boldsymbol{\nabla}\psi\cdot\boldsymbol{\nabla}\varphi')_1\,\mathrm{d}S, \tag{B 4}$$

$$\frac{\beta i\omega}{\gamma Pe}\hat{p}_g+\boldsymbol{\nabla}\cdot\hat{\boldsymbol{u}}_0 = 0, \tag{B 5}$$

where $\hat{p}_g$ is the amplitude of the pressure variation inside the bubble and $\hat{\boldsymbol{u}}_g$ is the amplitude of the velocity inside the bubble.

Now we proceed to determine the velocity field to leading order in β by neglecting

the pairwise interactions. The pressure inside the gas is uniform, and so the motion inside the bubble at $\boldsymbol{x}_1$ is still given by (3.34). The pressure outside the bubble can be determined from the Bernoulli's equation, which yields

$$\hat{p}_1 = -\rho_L[i\omega\hat{\varphi}_1 + (\nabla\hat{\varphi}\cdot\nabla\psi)_1]. \tag{B 6}$$

Since the compressibility of the liquid is neglected, we shall assume that the velocity potential is given by (cf. §3.3)

$$\hat{\varphi}_1 = \varphi^*(1 - i\boldsymbol{k}\cdot\boldsymbol{s}) + A_0 s^{-1} + \boldsymbol{A}_1\cdot\nabla s^{-1} + \ldots, \tag{B 7}$$

where A_0 and $\boldsymbol{A}_1$ are the strengths of the monopole and dipole, and $\varphi^* = \hat{\varphi}_0 e^{-i\boldsymbol{k}\cdot\boldsymbol{x}_1}$. The higher-order multipoles can be neglected when k is small and therefore they are not explicitly written in (B 7). Also, we note for later use that $\hat{\boldsymbol{u}}_0 = -i\boldsymbol{k}\varphi^*$ and $\hat{p}_0 = -i\omega\rho_L\varphi^*$ to this $O(1)$ approximation in β. The strengths of monopole and dipole can be determined from the boundary conditions at the bubble surface. Combining the kinematic and normal stress conditions, we now have that

$$\int_{s=R} \hat{p}_1 \boldsymbol{n}\,dS = 0, \tag{B 8}$$

$$\int_{s=R} \left\{\hat{p}_1 + \frac{3\gamma}{i\omega R}\frac{\partial\hat{\varphi}_1}{\partial s}\right\} dS = 0. \tag{B 9}$$

Substituting for the pressure from (B 6) into (B 8) and (B 9), and solving for the strengths of monopole and dipole, we obtain

$$\frac{A_0}{R} = \frac{\omega_r^2\varphi^*}{1-\omega_r^2(1+B^2)} - \frac{i\omega\varphi^*(-i\boldsymbol{k}\cdot\boldsymbol{V})}{\omega_c^2[1-\omega_r^2(1+B^2)]}, \tag{B 10}$$

$$\frac{\boldsymbol{A}_1}{R^3} = -i\boldsymbol{k}\varphi^* - \frac{A_0\boldsymbol{V}}{i\omega R^3}, \tag{B 11}$$

where $B = V/(R\omega)$. It is easy to verify that the expressions for the strengths of monopole and dipole are in agreement with those derived in §3.1 (cf. (3.12) and (3.13)) when $B = V = 0$. Now the pressure and velocity inside the bubble can be readily related to A_0 and $\boldsymbol{A}_1$ by means of

$$\hat{p}_g = \frac{3\gamma Pe\, A_0}{i\omega R^3} \quad \text{and} \quad \hat{\boldsymbol{u}}_g = \hat{\boldsymbol{u}}_0 + \frac{2\boldsymbol{A}_1}{R^3}, \tag{B 12}$$

so that all the terms in (B 4) and (B 5) can now be evaluated. Expressing φ^* and $-i\boldsymbol{k}\varphi^*$ in terms of $\hat{p}_0$ and $\hat{\boldsymbol{u}}_0$, and rearranging we finally arrive at the averaged momentum and continuity equations correct to $O(\beta)$:

$$i\omega\rho_L\left[\hat{\boldsymbol{u}}_0 - 3\beta\left\{\hat{\boldsymbol{u}}_0 - \frac{\boldsymbol{V}\hat{p}_0^*}{3\gamma^* Pe\,[1-\omega_r^2(1+B^2)]}\right\}\right] + \nabla\hat{p}_0^* = 0, \tag{B 13}$$

$$\frac{i\omega\beta\hat{p}_0^*}{[1-\omega_r^2(1+B^2)]\gamma^* Pe} + \nabla\cdot\hat{\boldsymbol{u}}_0 = 0, \tag{B 14}$$

where $\hat{p}_0^* = \hat{p}_0 - \rho_L\hat{\boldsymbol{u}}_0\cdot\boldsymbol{V}$ is the modified pressure. Once again, these equations reduce to the averaged momentum and continuity equations derived in §3 when $B = V = 0$. Eliminating now $\hat{p}_0^*$ and $\hat{\boldsymbol{u}}_0$ from the above equations yields the following dispersion relation:

$$k^2 = \frac{\beta\rho_L\omega^2}{\gamma^* Pe\,[1-\omega_r^2(1+B^2)]}\left[1 + \frac{\boldsymbol{k}\cdot\boldsymbol{V}}{\omega} - 3\beta\right]. \tag{B 15}$$

Thus we see that buoyancy affects the leading-order term in the dispersion relation

in two ways. It decreases the apparent natural frequency of the bubble by a factor $(1+B^2)^{\frac{1}{2}}$. More specifically, the factor $1/(1-\omega_r^2)$ is now replaced by $1/(1-(1+B^2)\omega_r^2)$. This is not surprising since the base flow generated by the buoyancy increases the pressure around the bubble. In the experiments of Micaelli (1982), B was about 10, and so the apparent natural frequency was considerably larger than the natural frequency of the bubbles. However, ω_r was only about 0.03, so that this corresponds to an error of about 10%. For larger frequencies, of course, $B = V/R\omega$ also decreases and in fact for ω comparable to the natural frequency, $B_c^2 = \rho_L V^2/(3\gamma^* Pe)$ is indeed very small. Thus the actual shift in the resonance frequency due to buoyancy is small.

The second effect of the buoyancy is the familiar Doppler shift due to a moving source. We find that the Doppler shift is primarily dependent on the average velocity of the bubble and not on the average velocity of the mixture. The latter is, of course, zero in the problem we have examined.

The $O(\beta^2)$ term in (B 15) is, of course, not exact but from the analysis of §3 it is easily seen that the corrections are at least $O(\omega_r^2)$. As mentioned earlier, however, the value of B is small whenever ω_r is $O(1)$. On the other hand, in the limit of very small ω_r, for which the comparison with the experiments of Micaelli is made, the $O(\beta^2)$ coefficients in the averaged momentum equations will in general be affected so that the $O(\beta)$ coefficient of λ_v will be a function of B and approach two different constants for the extreme values of B equal to 0 and ∞. The buoyancy also affects the $O(\beta)$ coefficient of λ_v by modifying the conditional probability density function.

REFERENCES

Abramowitz, M. & Stegun, I. A. 1972 *Handbook of Mathematical Functions with Formulas, Graphs, and Mathematical Tables.* National Bureau of Standards.

Acrivos, A. & Chang, E. Y. 1986 The transport properties of non-dilute suspensions. Renormalization via an effective continuum method. In *Physics and Chemistry of Porous Media, AIP Conf. Proc.* (ed. J. R. Banavar, J. Koplik & K. W. Winkler), vol. 154, p. 129.

Batchelor, G. K. 1967 *An Introduction to Fluid Dynamics.* Cambridge University Press.

Batchelor, G. K. 1969 Compression waves in a suspension of gas bubbles in liquid. *Fluid Dyn. Trans.* **4**, 425.

Batchelor, G. K. 1974 Transport properties of two-phase materials with random structure. *Ann. Rev. Fluid Mech.* **6**, 227.

Biesheuvel, A. & Spoelstra, S. 1989 The added mass coefficient of a dispersion of spherical gas bubbles in liquid. *Intl J. Multiphase Flow* **15**, 911.

Biesheuvel, A. & Wijngaarden, L. van 1984 Two-phase flow equations for a dilute dispersion of gas bubbles in liquid. *J. Fluid Mech.* **148**, 301.

Caflisch, R. E., Miksis, M. J., Papanicolaou, G. C. & Ting, L. 1985*a* Effective equation for wave propagation in bubbly liquids. *J. Fluid Mech.* **153**, 259.

Caflisch, R. E., Miksis, M. J., Papanicolaou, G. C. & Ting, L. 1985*b* Wave propagation in bubbly liquids at finite volume fraction. *J. Fluid Mech.* **160**, 1.

Carstensen, E. L. & Foldy, L. L. 1947 Propagation of sound through a liquid containing bubbles. *J. Acoust. Soc. Am.* **19**, 481.

Commander, K. W. & Prosperetti, A. 1989 Linear pressure waves in bubbly liquids: Comparison between theory and experiments. *J. Acoust. Soc. Am.* **85**, 732.

Foldy, L. L. 1945 The multiple scattering of waves. *Phys. Rev.* **67**, 107.

Fox, F. E., Curley, S. R. & Larson, G. S. 1955 Phase velocity and absorption measurements in water containing air bubbles. *J. Acoust. Soc. Am.* **27**, 534.

Hinch, E. J. 1977 An averaged-equation approach to particle interactions in a fluid suspension. *J. Fluid Mech.* **83**, 695.

HOBSON, E. W. 1931 *The Theory of Spherical and Ellipsoidal Harmonics*. Cambridge University Press.

HOWELLS, I. D. 1974 Drag due to the motion of a Newtonian fluid through a sparse random array of small fixed rigid objects. *J. Fluid Mech.* **64**, 449.

JEFFREY, D. J. 1973 Conduction through a random suspension of spheres. *Proc. R. Soc. Lond.* A **335**, 355.

KANG, I. S. & LEAL, L. G. 1988 Small-amplitude perturbations of shape for a nearly spherical bubble in an inviscid straining flow (steady shapes and oscillatory motion). *J. Fluid Mech.* **187**, 231.

KIM, S. & RUSSEL, W. B. 1985*a* The hydrodynamic interactions between two spheres in a Brinkman medium. *J. Fluid Mech.* **154**, 253.

KIM, S. & RUSSEL, W. B. 1985*b* Modelling of porous media by renormalization of the Stokes equations. *J. Fluid Mech.* **154**, 269.

KOCH, D. L. & BRADY, J. F. 1987 A non-local description of advection-diffusion with application to dispersion in porous media. *J. Fluid Mech.* **180**, 387.

KOL'TSOVA, I. S., KRYNSKII, L. O., MIKHALOV, I. G. & POKROVSKAYA, I. E. 1979 Attenuation of ultrasonic waves in low-viscosity liquids containing gas bubbles. *Akust. Zh.* **25**, 725. (English transl: *Sov. Phys. Acoust.* **25**, 409.)

LEVICH, V. G. 1962 *Physico-Chemical Hydrodynamics*. Prentice Hall.

MICAELLI, J.-C. 1982 Propagation d'ondes dans les écoulements diphasiques a bulles a deux constituants. Etude théorique et expérimentale. Thèse, Université de Grenoble.

MIKSIS, M. J. & TING, L. 1986 Wave propagation in a bubbly liquid with finite-amplitude asymmetric bubble oscillations. *Phys. Fluids* **29**, 603.

MIKSIS, M. J. & TING, L. 1987*a* Viscous effects on wave propagation in a bubbly liquid. *Phys. Fluids* **30**, 1683.

MIKSIS, M. J. & TING, L. 1987*b* Wave propagation in a multiphase media with viscous and thermal effects. *ANS Proc. Natl Heat Transfer Conf.*, p. 145.

PROSPERETTI, A. 1984 Bubble phenomena in sound fields: part one. *Ultrasonics* **22**, 69.

PROSPERETTI, A. & KIM, D. H. 1989 Pressure waves in bubbly liquids at small gas volume fractions. In *Fundamentals of Gas and Liquid Flows* (ed. E. E. Michaelides & M. P. Sharma), p. 19. ASME.

PROSPERETTI, A. & LEZZI, A. 1986 Bubble dynamics in a compressible liquids. Part 1. First-order theory. *J. Fluid Mech.* **168**, 457.

RUBINSTEIN, J. 1985 Bubble interaction effects on waves in bubbly liquids. *J. Acoust. Am.* **77**, 2061.

RUGGLES, A. E., SCARTON, H. A. & LAHEY, R. T. 1986 An investigation of the propagation of pressure perturbations in bubbly air/water flows. *First Intl Multiphase Fluids Transients Symp.* (ed. H. H. Safwat, J. Braun & U. S. Rohatgi). ASME.

SANGANI, A. S. & YAO, C. 1988 Bulk conductivity of composites with spherical inclusions. *J. Appl. Phys.* **63**, 1334.

SANGANI, A. S., ZHANG, D. & PROSPERETTI, A. 1991 The added mass, Basset, and viscous drag coefficients in non-dilute bubbly liquids undergoing small amplitude oscillatory motion. *Phys. Fluids* (submitted).

SCOTT, J. F. 1981 Singular perturbation applied to the collective oscillation of gas bubbles in a liquid. *J. Fluid Mech.* **113**, 487.

SHAQFEH, E. 1988 A nonlocal theory for the heat transport in composites containing highly conducting fibrous inclusions. *Phys. Fluids* **31**, 2405.

SILBERMAN, E. 1957 Sound velocity and attenuation in bubbly mixtures measured in standing wave tubes. *J. Acoust. Soc. Am.* **29**, 925.

TWERSKI, V. 1962 On scattering of waves by random distributions. I. Free-space scatterer formalism. *J. Math. Phys.* **3**, 700.

WIJNGAARDEN, L. VAN 1972 One-dimensional flow of liquids containing small bubbles. *Ann. Rev. Fluid Mech.* **4**, 369.

WIJNGAARDEN, L. VAN 1976 Hydrodynamic interaction between bubbles in liquid. *J. Fluid Mech.* **77**, 24.